12-4-2006

The Role of Ecological Interactions in Polymicrobial Biofilms and their Contribution to Multiple Antibiotic Resistance

Heather Adele O'Connell

THE ROLE OF ECOLOGICAL INTERACTIONS IN POLYMICROBIAL BIOFILMS AND THEIR CONTRIBUTION TO MULTIPLE ANTIBIOTIC RESISTANCE

by

HEATHER O'CONNELL

Under the direction of Eric Gilbert

ABSTRACT

The primary objectives of this research were to demonstrate that: 1.) antibiotic resistant bacteria can promote the survival of antibiotic sensitive organisms when grown simultaneously as biofilms in antibiotics, 2.) community-level multiple antibiotic resistance of polymicrobial consortia can lead to biofilm formation despite the presence of multiple antibiotics, and 3.) biofilms may benefit plasmid retention and heterologous protein production in the absence of selective pressure. Quantitative analyses of confocal data showed that ampicillin resistant organisms supported populations of ampicillin sensitive organisms in steady state ampicillin concentrations 13 times greater than that which would inhibit sensitive cells inoculated alone. The rate of reaction of the resistance mechanism influenced the degree of protection. Spectinomycin resistant organisms did not support their sensitive counterparts, although flow cytometry indicated that GFP production by the sensitive strain was improved. When both organisms were grown in both antibiotics, larger numbers of substratum-attached pairs at 2 hours resulted in greater biofilm formation at 48 hours. For biofilms grown in both antibiotics, a benefit to spectinomycin resistant organism's population size was detectable, but the only benefit to ampicillin resistant organisms was in terms of GFP production. Additionally, an initial

attachment ratio of 5 spectinomycin resistant organisms to 1 ampicillin resistant organism resulted in optimal biofilm formation at 48 hours. Biofilms also enhanced the stability of high-copy number plasmids and heterologous protein production. In the absence of antibiotic selective pressure, plasmid DNA was not detected after 48 hours in chemostats, where the faster growth rate of plasmid-free cells contributed to the washout of plasmid retaining cells. The plasmid copy number per cell in biofilms grown without antibiotic selective pressure steadily increased over a six day period. Flow cytometric monitoring of bacteria grown in biofilms indicated that 95 percent of the population was producing GFP at 48 hours. This research supports the idea that ecological interactions between bacteria contribute to biofilm development in the presence of antibiotics, and demonstrates that community-level multiple antibiotic resistance is a factor in biofilm recalcitrance against antibiotics. Additionally, biofilms may provide an additional tool for stabilizing high copy number plasmids used for heterologous protein production.

INDEX WORDS: Biofilm, *Escherichia coli*, Heterologous protein production, Microbial ecology, Multiple antibiotic resistance, Mutualism, Commensalism, Plasmid maintenance

THE ROLE OF ECOLOGICAL INTERACTIONS IN POLYMICROBIAL BIOFILMS AND THEIR CONTRIBUTION TO MULTIPLE ANTIBIOTIC RESISTANCE

by

HEATHER O'CONNELL

A Dissertation Submitted in Partial Fulfillment of the Requirements for the Degree of

Doctor of Philosophy

in the College of Arts and Sciences

Georgia State University

2006

THE ROLE OF ECOLOGICAL INTERACTIONS IN POLYMICROBIAL BIOFILMS AND THEIR CONTRIBUTION TO MULTIPLE ANTIBIOTIC RESISTANCE

by

HEATHER O'CONNELL

Major Professor: Eric Gilbert

Committee: Eric Gilbert

George Pierce

Sidney Crow

Electronic Version Approved:

Office of Graduate Studies

College of Arts and Sciences

Georgia State University

December 2006

ACKNOWLEDGMENTS

I thank Robert Simmons for his expert training with the CLSM. The vector pUCSpec was kindly provided by June Scott, Emory University. I thank Dr. Arne Heydorn and Dr. Molin for sharing the program COMSTAT and the accompanying technical support. I appreciate the feedback provided by Dan Rozen, Don Ahearn, and Kristala Prather on several manuscripts.

I am grateful for the highly motivational guidance by Dr. Eric Gilbert for the duration of both my undergraduate and graduate research, and to Drs. Pierce and Crow for their practical, application-driven insight. I thank B. Stubblefield, C. Niu, S. Gilbert, G. Kottkamp, J. Eppelbaum, J. Graves, M. Sanders, S. Taskaeva, B. Lovell, S. Afre, F. Mokuolu, C. Robbins, R. Mdodo, B. Cierny, A. Esfandiarinia, M. Ouattara, and B. Okorn for their assistance with experiments, and collegial camaraderie in the lab.

Personally, I would like to thank my husband, Daniel O'Connell, and my parents Robert and Karen Moulton; my good friends H. Rosen, M. Kuggeleijn, and the Transformers:2005 roleplaying group for their patience and support of my pursuit. This research was supported by the American Heart Association Southeast Affiliate (Grant # 0160196B).

TABLE OF CONTENTS

List of Tables

List of Figures

List of Abbreviations

AAD(9)	spectinomycin adenyltransferase
AB	antibiotics, 80 ppm spectinomycin and 100 ppm ampicillin
Amp^r	ampicillin resistant
Amp^R	ampicillin resistant
BISS	Biofilm Image Segmentation Software
bla	beta-lactamase gene
CMAR	community-dependent multiple antibiotic resistance
CLSM	confocal laser scanning microscopy
CFU	colony forming units
DNA	deoxyribonucleic acid
egfp	enhanced green fluorescent protein gene
EPS	exopolysaccharide
FCM	fuzzy c-means
FL1-H	relative green fluorescence
FSC	forward scatter
GFP	green fluorescent protein
HPP	heterologous protein production
HSV	hue saturation value
IPTG	isopropyl-beta-D-thiogalactopyranoside
LB	Luria-Bertani
LVQ	learning vector quantization
LVQNN	learning vector quantization neural network
MBPC	minimum biofilm preventative concentration
MIC	minimum inhibitory concentration
MW	molecular weight marker
NG	no growth
OD	optical density
PCN	plasmid copy number
RGB	red green blue
rGFP	recombinant green fluorescent protein
SOM	self-organizing maps
$Spec^R$	spectinomycin resistant
Spt^r	spectinomycin resistant
SSC	side scatter
TEM-1	beta-lactamase, encoded by a plasmid of clinical origin

CHAPTER 1 INTRODUCTION

1.1 BIOFILMS, NOSOCOMIAL INFECTION AND MULTIPLE ANTIBIOTIC RESISTANCE

1.1.1 Biofilms may have a negative impact on human health.

Biofilms are microbial communities adhered to a substratum, encased in expolysaccharide (EPS), and possessing altered gene expression relative to their planktonic counterparts (Donlan & Costerton, 2002). Biofilms may have a negative impact on human health. For example, biofilm associated bacteria cause diseases such kidney stones, endocarditis, and cystic fibrosis (Parsek & Singh, 2003). Nosocomial infections, those acquired by patients due to hospital stays, can arise from biofilms in several ways, and biofilm growth in drinking water and dental unit systems can act as a reservoir of infection (Parsek & Singh, 2003). Medical device infections involving biofilms are of particular concern. Indwelling devices such as artificial joints, artificial heart valves, venous and urinary catheters, and ventilators all become potential sources of recurrent infections once biofilms have been established (Adair *et al.*, 1999; Donlan & Costerton 2002; Puri *et al.*, 2002; Ronald, 2003; Triandafillu *et al.*, 2003). Consequently, understanding biofilm development could lead to their control, benefiting human health.

Biofilms increase the difficulties of treating infections with antibiotics. The nature of multispecies biofilm communities compound these difficulties for several reasons, described in the following sections. The contribution of ecological interactions

in multispecies, or polymicrobial, biofilm-based infections and their role in multiple antibiotic resistance, is currently limited. This research was designed to increase knowledge of the initial interactions between organisms in the early development of polymicrobial, antibiotic resistant biofilms.

1.1.2 The problem of multiple antibiotic resistance.

Antibiotics were discovered and rapidly developed in the first half of the twentieth century, and hailed as a major advancement in the health care field. This golden age was short-lived, however, with the rise of antibiotic resistance. There are many mechanisms of antibiotic resistance, such as target site modification, antibiotic modification, and efflux pumps (Jana & Deb, 2006; Piddock, 2006; Wilke *et al.*, 2005). Organisms resistant to multiple antibiotics are becoming a greater problem in hospitals, and some pathogens touting 'panresistant' traits have been identified (Paterson, 2006). In addition to these genetic elements, bacteria growing in biofilm environments enjoy a gamut of physiological advantages relative to those cells growing in the planktonic state.

1.1.3 Biofilm development.

A community of microbes attached to a surface is referred to as a biofilm. Biofilms typically form wherever a non-sterile fluid contacts a solid surface *et al.*, 2003). Biofilm formation begins when cells attach to a surface preconditioned with nutrients or electrostatic charges. The initial attachment to a substratum is reversible. Further growth and accumulation results in microcolony formation, and is accompanied by significant

physiological changes (Schembri *et al.*, 2003) such as flagella loss, fimbriation, reduced growth rate, exopolysaccharide (EPS) production, and signaling molecule production related to quorum sensing (Reisner *et al*., 2003). Mature biofilms feature structures such as channels, void spaces, and streamers. Individual cells can detach from the biofilm in response to changing nutrient needs or dispersal signals, or entire sections of biomass can be sloughed off and then colonize other areas (Stoodley *et al.*, 2002).

1.1.4 Benefits to cells growing in biofilms.

Several key features of biofilms benefit the component bacteria. Exopolysaccharide formation, diffusion gradients of electron acceptors and nutrients, the community metagenome, high cell density, antibiotic resistance exchange, and quorum sensing, all combine to enhance the chances of survival of individual cells (Kreft, 2004).

The EPS serves as a water and nutrient reservoir, and can present an additional barrier to immune system clearing. Most non-mucoid, non-pseudomonad biofilms used in research do not greatly delay physical diffusion of molecules into the biofilm. Molecules of approximately 400 g mol^{-1}, such as antibiotics or stains, can penetrate *E. coli* biofilms in the span of 10 minutes (Stone, 2002). The portions of biofilms closest to the bulk fluid, such as those on microcolony exteriors and channels, are the most metabolically active. Not only are these outer cells are the first to encounter nutrients and dissolved oxygen, but they are also the first to be exposed to toxins in their environment. In biofilm infections, antibiotic treatment and subsequent clearing by the immune system targets this more active, outer subpopulation. The bacteria deeper within the biofilm,

which had been dormant due to nutrient starvation, are protected by these ablative portions of the biofilm (Donlan & Costerton, 2002). Metabolically inactive bacteria may also further differentiate into persister cells, which can shift back into vegetative growth to repopulate the niche space and create new biofilm (Lewis, 2005).

Most biofilms found in nature are polymicrobial, meaning that they support multiple species of bacteria, fungi, and protozoa (Stoodley *et al.*, 2002). This diversity results in a much larger array of genetic tools, referred to as the metagenome, that are available to the community than would be at any single organism's disposal. The persistence of chronic infections is attributed to the persistence of polymicrobial biofilms (Ehrlich, 2005). Diversity allows survival during adversity (Brook, 2002; Von Canstein, 2002). In the event that a member organism dies off, polymicrobial biofilms may endure, due to possessing organisms whose metabolic pathways or other functions are redundant to the missing member.

1.2 BIOFILMS AND ANTIBIOTIC RESISTANCE

1.2.1 Biofilm infections are more difficult to eradicate than planktonic infections.

Biofilms contribute to the survival of bacteria despite antibiotic treatment, and bioilm related infections frequently require repeated courses of treatment (Costerton, 1999). Elimination of established biofilms may require up to 1000 times the MIC, the amount of antibiotic required to stop the growth of planktonic cells (Donlan & Costerton, 2002). Attached cells can tolerate antibiotic concentrations three to five times higher than their MIC (O'Connell *et al.*, 2006; Das *et al.*, 1998). Additionally, planktonic cells

that had been previously attached in a biofilm show a greater resistance to antibiotics (Mateus *et al.*, 2004; Pickering *et al.*, 2003), reflecting the large number of physiological changes that take place once the organisms attach to a surface.

1.2.2 Effect of diffusion gradients on antibiotic resistance in biofilms.

Antibiotic permeability does not appear to be constrained by diffusion gradients. The molecular weight of most antibiotics and their amphiphilic structure allows them to permeate most biofilms in the span of 10 minutes (Stone *et al.*, 2002). Instead, the metabolically active regions on the exterior of the biofilms may inactivate the antibiotic, particularly with enzymes with high turnover rates, like catalase in *Pseudomonas* biofilms (Stewart *et al.*, 2000). Thus, the effective antibiotic dose is sublethal, giving the bacteria time for induction and expression of other resistance phenotypes, such as the multidrug resistance operan *mar* (Maira-Littan *et al.*, 2000; Gilbert *et al.*, 2002).

Redox gradients also contribute to antibiotic resistance in biofilms. Even in well-aerated fluids, the oxygen concentrations approach zero near the substratum of biofilms more than 50 microns thick (Rasmussen & Lewandowski, 1998). This redox gradient reduces the efficacy of antibiotics such as phenazines and some glycopeptides. Reduced oxygen and nutrient concentrations within biofilms slow the growth rates of the interior organisms. A slower growth rate reduces the efficiency of antibiotics that target the cell wall, such as penicillins (Gilbert *et al.*, 1990).

1.2.3 Horizontal gene transfer in biofilms.

Antibiotic resistance genes are also more likely to be transferred between cells growing in biofilms relative to their planktonic counterparts (Fux *et al.*, 2005). In biofilms, the likelihood of plasmid exchange is increased (Molin, 2003) by two factors: higher cell density and pili production. Biofilms typically host more cells per mL than liquid suspensions of cells, increasing the chance that some member organisms possess plasmids. Additionally, the proximity of cells, and their fixed locations relative to each other, ensures that there will be a longer timeframe, and a more stable connection over a shorter distance, in which plasmid exchange can occur. Cell attachment to surfaces, and biofilm formation, has also been linked to pili formation (O'Toole & Kolter, 1998). Type IV pili production is a prerequisite for plasmid exchange (Molin, 2003), so increased production simultaneous with the presence of a large number of recipients, greatly enhances the potential for rapid dissemination of a plasmid in the biofilm.

1.3 ECOLOGICAL INTERACTIONS IN BIOFILMS

1.3.1 Biofilms are diverse ecosystems.

There is growing interest in the interactions between different species within biofilm communities. Most biofilms found in nature are polymicrobial, such as the microbial flora of oral biofilms (Li *et al.*, 2005). The large number of potential interactions between member species of polymicrobial biofilms has been likened to that people living in a city (Watnick & Kolter, 2000).

1.3.2 Commensalism.

An ecological interaction between two organisms in which one benefits, but the other is neither harmed nor helped, is known as commensalism, such as the ability of *Pseudomonas* to utilize the benzoate leaking from *Acinetobacter* cells (Christensen *et al.*, 2002). Biofilm commensalism was also described in wastewater treatment, where a strain of p-cresol degrading *Pseudomonas* was able to reduce the inhibitory effects of p-cresol on a second pseudomonad (Cowan *et al.*, 2000). A geneitically modified pseudomonad was able to aid other biofilm members by degrading toxic phenols (Erb *et al.*, 1997). The spatial organization of cells in biofilms results in the protection of at least one member species from disinfection by a chlorinated alkaline solution (Leriche *et al.*, 2003).

Another case involves beta-lactamase production of *Branhamella catarrhalis*, which can cause antibiotic treatment failure in inner-ear infections caused by streptococci (Budhani, 1998). This process, in which a non-target organism destroys antibiotics intended for a different, target pathogen is referred to as indirect pathogenesis (Brook, 1994; Kaieda *et al.*, 2005).

1.3.3 Mutualism.

Mutualism is an ecological interaction where both organisms benefit from each other's presence, such as in oral biofilms, where *Streptococcus* and *Actinomyces* aided each other in colonizing tooth surfaces (Palmer *et al.*, 2001). The degree to which an organism contributes to either a commensal or mutualistic relationship may vary. A

mutualism in which both organisms are essential, but do not contribute equally, could result in large numbers of the lesser contributor being supported by a smaller numbers of the greater contributor.

1.3.4. Competition.

Limited space and nutrients in biofilms can lead to competition between microorganisms. An example of this is the interaction between *Pseudomonas* and *Agrobacterium*, in which growth rate and motility impacted the fitness of each competitor (An *et al.*, 2006). Other factors, such as substrate concentration, can impact the ability of an organism to claim niche space in biofilms (Bollmann *et al.*, 2002).

1.3.5. Antagonism.

Bacteria, even when growing in biofilms, may behave antagonistically against other microorganisms. This type of interaction is typified by one organism's direct, deleterious impact on another. Temporal and spatial factors weigh heavily in these interactions. Typically, the first organism to colonize a surface inhibits potential competitors via compounds like bacteriocins (Kreth *et al.*, 2005; Rao *et al.*, 2005). Simultaneous colonization of a surface by the same organisms results in a longer interplay between the two, unlike the eventual out-competition that occurs in planktonic cultures (Riley & Gordon, 1999). Despite bacteriocin production that allows enteric organisms to successfully invade already established biofilms, the heterogeneity of the

biofilm environment allows the retention of bacteriocin-sensitive competitors (Tait & Sutherland, 2002).

1.4 PLASMIDS AND THEIR IMPACT ON THE BIOFILM LIFESTYLE

1.4.1 Economic significance of plasmids.

Several factors associated with biofilm growth enhance plasmid transmission and maintenance. Plasmids represent mobile genetic elements that can be exchanged between individual bacteria, even across species, genus, and families. This flexibility is a contributing factor to the rise of community-acquired antibiotic resistance in nosocomial infections (Wei *et al.,* 2005). In addition to their putative role in biofilm formation and their contribution to the proliferation of antibiotic resistance, plasmids are used extensively in industrial processes. Bioremediation, as well as fermentation and manufacturing precursors rely on organisms containing plasmids (Binnie *et al.,* 1997; Shintani *et al.,* 2006). These plasmids contain exogenous genes for production of enzymes, including operons that encode for entire metabolic pathways (Burlage *et al.,* 1989).

1.4.2 Role of biofilms in reducing plasmid loss.

The metabolic and resistance advantages that plasmids confer to their host are conditional, however. Many industrial applications involve high density, batch-fed systems (Baneyx, 1999; Belanger *et al.,* 2004). The microorganism receives no benefit from this, as energy typically invested in growth and division is diverted to

overexpression. Accumulation of waste products such as acetate also increases the stress placed on the cells (Kirkpatrick *et al.*, 2001). If there is no selective pressure to maintain the plasmid, the metabolic burden imposed by their maintenance makes the host less fit, causing it to be outcompeted. The slower growth rate of biofilm cells compared to their planktonic counterparts could aid plasmid retention in the absence of selective pressure (Bryers & Huang, 1995). Partitioning events, where one daughter cell may receive no plasmid during division, are less likely for a given amount of time. Partitioning is further reduced by slower growth of biofilm cells because the plasmids have more time to replicate per cell division, resulting in a larger plasmid dosage per daughter cell. Also, biofilm cells are attached to their substratum, preventing the washout of less quickly dividing, plasmid-bearing cells that would occur in chemostats.

1.5 HYPOTHESES

1.5.1 Statements of hypotheses regarding commensalism in antibiotic-exposed biofilms.

1.5.1.1 Rationale.

Thus far, the only observed examples of commensalism in biofilms via antibiotic detoxification have been in beta-lactamase producing bacteria. In a steady state chemostat culture, cells are well-mixed, minimizing any prolonged contact that one organism may have with another. Compared to planktonic culture, cells adjacent to each other in a biofilm experience fixed, long-term spatial interactions. In biofilms, a small number of antibiotic resistant organisms may be able to reduce the antibiotic

concentrations in their immediate area, even with resistance mechanisms that have lower rates of antibiotic modification.

1.5.1.2 Statements of hypotheses.

The objective of this work is to determine whether spectinomycin-sensitive bacteria will be able to establish and maintain a population despite inhibitory spectinomycin concentrations when cultivated with spectinomycin-resistant bacteria as a biofilm. Similarly, ampicillin-sensitive bacteria will be able to establish and maintain a population despite inhibitory ampicillin concentrations when cultivated with ampicillin-resistant organisms as a biofilm. This commensal interaction is hypothesized to be better supported in biofilms versus planktonic growth in chemostats, due to the prolonged, fixed positions of antibiotic sensitive organisms relative to their antibiotic resistant counterparts.

1.5.2 Statements of hypotheses regarding mutualism in biofilms exposed to multiple antibiotics.

1.5.2.1 Rationale.

Biofilm infections are often polymicrobial (Palmer, 2001; Stoodley *et al.,* 2002; Watnick & Kolter 2000). Each of the member organisms may possess separate antibiotic resistance mechanisms that inactivate the antibiotic. Colonization of the substratum by two reciprocally antibiotic resistant organisms in a close enough proximity to each other

could cause the local antibiotic concentrations to be reduced for a long enough time period to allow microcolony formation.

1.5.2.2 Statements of hypotheses.

The objective of this work is determine if the simultaneous detoxification of inhibitory concentrations of ampicillin and spectinomycin by two individual strains of bacteria will be sufficient to form a biofilm. A population equilibrium other than a one spectinomycin-resistant cell to one ampicillin-resistant cell may be necessary for optimal growth of biofilms that contain organisms with unequal detoxification rates.

1.5.3 Statements of hypotheses regarding plasmid maintenance and heterologous protein production in biofilms.

1.5.3.1 Rationale.

Heterologous protein production (HPP) has typically been carried out in chemostats, using plasmids as tools for gene overexpression. The metabolically demanding environment of the chemostat can promote to plasmid loss. Biofilm cells undergo fewer cell divisions per unit of time, and retain plasmid-containing member cells that might otherwise be washed out due to their slower growth rate. Biofilms have been used in the continuous production of ethanol (Kunduru & Pometto, 1996) and lactic acid (Cotton *et al.*, 2001).

1.5.3.2 Statements of hypotheses.

The objective of this work is to determine if the decreased growth rate of biofilm-attached *Escherichia coli* ATCC 33456 pEGFP cells will decrease the loss of the green fluorescent protein-encoding plasmid pEGFP in the absence of ampicillin selective pressure relative to planktonic growth.

CHAPTER 2

Applied and Environmental Microbiology, 2006, Jul. 72(7) p. 5013–5019

INFLUENCES OF BIOFILM STRUCTURE AND ANTIBIOTIC RESISTANCE MECHANISMS ON INDIRECT PATHOGENICITY IN A MODEL POLYMICROBIAL BIOFILM

Heather A. O'Connell, Greg S. Kottkamp, James L. Eppelbaum, Bryan A. Stubblefield, Sarah E. Gilbert, and Eric S. Gilbert

2.1 ABSTRACT

Indirect pathogenicity (IP), the commensal protection of antibiotic-sensitive pathogens by resistant microorganisms of low intrinsic virulence, can prevent the eradication of polymicrobial infections. The contributions of antibiotic resistance mechanisms and biofilm structure to IP within polymicrobial biofilms were investigated using a model two-member consortium. *Escherichia coli* ATCC 33456 was transformed with vectors conferring either ampicillin or spectinomycin resistance, creating two distinct populations with different resistance mechanisms. Each strain alone or the consortium was grown as biofilms in flow cells and planktonically in chemostats. Comparisons in survival and activity were made on the basis of MICs and minimum biofilm preventative concentrations, a newly introduced descriptor. In ampicillin-containing medium, commensal interactions were evident during both modes of cultivation, but the sensitive strain experienced a greater benefit in the chemostat,

indicating that the biofilm environment limited the commensal interaction between the Amp^r and Spt^r strains. In spectinomycin-containing medium, growth of the sensitive strain in chemostats and biofilms was not aided by the resistant strain. However, green fluorescent protein expression by the sensitive strain was greater in mixed-population biofilms (9% ± 1%) than when the strain was grown alone (2% ± 0%). No comparable benefit was evident during growth in the chemostat, indicating that the biofilm structure contributed to enhanced activity of the sensitive strain.

2.2 MATERIALS AND METHODS

2.2.1 Bacterial strains and plasmids.

Two antibiotic-resistant populations of *E. coli* ATCC 33456 (Shen, 1993) were prepared. One population was transformed with the plasmid pEGFP (Clontech, Palo Alto, CA), a pUC19-based vector conferring ampicillin resistance by the *bla* gene and green fluorescent protein (GFP) production via the *egfp* gene under control of the constitutive P*lac* promoter. The second population was transformed with the vector pUCSpec, a pUC18-derived plasmid that confers spectinomycin resistance via the AAD(9) determinant (Husmann *et al.*, 1997). In this research, *E. coli* ATCC 33456 pEGFP is referred to as the "Amp^r" strain and is resistant to ampicillin and sensitive to spectinomycin. *E. coli* ATCC 33456pUCSpec is referred to as the "Spt^r" strain and is resistant to spectinomycin and sensitive to ampicillin. Inocula were prepared from clonal populations that were stored at -82°C. Prior to use in flow cell experiments, the Amp^r strain was grown overnight at 37°C on Luria-Bertani (LB) agar plates containing 400

ppm ampicillin, and the Spt^r strain was grown on LB agar plates containing 100 ppm spectinomycin. For chemostat experiments, inocula of the Amp^r or Spt^r strain were grown overnight in a shaking incubator at 37°C and 200 rpm in LB broth containing either 400 ppm ampicillin or 100 ppm spectinomycin, respectively.

2.2.2 Chemicals.

Ampicillin and spectinomycin were obtained from Sigma (St. Louis, MO). Antibiotics were dissolved in ultrapure water, sterilized with 0.20µm-pore filters to create stock solutions, and stored at -20°C. Nitrocefin was obtained from Calbiochem (San Diego, CA). SYTO 59 was purchased from Molecular Probes, Inc. (Eugene, OR).

2.2.3 Biofilm cultivation.

Biofilms were cultivated using parallel-plate flow cells according to a previously described technique (Gilbert & Keasling, 2004). Briefly, cells were inoculated into medium reservoirs containing 200 ml LB broth to an optical density at 600 nm (OD_{600}) of 0.03 (0.015 of each strain in mixed-population biofilms) and were recirculated through the flow cell at 0.84 ml min^{-1} for 2 h to allow surface colonization. Antibiotics were present during recirculation at the same concentrations that were used for continuous (steady-state) flow, described below. After recirculation, the system was switched to continuous flow for 46 h (medium flow rate of 0.35 ml min^{-1}), introducing LB broth with antibiotics as required to the flow cell. The selected medium flow rate replaced the volume of the flow cell approximately once per minute and was chosen such that the

antibiotic concentration in the bulk fluid approximated steady-state conditions. Biofilms were grown for 48 h in order to allow GFP fluorescence to develop and the biofilm structure to mature and also to permit the cultivation of a large number of biofilms. Each growth condition was repeated at least in triplicate. Biofilms were imaged by confocal laser scanning microscopy (CLSM) as described below. Following CLSM imaging, biofilm cells were displaced from flow cells by introducing air into the channels and were resuspended in 1 ml sterile 50 mM phosphate buffer (pH = 7.2) using a pipette. Visual inspection of flow cells by microscopy following biofilm displacement indicated that greater than 99 percent of the cells not directly adhered to the glass substratum were recovered.

2.2.4 Confocal laser scanning microscopy.

Prior to imaging, biofilms were rinsed with sterile 50 mM potassium phosphate buffer (pH = 7.2; no autofluorescence detected) for 10 min and then stained with 20 μM SYTO 59 for 15 min and subsequently rinsed with sterile 50 mM potassium phosphate buffer for another 10 min. Intact biofilms were imaged nondestructively using a Zeiss LSM 510 confocal laser scanning microscope (Zeiss, Thornwood, NY) equipped with a Fluor 40× oil immersion lens. Samples were excited simultaneously at wavelengths of 488 nm and 523 nm. Four image stacks of each biofilm were taken at different locations throughout the flow cell, using a 1-μm z-step increment.

2.2.5 COMSTAT analysis.

Quantitative analysis of CLSM images of biofilms was conducted using the digital image analysis program COMSTAT (Heydorn *et al.*, 2000). For COMSTAT analysis, the following settings were used: pixel intensity threshold of 30; minimum colony size of 100 pixels, representing a cluster of five cells.

2.2.6 Chemostat experiments.

Chemostats were made from 250-ml sidearm flasks. Flasks were sealed with a rubber stopper containing a 3.2-mm-inside-diameter Pharmed tube that extended to the bottom of the flask for influent media and another tube for the intake of air, which passed through a 0.20-μm-pore-size filter. Sterile LB broth with antibiotics as required was contained in 2-liter Pyrex bottles incubated in a 37°C water bath and pumped into the chemostat using a peristaltic pump (Cole Parmer) through autoclaved 3.2-mm-inside-diameter Pharmed tubing. The sidearm flask was located on a heated magnetic stir plate at a setting that maintained a temperature of 37°C ± 0.5°C. A magnetic stir bar kept the flask contents well mixed, and effluent flowed out of the sidearm into a sterile, hooded funnel leading to a waste vessel. Samples were collected by extending a sterile microcentrifuge tube held by flame-sterilized tweezers into the sterile hood to collect effluent. A Bunsen burner was stationed next to the chemostat to maintain aseptic conditions. At each time point, a sample was collected to measure turbidity and a second sample was collected, centrifuged, resuspended in 10% glycerol, and stored at -82°C for analysis by plate count. The cell densities of cultures that were stored frozen at -82°C

prior to dilution plate counting were 83% ± 6% of those of cultures that were not frozen prior to plating. Freezer storage did not alter the specific fluorescence of GFP-containing cells. Dilution rates were set to maintain the sensitive strain at 55 percent (Spt^r strain) or 60 percent (Amp^r strain) of its maximum growth rate in LB medium. With ampicillin in the medium, the pump flow was maintained at 4.5 ml min^{-1},corresponding to a complete reactor displacement every 64 min. With spectinomycin in the medium, the pump flow was maintained at 3.8 ml min^{-1}, corresponding to a complete reactor displacement every 76 min. The inoculum concentration of the resistant strain was always an OD_{600} of 0.40, corresponding to 2×10^8 CFU ml^{-1}. The inoculum concentration of the sensitive strain was always 0.04. Preliminary work with ampicillin-containing medium indicated that when the sensitive strain was inoculated at higher initial optical densities, the population size declined and stabilized at an OD_{600} of approximately 0.04. Chemostats were run in at least duplicate for each condition.

2.2.7 Determination of MIC and MBPC.

Antibiotic MIC determinations were performed as described by Jorgensen and Turnidge (Jorgensen & Turnidge, 2003). The concentration of antibiotic required to prevent the formation of biofilm by viable cells adhering to the flow cell substratum during the recirculation phase was designated the minimum biofilm preventative concentration (MBPC). MBPCs were determined by measuring the concentration at which biofilm biomass as calculated by COMSTAT equaled 0 μm^3 μm^{-2}, indicating that

only cells which adhered to the flow cell substratum during its inoculation were present. At the MBPC, the areal cell density was 3.5×10^3 CFU mm^2.

2.2.8 Nitrocefin assay.

The beta-lactamase potential of the Amp^r strain during growth in biofilms and chemostats was measured using the chromogenic substrate nitrocefin (O'Callaghan *et al.*, 1972). Briefly, Amp^r cells were resuspended in sterile 50 mM phosphate buffer, adjusted to an OD_{600} of 0.40, and incubated with 0.1 mM nitrocefin for 5 min at 37°C. Activity was measured by using a spectrophotometer (486 nm, as per the manufacturer's recommendation) at 0 and 5 min. All assays were carried out in at least triplicate, and statistical significance was determined using Student's *t* test.

2.2.9 Flow cytometry.

Flow cytometry was performed with a Becton-Dickinson FACSCalibur flow cytometer (BD Biosciences, San Jose, CA). Cells were washed and resuspended in sterile 50 mM phosphate buffer to an OD_{600} of 0.03 prior to analysis. Samples were excited at a wavelength of 488 nm with an argon laser, and 10,000 events were collected. Fluorescence was measured using logarithmic gain, and side scatter (SSC) was measured using linear gain. Six-micrometer-diameter beads (BD Biosciences, San Jose, CA) were used as size controls.

2.2.10 Plate counts.

Cells recovered from biofilms or chemostats were resuspended in sterile 50 mM phosphate buffer, serially diluted, and plated on LB agar plates supplemented with antibiotics as necessary. Plates were incubated overnight at 37°C. Biofilms resuspended to an OD_{600} of 1.0 corresponded to an average cell density of 7.7×10^8 CFU ml^{-1} (n = 8), whereas the average cell density of suspensions of chemostat cells with an OD600 of 1.0 corresponded to 6.4×10^8 CFU ml-^{1} (n = 10).

2.2.11 Growth kinetics.

Specific growth rates were determined from hourly measurements of optical densities (600 nm) during growth of each strain in LB broth in batch culture. Triplicate test tubes were inoculated to an initial OD_{600} of 0.03 from liquid cultures in mid-log-phase growth.

2.3 RESULTS

2.3.1 Growth kinetics.

The specific growth rates of the Spt^r and Amp^r strains growing exponentially in LB broth without antibiotics were 1.7 h^{-1} and 1.3 h^{-1}, respectively. The measured MIC for the Spt^r strain exposed to ampicillin was 16 ppm **(Figure 2.1A)**, and the measured MIC for the Amp^r strain exposed to spectinomycin was 30 ppm **(Figure 2.1B)**. These values were similar to MICs of 8 to 16 ppm reported elsewhere for ampicillin (Butler *et al.*, 1999; Lorian, 1996) and 12.5 to 50 ppm for spectinomycin (Kucers, 1979).

2.3.2 Phenotype stability.

In order to assess the stability of the relevant phenotypes, single-strain biofilms were grown for 48 h in the absence of antibiotic selective pressure. Biofilm-grown cells of the Amp^r strain were estimated by flow cytometry to be 97% ± 1% fluorescent. Biofilm-grown cells of the Spt^r strain were plated on LB agar with and without spectinomycin and were determined to be 103% ± 16% resistant to spectinomycin (n = 7).

2.3.3 Exchange of antibiotic resistance determinants in biofilms.

To check if antibiotic resistance determinants were exchanged between the Amp^r and Spt^r strains during growth in biofilms, cells from resuspended mixed-population biofilms were cultured on plates containing either ampicillin or spectinomycin. Eight biofilms cultivated in ampicillin-containing medium and eight biofilms cultivated in spectinomycin-containing medium were tested. Cells that grew were inoculated into LB broth containing twice the MIC of the reciprocal antibiotic. Out of 16 biofilms that were screened, only 1 spontaneous mutant, originally grown in ampicillin, was found to be resistant to both antibiotics.

2.3.4 Nitrocefin assay of beta-lactamase potential. The beta-lactamase potential of Amp^r cells grown in chemostats or 48-h biofilms were compared. Cells from chemostats showed a greater potential (P = 0.042) to cleave nitrocefin than biofilms cells (per 1×10^8 cells): 0.75 ± 0.17 ppm min^{-1} in the chemostat and 0.49 ± 0.08 ppm min^{-1} in biofilms.

2.3.5 Commensal protection in biofilms.

The MBPC for the Spt^r strain was 50 ppm ampicillin (Fig. 1A), and the MBPC for the Amp^r strain was 40 ppm spectinomycin (Fig. 1B). In the absence of ampicillin, the Spt^r strain developed robust biofilms with an overall spongiform morphology, with individual cells exhibiting the typical coccobacillus shape **(Figure 2.2A)**. The average thickness of these biofilms was 50 μm. Exposure to sublethal concentrations of ampicillin caused the formation of filamentous structures **(Figure 2.2B)**, and these biofilms had a maximum height of approximately 6 μm at ampicillin concentrations greater than 13 ppm. The Amp^r strain formed an extensive biofilm of fluorescent cells in the absence of antibiotics **(Figure 2.2D)**. Concentrations of spectinomycin greater than 20 ppm caused deformation of cells into filaments and a reduction in GFP expression **(Figure 2.2E, Figure 2.3)**. Amp^r biofilms were approximately 35 μm thick through 35 ppm spectinomycin but then decreased in size until the MBPC of 40 ppm was reached. The ability of the resistant strain to prevent morphological damage to the sensitive strain in mixed-population biofilms was considered. In the presence of 8 ppm ampicillin, no abnormally shaped Sptr cells were evident in mixed biofilms **(Figure 2.2C)**, in contrast to results with their growth alone. In the presence of 20 ppm spectinomycin, morphological damage was minimal in mixed biofilms **(Figure 2.2F)**. The sensitive-cell population size decreased substantially with increasing antibiotic concentration **(Figure 2.4)**; thus, comparisons were made at low antibiotic concentrations where the sensitive population was adequately represented.

In biofilms exposed to ampicillin, the growth of the Spt^r population was aided by growth with the Amp^r strain. By 33 ppm ampicillin, the number of viable Spt^r cells in single-strain biofilms was an order of magnitude lower than in mixed population biofilms, and no viable Spt^r cells were recovered following continuous exposure to ampicillin concentrations greater than 100 ppm **(Figure 2.4A)**. In contrast, populations of the Spt^r strain with cell densities greater than 10^3 CFU mL^{-1} were present in mixed-population biofilms exposed to 625 ppm ampicillin, 12.5 times greater than the Spt^r strain MBPC. In biofilms exposed to spectinomycin, there was no evidence of commensal protection based on Amp^r cell numbers **(Figure 2.4B)**. However, a higher percentage of Amp^r cells producing GFP were evident in mixed-population biofilms than in single-strain Amp^r biofilms **(Figure 2.5)**. Analysis by flow cytometry indicated a decrease in the size and brightness of the fluorescent subpopulation within single-strain Amp^r biofilms as a function of increasing spectinomycin concentration, with a substantial loss of fluorescence at spectinomycin concentrations greater than 33.3 ppm **(Figure 2.5; Figure 2.6, middle row)**. In contrast, the fluorescent Amp^r strain subpopulation in mixed-population biofilms stabilized at approximately 9% ± 1% of the total biofilm population by 33.3 ppm spectinomycin and was significantly larger than the fluorescent population in single-strain Amp^r biofilms (2% ± 0% fluorescent) for spectinomycin concentrations of 33.3 ppm and higher **(Figure 2.5; Figure 2.6, bottom row)**.

2.3.6 Commensal protection in chemostats.

The survival of the sensitive Spt^r strain was enhanced by the presence of the resistant Amp^r strain in the chemostat **(Figure 2.7A)**. In the absence of the Amp^r strain, the Spt^r strain was almost completely displaced from the chemostat in 64 min, corresponding to a single reactor volume replacement. In contrast, with the Amp^r strain present, the Spt^r strain population was approximately 3 orders of magnitude larger than the Spt^r strain population grown alone after 3 h, a period of time corresponding to more than two reactor volume replacements **(Figure 2.7A)**. The Spt^r strain survived in chemostats containing 625 ppm ampicillin, corresponding to 39 times the MIC. In mixed culture, the decline in the Spt^r population as a function of increasing ampicillin concentration was nearly 2 orders of magnitude greater in biofilms than in the chemostat **(Figure 2.8)**. There was no evidence of enhanced survival of the Amp^r strain in coculture with the Spt^r strain in spectinomycin-containing medium **(Figure 2.7B)**, nor was there any beneficial effect on GFP fluorescence (data not shown). Populations of the Amp^r strain declined steadily over a 3-h period to approximately 2 to 3% of their initial concentration. This behavior was observed in both 100 and 150 ppm spectinomycin, corresponding to 3.3 and 5 times the MIC, respectively.

2.4 DISCUSSION

In well-mixed planktonic cultures, cells that cannot coaggregate move past one another and do not establish interactions that have a spatial component. In contrast, in biofilms, cells are primarily fixed in space and must contend with intercellular

relationships in three dimensions. During growth in either ampicillin- or spectinomycin-containing medium, biofilm structure influenced the extent of commensal interactions between the consortium members. In ampicillin-containing medium, the biofilm environment reduced the commensal benefit to the Spt^r strain in two ways. First, the cells competed for space. In the biofilm setting, the Amp^r strain outcompeted the Spt^r strain by accumulating in the limited available space, whereas in the chemostat the size of the Amp^r population was restricted by washout, allowing a substantial population of the Spt^r strain to persist (due to its faster specific growth rate). The faster initial growth of the Amp^r strain in the biofilm also could have established a gradient of nutrients favoring its own growth (Kreft, 2004). Second, the beta-lactamase activity was greater in the chemostat than in the biofilm. The difference in average beta-lactamase activity most likely occurred because the population in the chemostat was in the exponential growth phase, whereas the biofilm contained a subpopulation of older, less-active cells. Thus, while these data support the observations of others that IP occurs in biofilms (Budhani, 1998), they demonstrate that the biofilm environment limited the commensal interaction between the Amp^r and Spt^r strains in the presence of ampicillin. In spectinomycin-containing medium, no protection was afforded to the sensitive Amp^r strain in the chemostat with respect to population size or GFP expression. Similarly, in terms of population size, the Amp^r strain received no benefit from the Spt^r strain in biofilms. However, a commensal interaction was evident in biofilms in terms of enhanced GFP expression in the Amp^r strain. The commensal interaction likely resulted from the development of microenvironments with reduced spectinomycin concentrations resulting

from the enzyme-catalyzed detoxification of spectinomycin by the Spt^r strain. The reduction in Amp^r cells with abnormal morphology in the commensal environment that was observed by CLSM also supports the concept of spectinomycin-reduced microenvironments within the mixed biofilm. Alternatively, the greater biomass that formed in the mixed biofilms may have also contributed to enhanced Amp^r strain resistance to spectinomycin.

Two methods-related aspects of this work warrant discussion. First, the concept of MBPC, the concentration of antibiotic required to prevent biofilm formation, was introduced. Existing parameters emphasize the concentration of chemical required to eliminate biofilms already attached to a surface. For example, the minimum biofilm eradication concentration measures the concentration of antibiotic required to kill an already-established biofilm (Ceri *et al.,* 1999), and the minimum biofilm inhibitory concentration measures the antibiotic concentration required to inhibit growth of individual cells shed from an established biofilm (Pickering *et al.,* 2003). In contrast, the MBPC describes the concentration of an agent required to keep a surface free of biofilm. Second, GFP fluorescence was used to characterize the quality of the biofilm environment for *E. coli* activity. GFP fluorescence requires low levels of oxygen (Hansen *et al.,* 2001; Tsien, 1998), is pH dependent (Patterson *et al.,* 1997), and may be inhibited when cells are challenged with antibiotics. Thus, a decrease in GFP fluorescence may indicate suboptimal conditions for an aerobic neutrophile like *E. coli*. Conversely, the persistence of localized GFP fluorescence under inhibitory conditions, as was detected in

mixed biofilms exposed to spectinomycin, indicated the presence of microenvironments with suitable conditions for Amp^r strain fluorescence.

The mechanism of antibiotic resistance substantially influenced the extent of the commensal interaction between the Amp^r and Spt^r strains. In the case of ampicillin, detoxification by the TEM-1 beta-lactamase produced by the Amp^r strain facilitated the growth of a significant population of sensitive bacteria. TEM-1 beta-lactamase has a high affinity for ampicillin (*Km* = 14 μM [~5 ppm]) (Livermore *et al.*, 1986) and hydrolyzes ampicillin without an energy input, leading to efficient antibiotic inactivation. In contrast, the inactivation of spectinomycin by the Spt^r strain provided a small benefit to spectinomycin-sensitive cells. The spectinomycin adenyltransferase AAD(9) determinant inactivates spectinomycin by adenylation at the 9-OH position in an ATP-consuming reaction (LeBlanc *et al.*, 1991), and the associated energy cost most likely inhibited extensive antibiotic detoxification. The potential for commensal interactions to cause IP in response to other antibiotics is largely uninvestigated to date. Antibiotics that are enzymatically degraded or modified could potentially be susceptible, including aminoglycosides, macrolides, chloramphenicol, and rifamycin (Wright, 2005). In the case of IP caused by beta-lactamase-producing bacteria, administration of amoxicillin and the beta-lactamase inhibitor clavulanic acid reduced the extent of treatment failure (Brook, 2002) and helped eliminate penicillin-sensitive pneumococci in a model biofilm (Budhani, 1998). Understanding the factors that give rise to IP in polymicrobial biofilms could facilitate narrow-spectrum antibiotic therapies and help reduce incidences of treatment failure.

TABLE 2.1 Survival of *E. coli* ATCC 33456 pUCSpec ($Spec^R$) in mixed culture exposed to ampicillin

Mode of cultivation	Maximum ampicillin concentration with commensal protection[a], ppm	Relative amount of commensal protection[b]	Percent $Spec^R$ in total population	
			Low ampicillin concentration (2 × MIC or MBPC)	High ampicillin concentration (10 × MIC or MBPC)
Biofilm	625	12.5	0.08 ± 0.07	0.002 ± 0.001
Chemostat[c]	>625[d]	39	17.7 ± 1.5	3.2 ± 2.2
Batch	32	2	0.002 ± 0.000	NG[e]

[a]For comparative purposes, commensal protection was defined as the survival of $>10^4$ CFU mL^{-1} of $Spec^R$

[b]Relative commensal protection was calculated using the following formula: the maximum antibiotic concentration with commensal protection was divided by either the MIC for batch- and chemostat-grown cells or the MBPC for biofilm-grown cells. See text for definitions.

[c]Concentration where $Spec^R$ density was stable at least one reactor volume following first reactor volume replacement

[d]625 ppm ampicillin was the highest tested concentration in the chemostat. The $Spec^R$ cell density was 5×10^5 CFU mL^{-1} at this concentration. See Figure 7A.

[e]NG = no growth

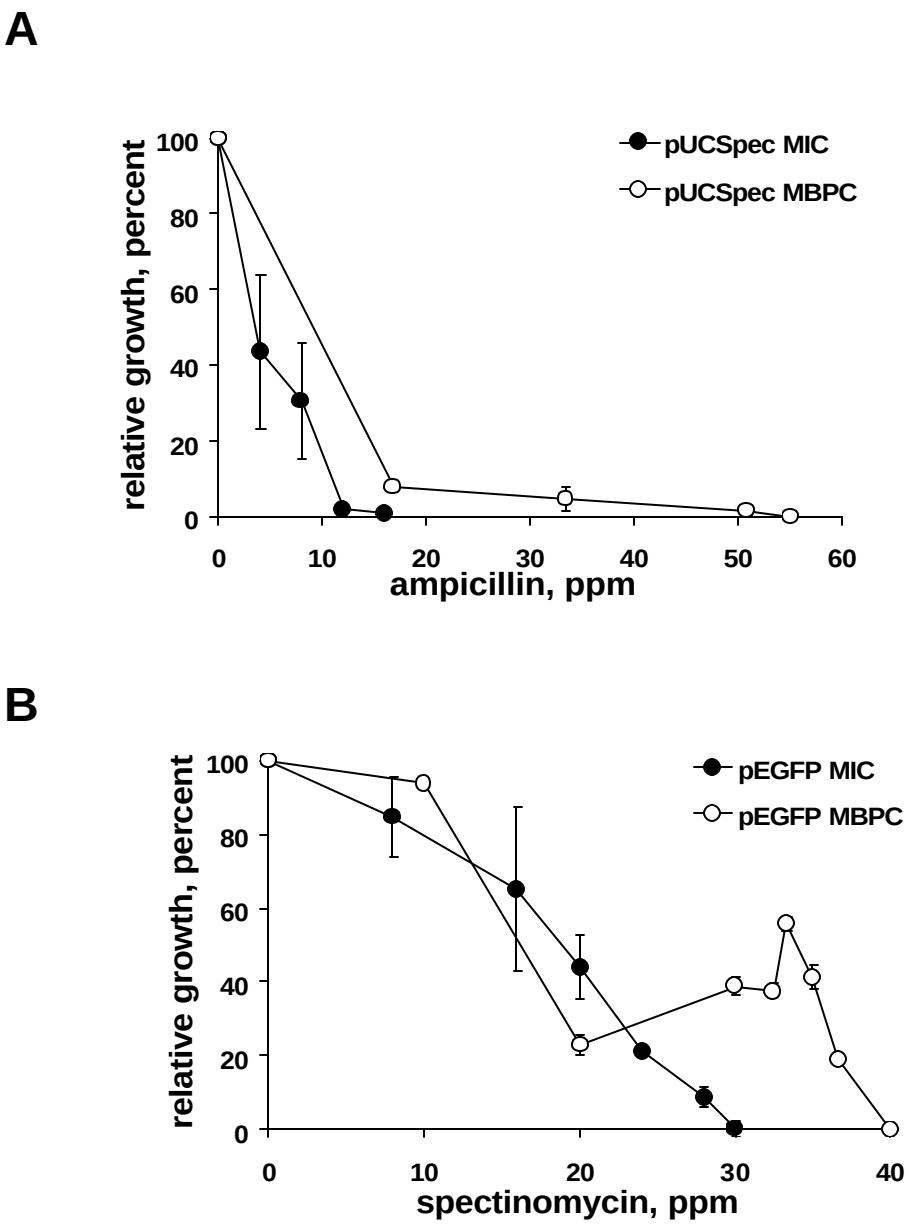

Figure 2.1. Antibiotic concentrations required to prevent planktonic or biofilm growth. MICs for each strain were determined in batch culture. The antibiotic concentration at which attached cells were unable to form a biofilm within 48 h was termed the minimum biofilm preventative concentration, MBPC. A: Spt^r in ampicillin-containing medium. B: Amp^r in spectinomycin-containing medium. Closed symbols, MIC. Open symbols, MBPC.

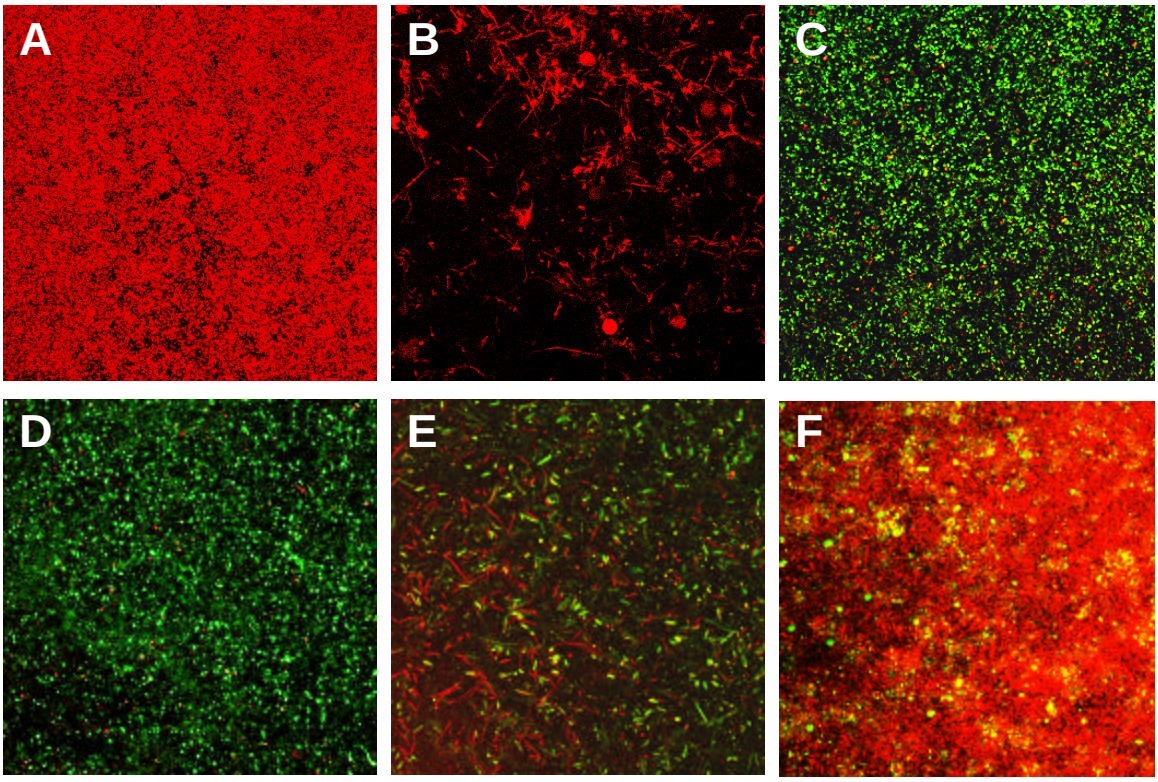

Figure 2.2. Prevention of morphological damage to antibiotic sensitive bacteria during growth with a resistant strain. Biofilms of each strain alone or the two strains grown together were imaged by CLSM. Representative images of the substratum are shown. A: Spt^r in LB broth. B: Spt^r in LB broth + 8 ppm ampicillin. C: Amp^r and Spt^r in LB broth + 8 ppm ampicillin. D: Amp^r in LB broth. E: Amp^r in LB broth + 20 ppm spectinomycin. F: Amp^r and Spt^r in LB broth + 20 ppm spectinomycin. Magnification: 400X.

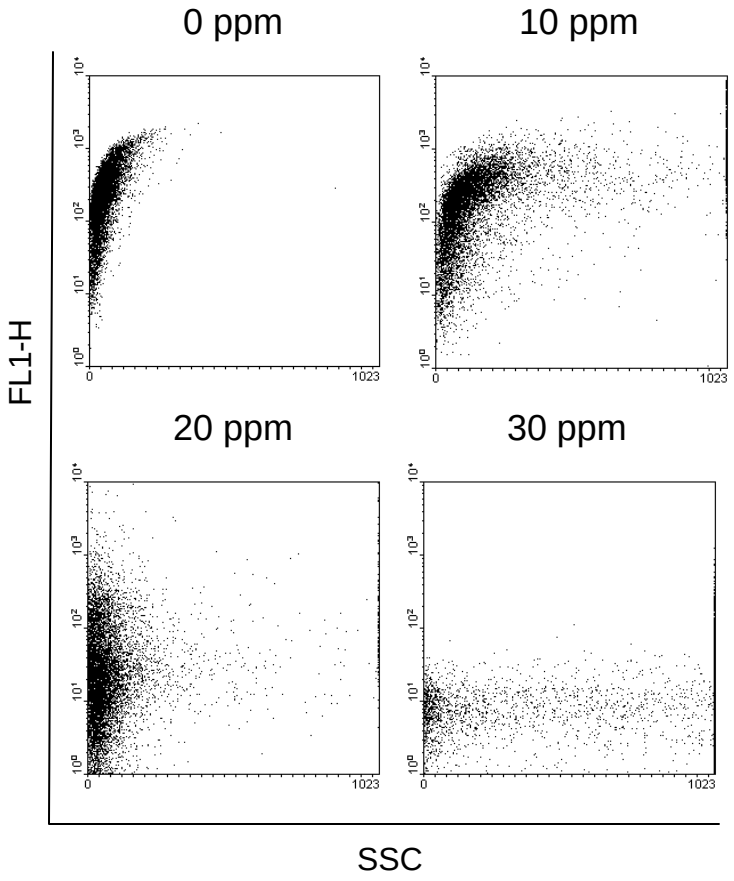

Figure 2.3. Flow cytometry scatter plots of Amp^r biofilms grown in spectinomycin-containing media. Representative flow cytometry scatter plots showing the distribution of fluorescent events in Amp^r biofilms grown alone in media containing subinhibitory concentrations of spectinomycin. X-axis: Side scatter (SSC). Y-axis: GFP fluorescence (FL1-H).

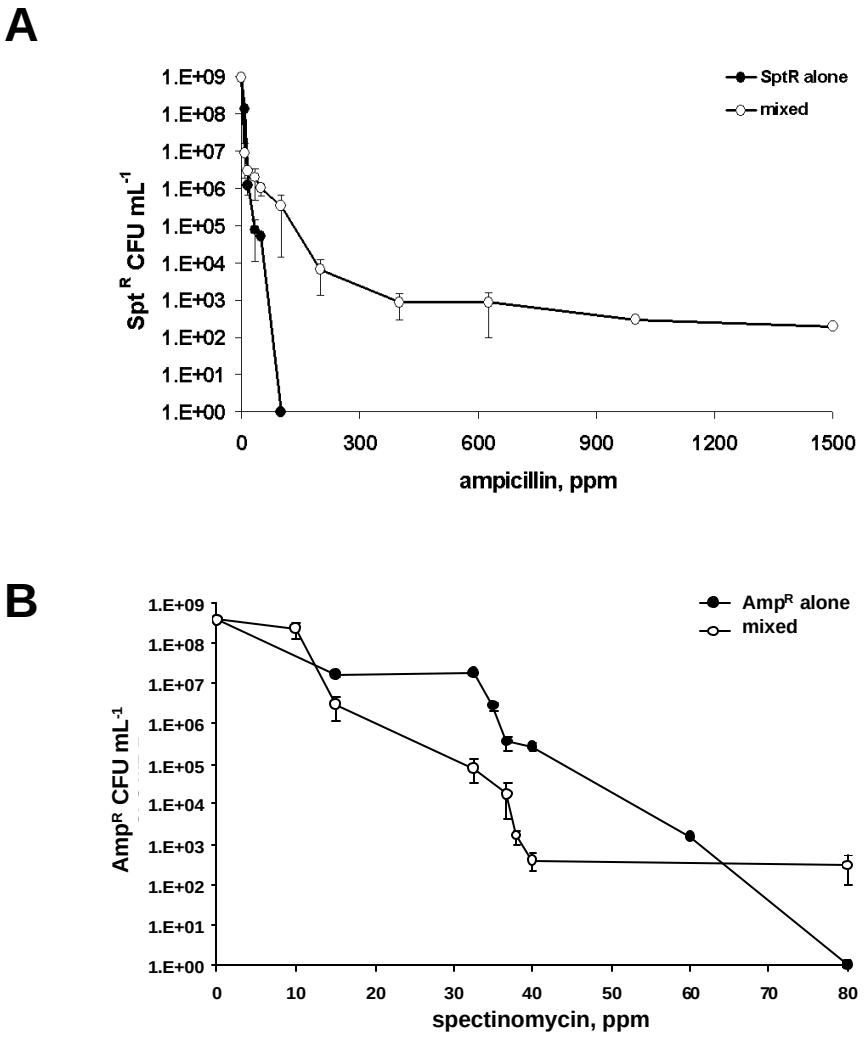

Figure 2.4. Commensal protection in biofilms. Antibiotic sensitive organisms grown in biofilms either alone (closed symbols) or with the resistant strain (open symbols) were enumerated by plate counts. A: Spt^r in ampicillin-containing medium. B: Amp^r in spectinomycin-containing medium.

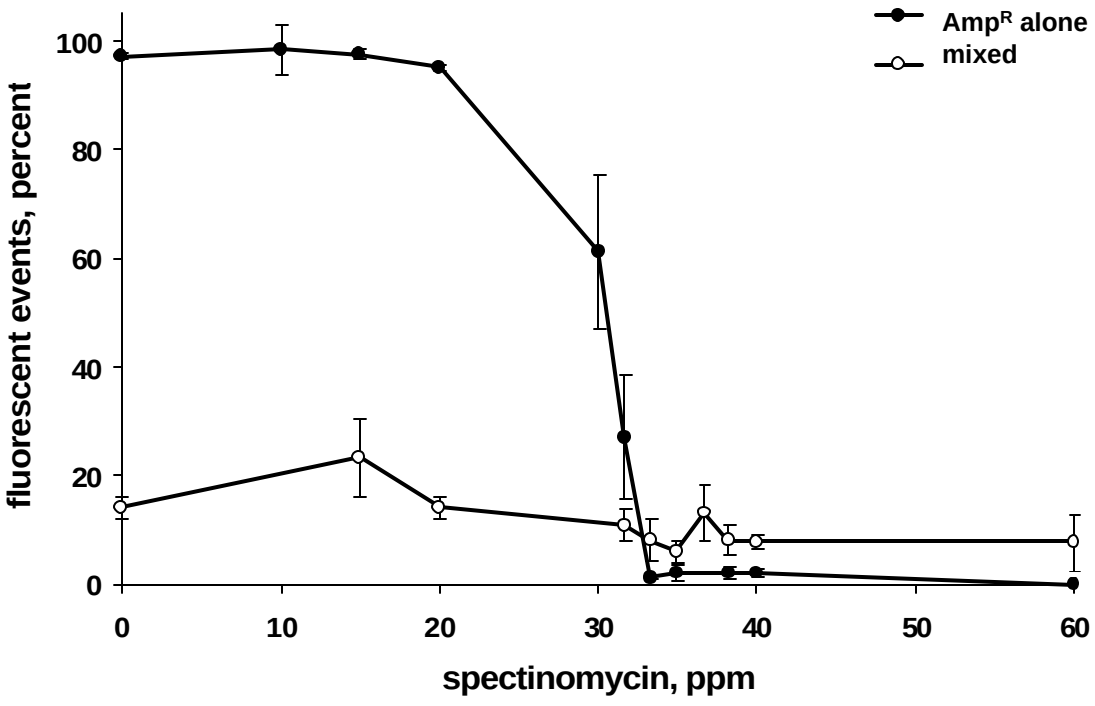

Figure 2.5. Flow cytometry analyses of Amp^r populations grown alone or together with Spt^r in spectinomycin-containing medium. Amp^r grown alone, (closed circles). Amp^r and Spt^r grown together, (open circles).

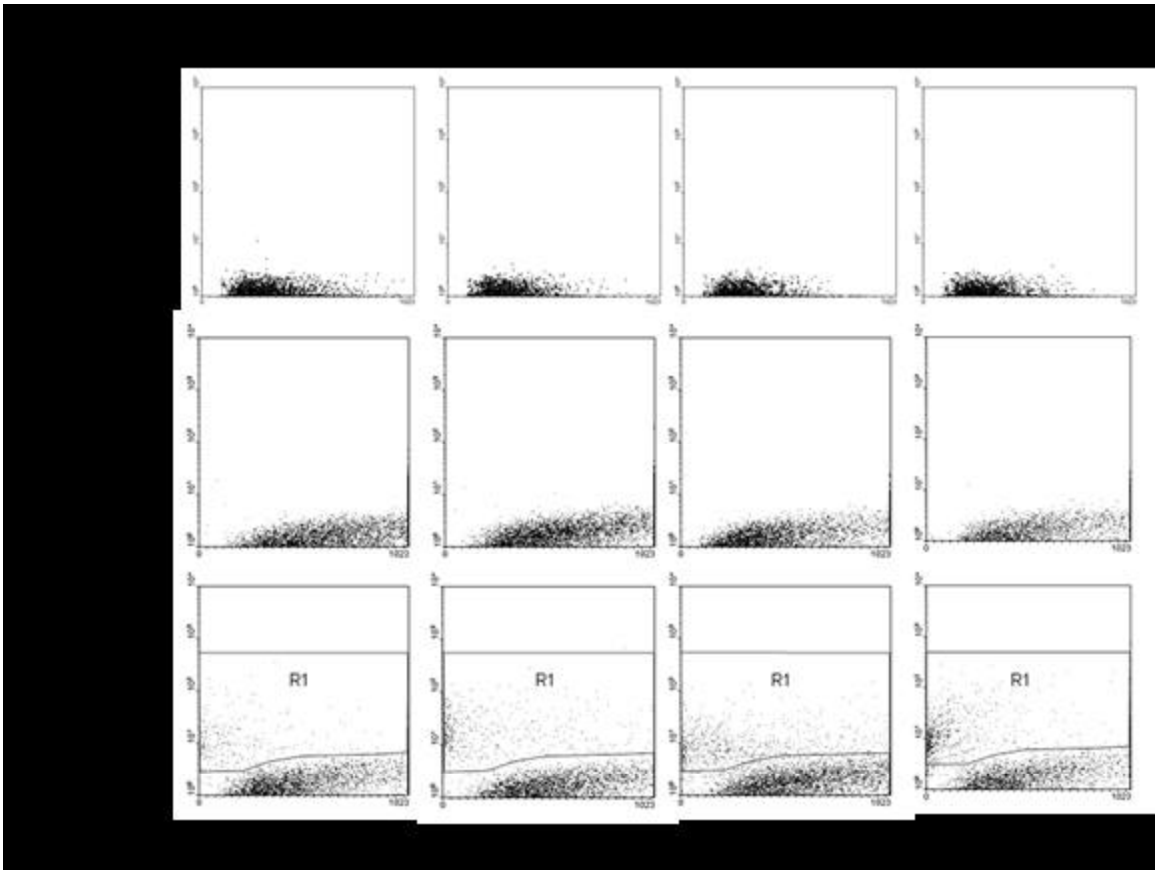

Figure 2.6. Representative scatter plots of biofilms grown in media containing 33.3 to 40 ppm spectinomycin. Top row: Spt^r alone. Middle row: Amp^r alone. Bottom row: mixed biofilms, with fluorescent populations indicated by the R1 region. X-axis: Side scatter (SSC). Y-axis: GFP fluorescence (FL1-H).

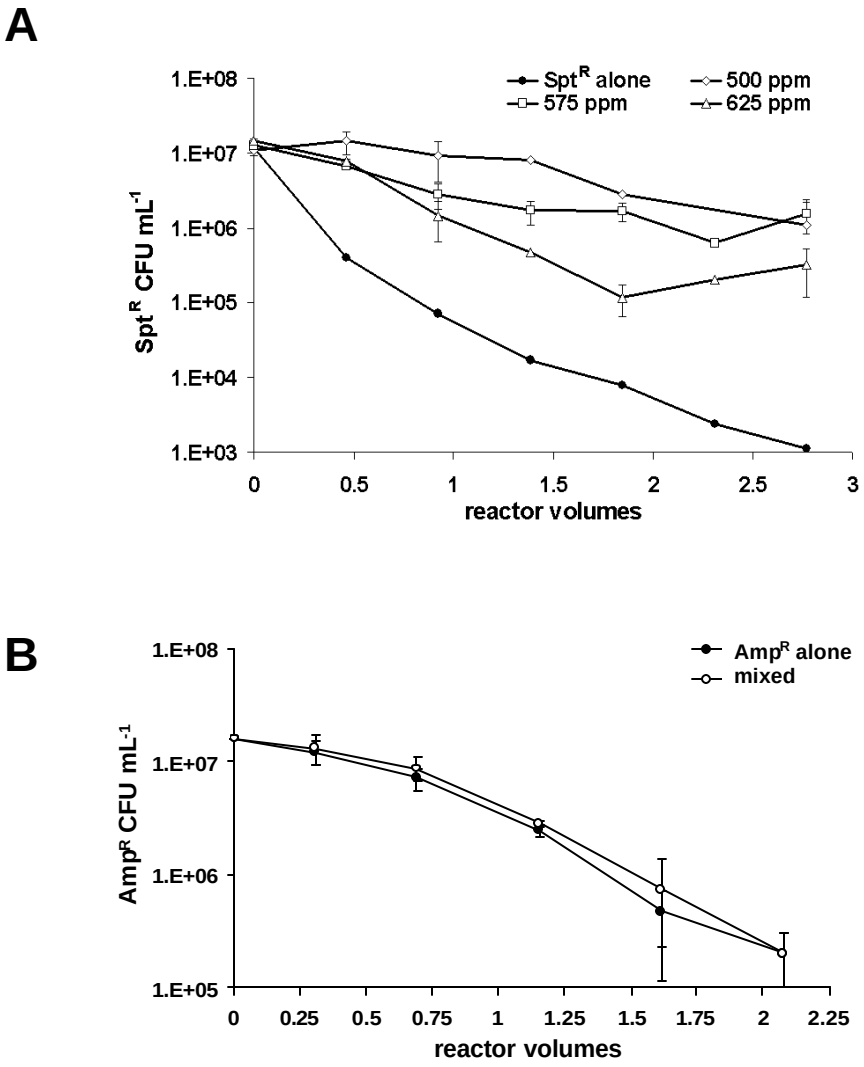

Figure 2.7. Commensal protection in chemostats. Antibiotic sensitive organisms grown in chemostats either alone (closed symbols) or with the resistant strain (open symbols) were enumerated by plate counts. A: Spt^r in ampicillin-containing medium. B: Amp^r in spectinomycin-containing medium.

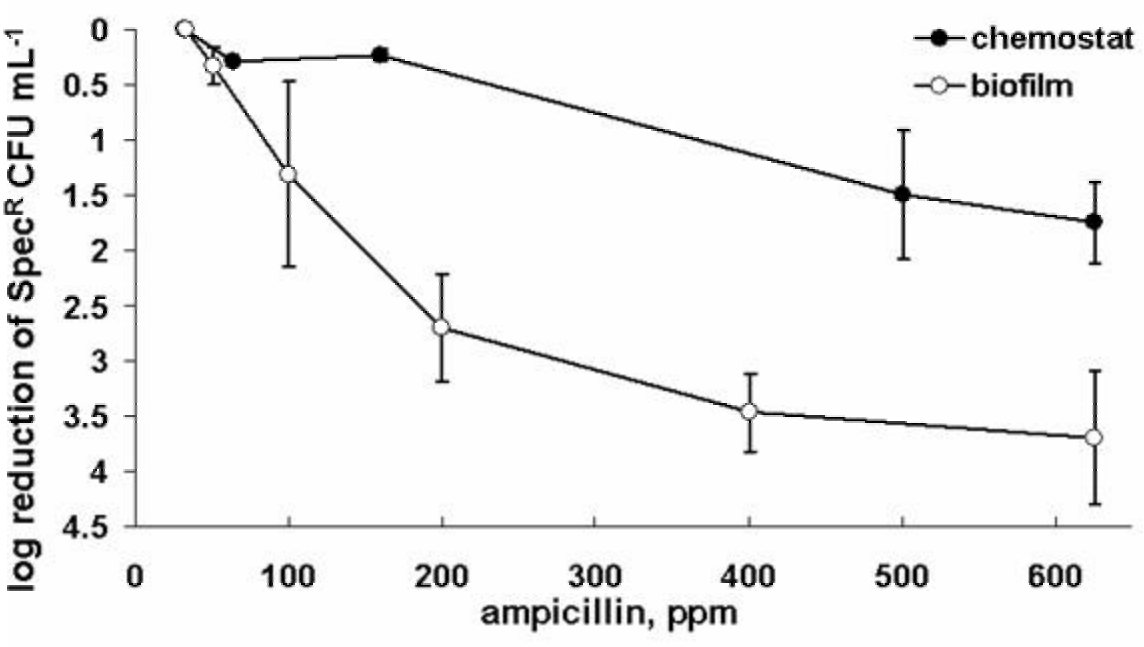

Figure 2.8. Commensal protection in batch culture. Antibiotic sensitive organisms grown in batch culture either alone (closed symbols) or with the resistant strain (open symbols) were enumerated by plate counts after 5 h of growth. A: Spt^r in ampicillin-containing medium. B: Amp^r in spectinomycin-containing medium.

CHAPTER 3
COMMUNITY-DEPENDENT MULTIPLE ANTIBIOTIC RESISTANCE IN A POLYMICROBIAL BIOFILM

3.1 INTRODUCTION

Multidrug resistant bacteria have been widely recognized for increasing the severity and frequency of nosocomial infections (Karlowsky *et al.,* 2006; Naiemi *et al.,* 2005, Obritsch *et al.,* 2004). Recently, antibiotic treatment regimens involving two or more antibiotics, referred to as combination therapies, have been employed for treatment of polymicrobial infections (LaPlante *et al.,* 2006; Lin *et al.,* 2006; Matthaiou *et al.,* 2006) and antibiotic resistant strains (Rahal, 2006; Sader & Jones, 2005). The use of novel antibiotic combinations and antibiotic cycling may prolong the effectiveness of antibiotic therapies (Kollef, 2006; Rossolini & Mantengoli, 2005). Alternatively, combination therapies could create conditions that select for novel types of antibiotic resistance. We hypothesized that two populations of microorganisms, each with a different antibiotic resistance, could cooperate to resist the effects of two simultaneously administered antibiotics selected to target each population. This kind of mutualistic interaction would constitute a community-dependent mode of multiple antibiotic resistance (CMAR).

To investigate the possibility of mutualistic interactions facilitating multiple antibiotic resistance, a two-member model consortium based on *Escherichia coli* ATCC 33456 was used. The two-member model was used previously to analyze commensal interactions that enhanced antibiotic resistance, an interaction known as indirect pathogenicity (O'Connell *et al.,* 2006). The model was comprised of one strain harboring

a plasmid encoding beta-lactamase and thus resistant to ampicillin, and a second strain with a plasmid carrying spectinomycin adenyltransferase, enabling resistance to spectinomycin. Ampicillin and spectinomycin were selected for use in the model because of (a) the sensitivity of *E. coli* ATCC 33456 to both in the absence of a heterologous resistance gene, and (b) the ability of these antibiotics to be permanently inactivated by the encoded resistance genes. Both plasmids belonged to the same incompatibility group, preventing their exchange between the two populations. Additionally, the ampicillin resistant strain expressed green fluorescent protein, allowing it to be distinguished from the other strain following counterstaining with a red dye.

Many nosocomial infections involve microbial biofilms, or communities of microorganisms attached to surfaces (Manago *et al.*, 2006; Amaral *et al.*, 2005; Braxton *et al.*, 2005; O'Donnell *et al.*, 2005). We hypothesized that biofilms would be likely environments to observe CMAR development because the fixed positions of cells within the biofilm would potentially foster mutually beneficial antibiotic detoxification. To determine whether biofilm structure contributed to the development of mutualistic interactions, the two-member consortium was grown in the presence of steady state antibiotic concentrations in flow cells (sessile growth) or chemostats (planktonic growth). The occurrence of any mutualistic interactions was identified by comparing the growth of each consortium member alone with its growth in the mixed population. By considering the two types of cultivation, it was possible to determine whether the biofilm environment contributed to multiple antibiotic resistance by the mixed population.

3.2. MATERIALS AND METHODS

3.2.1. Bacterial strains and plasmids.

Two populations of *E. coli* ATCC 33456 were transformed with pUC family vectors bearing antibiotic resistance determinants. The first population contained the plasmid pEGFP (Clontech, Palo Alto, CA), which encodes ampicillin resistance and a red-shifted green fluorescent protein (GFP). *E. coli* ATCC 33456 pEGFP is designated as "Amp^R. The second population was transformed with the plasmid pUCSpec, which confers spectinomycin resistance via the AAD(9) determinant (Husmann *et al.,* 1997). *E. coli* ATCC 33456 pUCSpec is referred to as "$Spec^R$". For biofilm experiments, Amp^R was grown overnight at 37°C on Luria-Bertani (LB) agar plates containing 400 ppm ampicillin, and $Spec^R$ was grown on LB agar plates containing 100 ppm spectinomycin. For chemostat experiments, Amp^R or $Spec^R$ were grown overnight in a shaking incubator at 37°C and 200 rpm in LB broth containing either 400 ppm ampicillin or 100 ppm spectinomycin, respectively.

Several controls were performed to ensure plasmid stability, and are elaborated upon in O'Connell et al. (2006). The specific growth rates of $Spec^R$ and Amp^R growing exponentially in LB broth without antibiotics were 1.7 hr^{-1} and 1.3 hr^{-1} respectively. The Amp^R and $Spec^R$ phenotypes were stable over a period of 48 h with no antibiotic selective pressure when grown in biofilms, and no exchange of antibiotic determinants when Amp^R and $Spec^R$ were cocultured in biofilms was detected.

3.2.2. Antibiotics.

Ampicillin and spectinomycin were purchased from Sigma (St. Louis, MO). Stock solutions were created by dissolving the antibiotic powder in double deionized water, and passed through 0.20 μm pore filters for sterilization, and stored at -20°C.

3.2.3. Biofilm cultivation.

Biofilms were grown in flow cells according to a previously described technique (Gilbert & Keasling, 2004). Briefly, cells were inoculated into media reservoirs containing 200 mL LB broth to the desired OD_{600} and were recirculated through the flow cell at 0.84 mL min^{-1} for 2 hours to allow surface attachment. For experiments involving antibiotics, 80 ppm spectinomycin and 100 ppm ampicillin were present for both recirculation and continuous (steady state) flow. At 2 h, initial attachment studies were imaged by confocal laser scanning microscope, as described below. For biofilm growth studies, the system was then switched to continuous flow for 46 h, maintaining steady state concentrations by replacing the flow cell volume at a rate of approximately one volume per minute (media flow rate of 0.35 mL min^{-1}). Each growth condition was repeated at least in triplicate. Following CLSM imaging, biofilm cells were displaced from flow cells by introducing air into the channels and were resuspended in sterile 50 mM phosphate buffer (pH = 7.2) using a pipette for plate counting.

3.2.4. Confocal laser scanning microscopy.

Sterile 50 mM potassium phosphate buffer (pH = 7.2) was used to rinse biofilms for 5 min. Subsquently, biofilms were stained with 20 μM SYTO 59 (Molecular Probes, Eugene, OR) for 15 min, and rinsed a second time with sterile 50 mM potassium phosphate buffer for 5 min. A Zeiss LSM 510 confocal laser scanning microscope (Zeiss, Thornwood, NY) was used to image the flow cells without disrupting the biofilm structures. Imaging took place with dual excitation at wavelengths of 488 nm and 523 nm, using a Fluor 40X oil immersion lens. Four image stacks of each biofilm were taken at the middle of the flow cell's length, using a 1 μm vertical step increment.

3.2.5. Biofilm Image Segmentation Software analysis.

Biofilm Image Segmentation Software (BISS) was developed in conjuction with the Department of Computer Sciences, Georgia State University (Belkasim *et al.*, 2004). Briefly, each image was segmented into discrete red, green, or black pixels. By selecting how many Amp^R (green) and $Spec^R$ (red) cells are in a group, and the radius in pixels to search, users can calculate the number of cells of each strain attached to the glass, the distance between individual attached Amp^R and $Spec^R$ cells, and the number of Amp^R and $Spec^R$ interactions in each 2 hour CLSM image.

3.2.6. COMSTAT analysis.

CLSM images of biofilms were analyzed quantitatively using the digital image analysis program COMSTAT (Heydorn *et al.*, 2000) with a user-defined pixel intensity threshold of 30.

3.2.7. Chemostat experiments.

Chemostats were made from 250 mL sidearm flasks sealed with a rubber stopper. Two 3.2 mm i.d. Pharmed tubes extended to the bottom of the flask, one for influent media, and another for the intake of air, which passed through a 0.20 μm pore size filter. Sterile media were contained in 2 L Pyrex bottles, and were pumped into the chemostat using a peristaltic pump (Cole Parmer, USA) through autoclaved 3.2 mm i.d. Pharmed tubing. A magnetic stir bar kept the flask contents well mixed, and effluent flowed out of the sidearm into a sterile, hooded funnel leading to a waste vessel. The entire setup fit into an incubator that was maintained at a temperature of 37°C ± 0.5°C. At each time point, a sample was collected to measure turbidity and a second sample was collected, centrifuged, resuspended in 10% glycerol and stored at -80°C for analysis by plate count. Dilution rates were set to maintain the sensitive strain at 55 percent ($Spec^R$) or 60 percent (Amp^R) of its maximum growth rate in LB medium. The pump flow was maintained at 3.8 mL min^{-1}, corresponding to a complete reactor displacement every 76 minutes. The total inoculum concentration of the cells was either OD_{600} = 0.50, corresponding to 3×10^8 CFU mL^{-1}, or OD_{600} = 0.05, corresponding to 3×10^7 CFU mL^{-1}. Chemostats were run in at least duplicate for each condition.

3.2.8. Plate counts.

Cells recovered from biofilms or chemostats were resuspended in sterile 50 mM phosphate buffer, serially diluted, and plated on LB agar plates containing either 400 ppm ampicillin or 100 ppm spectinomycin. Plates were incubated overnight at 37°C.

3.3. RESULTS

We hypothesized that it was possible to affect the number and proportions of Amp^R and $Spec^R$ cells colonizing the substratum by manipulating their concentrations in the liquid medium during the recirculation phase (e.g. the first two hours of the experiment). First we investigated the ability of each strain alone to attach to the flow cell substratum. Confocal microscopy determined that there was an increase in cells attached to the substratum as a function of the cell density during recirculation **(Figures 3.1, 3.2)**. We also found that $Spec^R$ adhered twice as effectively as Amp^R. Next we considered whether synergism or antagonism between the two strains might alter their abilities to attach to the flow cell surface when these two strains were recirculated concurrently. We found that $Spec^R$ adhered to the flow cell substratum nearly three times more efficiently in the presence of Amp^R relative to its growth alone **(Figures 3.1, 3.2)**. On the other hand, $Spec^R$ did not affect the adhesion of Amp^R relative to its growth alone. Thus, in order to establish populations of cells attached to the substratum with specific ratios of cell types, inoculum conditions were worked out empirically **(Table 3.1)**. BISS analysis of the number of pairs formed by cocultures correlated with increasing inoculum density. When a maximum distance of 5 pixels (2 μm) was used, an OD_{600} of 0.01 yielded 1.4 ±

0.9 pairs, 0.03 yielded 5.0 ± 1.3 pairs, and 0.06 yielded 11.7 ± 2.3 pairs. Increasing the maximum distance to 10 pixels (4 μm) resulted in 5.3 ± 1.7 pairs for OD_{600} of 0.01, 33.8 ± 4.8 pairs for OD_{600} of 0.03, and 43.6 ± 5.2 pairs for OD_{600} of 0.06. The basis of the beneficial interaction between $Spec^R$ and Amp^R leading to enhanced surface adhesion by $Spec^R$ is presently unknown.

To determine whether areal cell density was an important factor for the initiation of biofilm development in the presence of two antibiotics, we compared biofilm development at the 10 $Spec^R$: 1 Amp^R attachment ratio using OD_{600} values ranging from 0.01 to 0.06. In no case could either of the two strains form a biofilm if they were inoculated into the flow cell alone **(Figure 3.3A)**. Quantitative digital image analysis of coculture biofilm structure visualized by CLSM revealed that in the presence of both antibiotics, at areal cell densities greater than 150 cells per field (0.053 mm^2; 2000 – 3000 cells per mm^2), microcolonies were consistently observed and confluent biofilm began to form **(Figure 3.3B)**. In contrast, at areal cell densities of 40 cells per 0.053 mm^2 (800 cells per mm^2) or less, few microcolonies developed and no confluent biofilm was observed.

We hypothesized that the greater biofilm formation in flow cells with initial areal cell densities greater than 150 cells per field occurred because Amp^R and $Spec^R$ cells attached to the substratum after the recirculation phase were more likely to be in close spatial proximity to one another, due to the greater number of attached cells, in comparison to flow cells with initial areal cell densities less than 40 cells per field. To test this hypothesis, we used the biofilm image analysis program BISS to measure the

average intercellular distance between Amp^R and $Spec^R$ cells attached to the substratum after 2 h for the three tested initial cell densities. At least eight fields, representing two or more replicates, were tested by selecting an area containing a single Amp^R cell (green cell) and the six closest surrounding $Spec^R$ cells (red cells). The average distance between a green cell and its surrounding red cells decreased with increasing inoculation density. An OD_{600} of 0.01 resulted in an average green to red intercellular distance to be 18.4 ± 7.9 microns, OD_{600} 0.03 yielding 15.3 ± 5.6 microns, and OD_{600} of 0.06 resulting in 9.8 ± 3.9 microns.

To evaluate whether the greater biofilm formation in flow cells with initial areal cell densities greater than 150 cells per field occurred simply because more Amp^R and $Spec^R$ cells were attached to the substratum after the recirculation phase compared to flow cells initially seeded with 40 cells per field, we examined biofilms cultivated in antibiotic-free LB medium under identical conditions to those used for cultivation of biofilms in the presence of both ampicillin and spectinomycin. We found that during growth in antibiotic-free media, biofilm formation was independent of initial areal cell density ($p = 0.454$) **(Table 3.2)**, in contrast to the behavior of the model polymicrobial biofilm in the presence of antibiotics ($p = 0.004$).

To determine whether the ratio of microorganisms was important for the initiation of biofilm development in the presence of two antibiotics, we compared biofilm development under conditions where the initial areal cell density was constant, but the ratio of resistant to sensitive organisms varied. In the presence of both antibiotics, it was essential that there be more $Spec^R$ cells than Amp^R cells at the substratum in order for

biofilm development to occur **(Figure 3.3C)**. Amp^R growth in coculture was similar to Amp^R growth alone in terms of biomass ($p = 0.462$) and substratum coverage ($p = 0.667$) **(Table 3.3)**. The 5 $Spec^R$ to 1 Amp^R ratio benefited Amp^R in terms of maximum height ($p = 0.002$) and the number of green colonies growing above the substratum, indicating that Amp^R growth occurred after the initial cell attachment phase. During growth in antibiotic-free media, the increasing ratio of $Spec^R$ to Amp^R cells correlated with larger $Spec^R$ maximum height ($p = 0.00008$), Amp^R maximum height ($p = 0.0324$), and Amp^R substratum coverage ($p = 0.002$). For both organisms, growth alone in LB yielded values greater than or similar to the largest values from coculture.

To determine whether the biofilm environment was important for the growth of the co-culture in the presence of two antibiotics, we compared growth of the two strains in chemostats (planktonic growth) with growth in flow cells (biofilm growth). In the presence of two antibiotics, and at a ratio of 1:1, the two strains could not establish a stable relationship at cell densities ranging from 2.1×10^7 CFU mL^{-1} ($OD_{600} = .03$) to 3.5×10^7 CFU mL^{-1} ($OD_{600} = 0.50$). For chemostats inoculated at an OD_{600} of 0.5, $Spec^R$ populations declined less than 3 orders of magnitude in coculture for all tested inoculation ratios **(Figure 3.4A).** Only the 5 $Spec^R$ to 1 Amp^R ratio resulted in a less than 3 log reduction in Amp^R populations **(Figure 3.4B).** At lower inoculation densities, both Amp^R and $Spec^R$ populations declined 3.5 orders of magnitude over the course of the experiment.

3.4. DISCUSSION

In this research, two strains were able to attach to a surface and produce biofilms, despite simultaneous exposure to two antibiotics at concentrations twice that which prevented the growth of the sensitive strains alone in a single antibiotic. All events that contributed to this survival had to be established in the first two hours, because the biofilms were treated identically after that point. Also, neither strain alone was able to grow in the presence of both antibiotics. This result indicates that an interaction between the strains was necessary to foster biofilm development.

An essential feature for establishing the growth of the biofilm is the number of cells attached to the substratum in the first two hours. At low initial cell density, only a small number of microcolonies were detected at 48 hours. This is most likely because the two strains did not attach within a suitable proximity to one another to detoxify the antibiotics for one another. Simultaneous detoxification of both antibiotics by both organisms was a requirement for biofilm development. Thus, it is reasonable to assume that the two strains must be in some physical proximity to one another on the substratum at the beginning of the experiment in order for this to happen. Several pieces of data support this concept. First, the amount of biofilm that formed was greater when more cells were attached to the substratum. Second, analysis by BISS determined that the average intercellular distance was smaller at high cell density, and there were correspondingly more pairs within the user defined intercellular distances of 5 and 10 pixels. At this time, the greatest possible physical intercellular distance that can result in mutual detoxification is unknown. Enumeration of other groupings (e.g. two of one

strain and one of another) at different intercellular distances showed a similar trend relative to the number of cells attached to the substratum. An alternative hypothesis that the amount of biofilm formed by 48 h could simply be a function of the total number of cells attached to the substratum at 2 h was rejected because in the absence of antibiotics the amount of biofilm that formed was similar under all tested conditions **(Table 3.3)**.

Cell number alone was not sufficient to explain the observed growth; the ratio of the two strains influenced whether biofilm formed. A ratio of 5:1 $Spec^R$ to Amp^R was superior to the other tested ratios. This result was consistent with previously observed behavior where the antibiotic detoxification activity of $Spec^R$ was significantly less than that of Amp^R, most likely because of the difference in the energetics of the two detoxification mechanisms (O'Connell *et al.*, 2006). The importance of cell ratio was underscored by work with the chemostat, which also showed that a ratio of 5:1 could enhance the growth of the co-culture, even in planktonic culture, compared to other ratios of strains. However, while this work showed that biofilm structure was not essential for the survival and establishment of the co-culture, a comparison of growth in biofilms versus chemostat showed that orders of magnitude fewer cells were required to establish a successfully growing co-culture in flow cells. This result demonstrates that an important function of surfaces in the formation of polymicrobial biofilms is to nucleate the interacting populations, which can subsequently self-propogate.

The significance of this work is that a single cell resistant to one antibiotic could hypothetically attach to a surface colonized by a different species resistant to another antibiotic and establish a multiple antibiotic resistant infection. This could be significant

in terms of treatment failure of combination therapies. Early attachment can cause decreases in cell susceptibility to biocide concentrations greater than the minimum inhibitory concentration, or MIC (Das *et al.*, 1998). From a bacterial perspective, this now sublethal concentration could allow time for the induction of resistance phenotypes such as the multiresistance operon *mar* (Maira-Litran *et al.*, 2000; Gilbert *et al.*, 2002). We propose that in infections treated by multiple antibiotics, the attachment of reciprocally resistant organisms can reduce of antibiotic concentrations enough to create a similar window of opportunity.

A requirement for the CMAR biofilm to become established is that both strains must inactivate their respective antibiotics enzymatically, such that the partner strain can experience a benefit. Antibiotics in common use as combination therapies, such as beta-lactams and aminoglycosides, are inactivated by resistance mechanisms that are commonly found (Aslangul *et al.*, 2006; Jana & Deb 2006; Ramphal & Ambrose 2006; Brook, 2004); thus, the proposed model does not have extreme requirements. Many commons surfaces on the body are coated with a coating of cells, e.g. the ear, the GI tract. In these environments, if the surface is colonized by a strain resistant to one antibiotic, in principle a cell of a second strain resistant to a different antibiotic could join the established biofilm and form a CMAR biofilm infection. At present, whether this type of mutualistic interaction forms in the clinic contributing to nosocomial infections is unknown. However, because it can easily be demonstrated in the laboratory suggests that it is plausible.

TABLE 3.1. BISS-directed inoculum engineering to obtain specific attachment ratios

Desired cell attachment ratio	$Spec^R$ OD or volume	Amp^R OD or volume	Required liquid ratio
10 $Spec^R$: 1 Amp^R	0.015[a]	0.015	1 $Spec^R$: 1 Amp^R
5 $Spec^R$: 1 Amp^R	0.006	0.024	1 $Spec^R$: 4 Amp^R
1 $Spec^R$: 1 Amp^R	0.003	0.027	1 $Spec^R$: 9 Amp^R
1 $Spec^R$: 5 Amp^R	25 μL of 1/10[b] dilution of 0.10 OD_{600}	0.04	1 $Spec^R$: 800 Amp^R

[a] OD_{600} of 200 mL used in recirculation phase of biofilm growth
[b] volume added to 200 mL used in recirculation phase of biofilm growth

TABLE 3.2. $Spec^R$ and Amp^R cell behavior alone and in coculture based on cell numbers attached to the substratum

Cell number at substratum	biomass, $\mu m^3/\mu m^2$		maximum height, μm		percent substratum coverage	
	AB	LB	AB	LB	AB	LB
$Spec^R$ alone[a]	0.0002 ± 0.0001	5.74 ± 0.66	2 ± 1	32 ± 2	0.02 ± 0.01	84 ± 3
$Spec^R$ in 40 cells mixed	0.15 ± 0.12	1.91 ± 1.57	13 ± 3	30 ± 10	2 ± 1	38 ± 15
$Spec^R$ in 150 cells mixed	0.38 ± 0.15	2.20 ± 1.38	15 ± 4	30 ± 4	4 ± 3	40 ± 5
$Spec^R$ in 400 cells mixed	0.36 ± 0.36	6.78 ± 3.40	23 ± 6	26 ± 7	6 ± 4	71 ± 7
Amp^R alone[a]	0.014 ± 0.002	1.22 ± 0.88	6 ± 1	22 ± 4	0.4 ± 0.0	19 ± 10
Amp^R in 40 cells mixed	0.02 ± 0.02	0.60 ± 0.50	4 ± 3	22 ± 9	0.5 ± 0.41	21 ± 10
Amp^R in 150 cells mixed	0.01 ± 0.01	0.21 ± 0.20	7 ± 2	25 ± 4	0.2 ± 0.1	10 ± 6
Amp^R in 400 cells mixed	0.01 ± 0.01	0.98 ± 1.10	9 ± 3	27 ± 7	0.4 ± 0.3	20 ± 8

[a] approximately 300 cells attached to the substratum

[b] standard error of the mean used

[c] standard deviation used

TABLE 3.3. $Spec^R$ and AmpR cell behavior alone and in coculture, 150 cells at substratum, different cell type ratios.

$Spec^R$ to Amp^R ratios	biomass, $\mu m^3/\mu m^2$		maximum height, μm		percent substratum coverage		number of green colonies above substratum
	AB	LB	AB	LB	AB	LB	
$Spec^R$ alone[a]	0.0002 ± 0.0001	5.74 ± 0.66	2 ± 1	32 ± 2	0.02 ± 0.01	84 ± 3	NA
5 : 1 mixed	0.39 ± 0.32	4.60 ± 2.62	25 ± 11	40 ± 10	4.8 ± 2.7	49 ± 23	NA
1 : 1 mixed	0.04 ± 0.03	2.99 ± 1.76	20 ± 7	27 ± 10	1.7 ± 1.0	46 ± 22	NA
1 : 5 mixed	0.13 ± 0.13	2.64 ± 0.55	5 ± 2	26 ± 2	0.6 ± 0.2	52 ± 7	NA
Amp^R alone[a]	0.01 ± 0.00	1.22 ± 0.88	6 ± 1	22 ± 4	0.4 ± 0.0	19 ± 10	0 ± 0
5 : 1 mixed	0.01 ± 0.01	0.37 ± 0.27	11 ± 0	22 ± 8	0.4 ± 0.5	15 ± 9	12 ± 4
1 : 1 mixed	0.01 ± 0.01	0.45 ± 0.45	8 ± 3	21 ± 13	0.3 ± 0.3	6 ± 1	2 ± 2
1 : 5 mixed	0.02 ± 0.02	0.14 ± 0.05	5 ± 2	14 ± 3	0.3 ± 0.1	2 ± 0	1 ± 1

[a] approximately 300 cells attached to the substratum

NA = not applicable

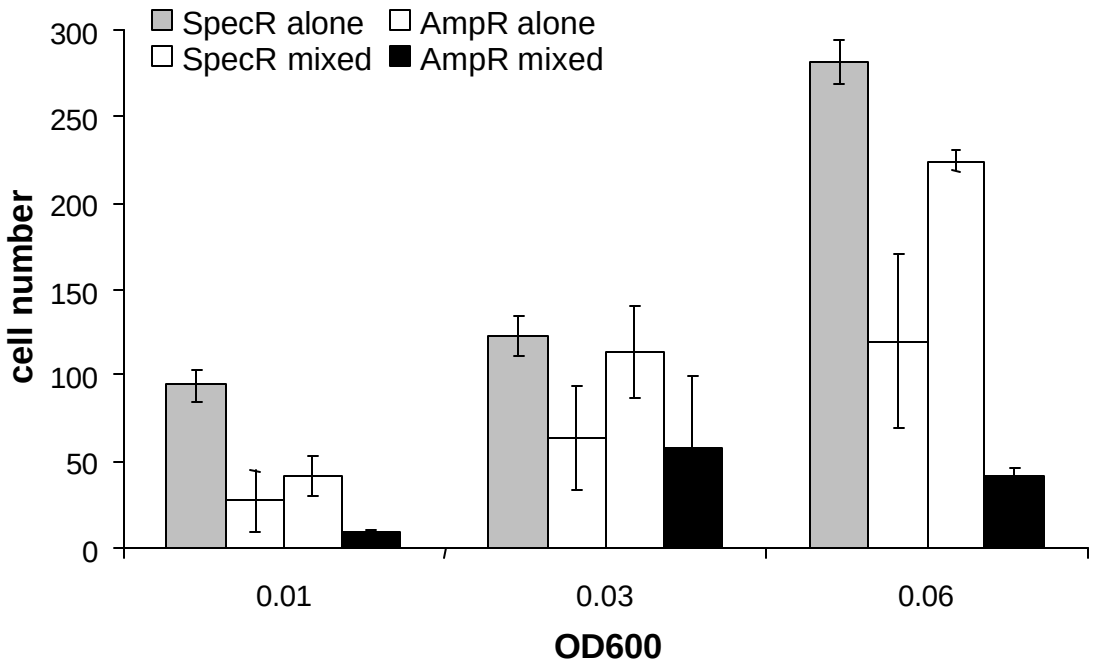

Figure 3.1. Initial attachment of Amp^R and $Spec^R$ cells grown in both antibiotics. attachment of Amp^R (green series) or $Spec^R$ (red series) based on optical density (OD_{600}).

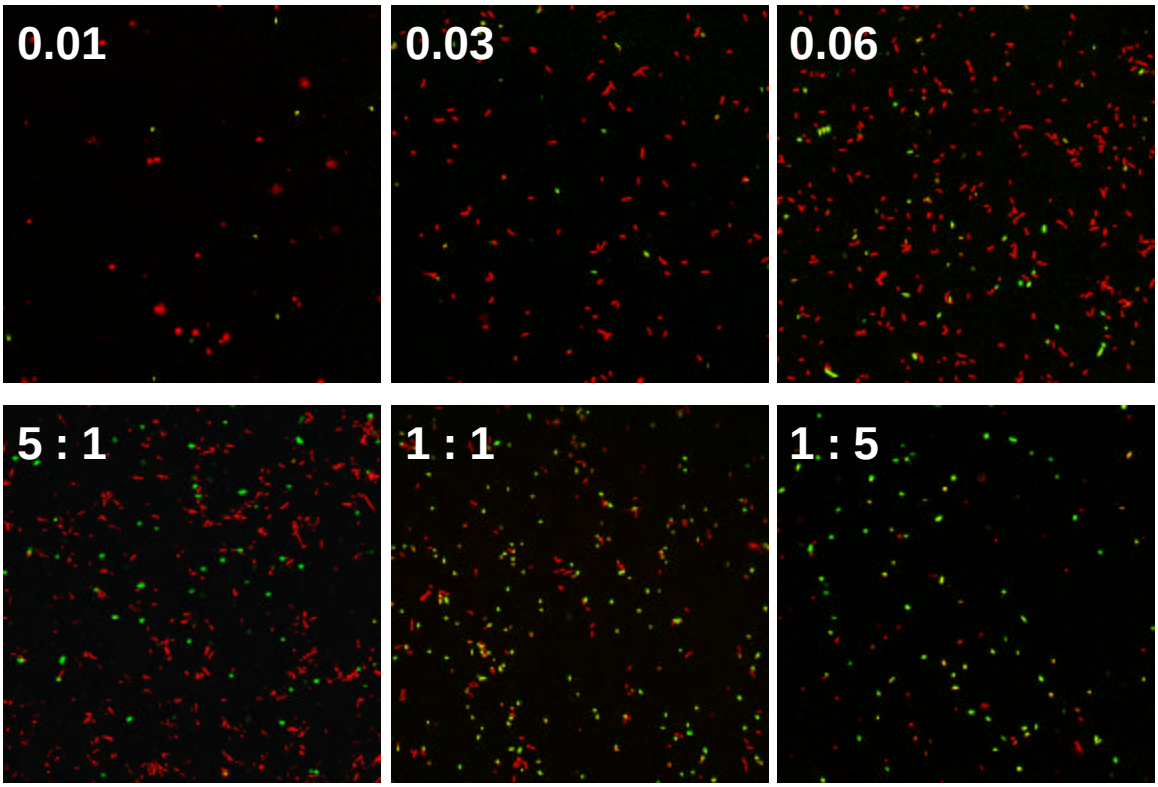

Figure 3.2. Substratum images of initial attachment of mixed cultures in 80 ppm spectinomycin and 100 ampicillin at 2H. 400× magnification, all images to scale. Top row: Inoculum consisting of equal cell numbers of Amp^R and $Spec^R$. Total OD_{600} values: 0.01, 0.03, or 0.06. Bottom row: OD_{600} 0.03 inoculum with varying cell attachment ratios: 5 $Spec^R$ to 1 Amp^R, 1 $Spec^R$ to 1 Amp^R, 1 $Spec^R$ to 5 Amp^R. Representative images shown.

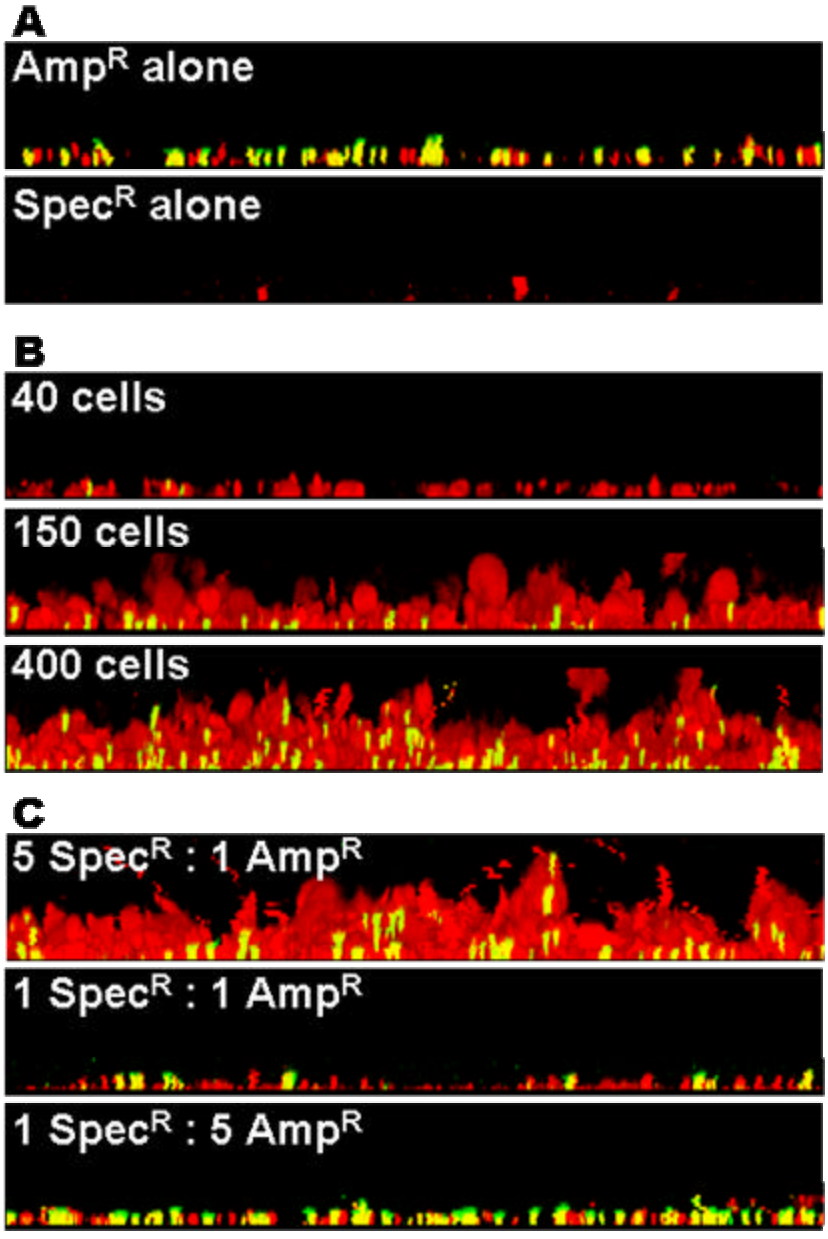

Figure 3.3. Cross-section images of 48 hour growth of single or mixed cultures 80 ppm spectinomycin and 100 ampicillin. 400× magnification, all images to scale and imaged to 36 microns above the substratum. A: Single-organism controls, with approximately 300 cells attached to the substratum. B: Equal cell numbers of Amp^R and $Spec^R$ in liquid inocula, with varying cell numbers attached to the substratum after 2 h recirculation. C: Approximately 150 cells attached to the substratum, with varying cell attachment ratios. Representative images shown.

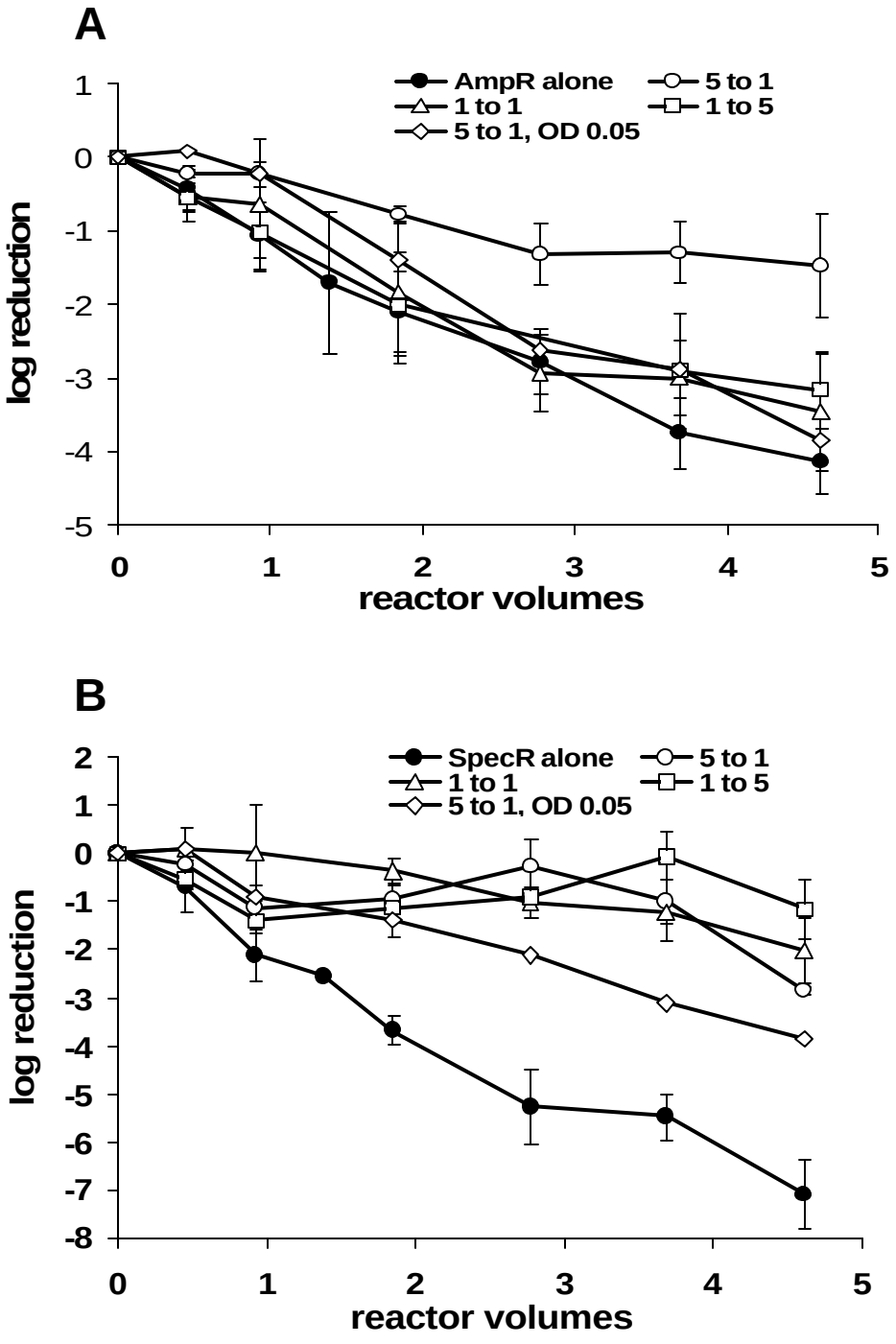

Figure 3.4. Chemostats: A: Amp^R grown alone or in differing ratios with $Spec^R$. B: $Spec^R$ grown alone or in differing ratios with Amp^R.

CHAPTER 4

ENHANCED HIGH COPY NUMBER PLASMID MAINTENANCE AND HETEROLOGOUS PROTEIN PRODUCTION IN AN *ESCHERICHIA COLI* BIOFILM

Heather A. O'Connell, Chen Niu and Eric S. Gilbert

4.1 ABSTRACT

Escherichia coli has been widely used for heterologous protein production (HPP). To determine whether a biofilm environment could benefit *E. coli* HPP using high copy number plasmids, we compared plasmid maintenance and HPP by *E. coli* ATCC 33456 containing plasmid pEGFP (a pUC family vector) cultivated in biofilms and in suspended culture. Cells were grown with or without antibiotic selective pressure in flow cells or chemostats for up to six days. In biofilms, antibiotic selective pressure increased the plasmid copy number (PCN), but by 144 h, biofilms grown in antibiotic-free media had comparable plasmid concentrations. In the chemostat, the PCN declined steadily, although 100 ppm ampicillin in the medium slowed the rate of plasmid loss. Production of green fluorescent protein (GFP), a representative heterologous protein, was quantified by flow cytometry. In biofilms, at ampicillin concentrations = 33 ppm, strongly fluorescent cells comprised more than half of the population by 48 h. In the chemostat, more than 50 percent of the population was non-fluorescent by 48 h in media containing 100 ppm ampicillin, and strongly fluorescent cells were < 10 percent of the population. Biofilm structure was determined by confocal microscopy. Maximum biofilm thickness

ranged from 30 to 45 microns, with no significant changes in biofilm structure after 48 h. Plasmid multimer percentages were similar to inocula for cells cultivated in either biofilms or the chemostat. The results indicate that the biofilm environment enhanced both plasmid maintenance and cellular GFP concentrations, and that low levels of antibiotic increased the beneficial effect.

4.2 METHODS

4.2.1 Strains and plasmids:

E. coli ATCC 33456 pEGFP contained the plasmid pEGFP, a pUC19-based vector encoding ampicillin resistance and a red-shifted *egfp* gene (Clontech, Mountain View, CA). Cells were cultured at 37°C in Luria-Bertani (LB) medium. *E. coli* ATCC 33456 pEGFP was maintained in medium containing 400 ppm ampicillin. No IPTG was added to the medium to avoid suppression of HPP, previously reported in cells containing high copy number plasmids (Jones *et al.*, 2000). The minimum inhibitory concentration (MIC) of ampicillin for *E. coli* ATCC 33456 was 16 ppm, as determined by the method of Jorgensen and Turnidge (Jorgensen & Turnidge, 2003). 16 ppm ampicillin was not lethal to attached cells, but reduced biofilm formation by 90 percent relative to growth in the absence of ampicillin (O'Connell *et al.*, 2006). Inocula for biofilm experiments were prepared by growing overnight cultures on antibiotic-containing plates with cells taken from clonal populations stored at -80°C. Inocula for chemostat experiments were prepared by growing frozen stock overnight at 37°C in 150 mL of LB containing 400 ppm ampicillin.

4.2.2 Chemostat experiments.

Chemostats were made from 250 mL sidearm flasks. Flasks were sealed with a rubber stopper containing a 3.2 mm i.d. Pharmed tube that extended to the bottom of the flask for influent media and another tube for the intake of air, which passed through a 0.2 μm pore size filter. Sterile media were contained in 5 L Pyrex bottles and were pumped into the chemostat using a peristaltic pump (Cole Parmer, USA) through autoclaved 3.2 mm i.d. Pharmed tubing. The sidearm flask was located on a magnetic stir plate that kept the flask contents well mixed, effluent flowed out of the sidearm into a sterile, hooded funnel leading to a waste vessel. The entire system was contained within an incubator with a maintained internal temperature of 37° C ± 0.5° C. Samples were collected by reaching a sterile microcentrifuge tube held by flame-sterilized tweezers into the sterile hood to collect effluent. Surfaces were sprayed with ethanol before and after handling to maintain sterility. At each time point, samples were collected to measure turbidity, to enumerate colonies by plate count, or to extract plasmid. Dilution rates were selected to maintain *E. coli* ATCC 33456 pEGFP in an active physiological state without risking washout, and thus were set to maintain the doubling time for the population at 75 percent of its maximum growth rate in LB medium ($\mu max = 1.3\ h^{-1}$). This corresponded to a pump flow of 4.7 mL min^{-1}, resulting in a complete reactor displacement every 62 minutes. The inoculum concentration was always $OD_{600} = 0.40$ (measured with an Ultrospec 2000 spectrophotometer; Pharmacia Biotech, UK), corresponding to 2×10^8

CFU mL^{-1}. Chemostats were run in at least duplicate for each condition that was investigated.

4.2.3 Biofilm growth and analysis.

Biofilms were cultivated using a parallel plate flow cell according to a previously described technique (Gilbert & Keasling, 2004). Briefly, cells were inoculated into media reservoirs to an OD_{600} of 0.03 and were recirculated through the flow cell at 0.84 mL min^{-1} for 2.5 hours to allow surface colonization. Subsequently, the system was switched to continuous (one-way) flow for the duration of the experiment (media flow rate of 0.35 mL min^{-1}). The selected media flow rate replaced the volume of the flow cell approximately once per minute, and was chosen such that the antibiotic concentration in the bulk fluid approximated steady state conditions, nutrients were not limiting and planktonic cells were removed from the flow cell. Liquid flow in the flow cell was laminar (Re = 32). Biofilms were grown at least in triplicate for all experiments. Quantitative analysis of CLSM images of biofilms was conducted using the digital image analysis program COMSTAT (Heydorn *et al.,* 2000). A constant pixel intensity threshold value of 30 and a minimum colony size of 100 pixels was used. To determine viability of *E. coli* ATCC 33456 cultivated in ampicillin-containing media, biofilms were stained with LIVE/DEAD BacLight bacterial viability stain (Invitrogen, USA) per manufacturer's instructions.

4.2.4 Confocal laser scanning microscopy.

Confocal laser scanning microscopy (CLSM) was performed with a Zeiss LSM 510 confocal laser scanning microscope (Carl Zeiss, Thornwood, NY) using a 40X oil immersion lens. An argon laser operating at 488 nm was used for excitation of cells. Eight image stacks were taken for each biofilm.

4.2.5 Flow cytometry.

Following imaging by CLSM, air was introduced into the flow cells to displace the biofilms. Visual inspection of flow cells by microscopy following biofilm displacement indicated that greater than 99 percent of the cells not directly adhered to the glass substratum were recovered. Displaced biofilms were resuspended by pipetting and were subsequently centrifuged at 9.8 × g for 2 min. The supernatant was discarded, the samples were resuspended in 50 mM sterile potassium phosphate buffer, and then diluted to an optical density (600 nm; OD_{600}) of 0.03 (approximately 2×10^7 cells mL^{-1}). Prior to analysis, cells were resuspended in 50 mM sterile potassium phosphate buffer, and were injected within 10 minutes into a Becton-Dickinson FACSCalibur flow cytometer (BD Biosciences, USA). Fluorescence intensity was determined by excitation at 488 nm. Forward scatter (FSC) and side scatter (SSC) were processed in linear gain, while fluorescence emissions (FL1-H) of between 515-545 nm were processed in logarithmic gain. Forward scatter data indicated that 85 percent of counted events for the resuspended biofilms were in the same range as for planktonic cells, indicating little to no clumping of resuspended cells. 10,000 events were collected for each biofilm.

4.2.6 Plasmid analysis.

Cells for plasmid extraction were normalized in 50 mM sterile potassium phosphate buffer to approximately 1.5×10^9 cells. Plasmid DNA was extracted from each resuspended sample using a kit (Qiagen, Valencia, CA). DNA was separated on 0.7% agarose gels containing 0.5 $\mu g\ mL^{-1}$ ethidium bromide at 85V for 120 minutes. Band intensity was evaluated densitometrically using digital image analysis software (LabWorks v. 4.0.0.8; Upland, CA), using the method of Asaka et al (Asaka et al. 1994) with minor modifications. Briefly, DNA concentrations were determined using a 2 – 10 kbp supercoiled plasmid marker containing 30 ng DNA μL^{-1} per band, which served as both a molecular weight marker and an internal standard for normalizing DNA concentrations between gels (Promega, Madison, WI). DNA concentrations were divided by the number of cells in the extracted sample and the molecular weight of the pEGFP plasmid to obtain the number of plasmid copies per cell. The mean of triplicate samples was used to calculate PCN.

4.2.7 GFP concentration.

GFP concentrations were determined by correlating fluorometry values of cell lysates prepared by sonication with an rGFP standard (Roche Applied Biosciences, USA) using a Bio-Rad VersaFluor fluorometer (Bio-Rad, Inc., Hercules, CA) after the method of Remans et al. (Remans *et al.*, 1999). GFP concentrations for biofilm cells were determined from cell suspensions with $OD_{600} = 1.0$. Total protein was determined using

the BCA assay (Pierce Biotechnology, Inc., Rockford, IL). Monitoring GFP production by flow cytometry and fluorometry is linear in relation to the amount of protein produced down to μL^{-1} concentrations (Hedhammar *et al.*, 2005; Remans *et al.*, 1999), is non-destructive to GFP-producing cells, can measure GFP production in single cells, and can differentiate cells based on the degree of their GFP expression.

4.3 RESULTS

4.3.1 Effect of ampicillin on biofilm cells.

Biofilms of *E. coli* ATCC 33456 pEGFP grown in LB broth plus 16 ppm ampicillin had typical coccobacillus morphology. In contrast, *E. coli* ATCC 33456 cells grown under the same conditions failed to produce a confluent biofilm, and were comprised of cells with filamentous and bulbous morphologies. Viability staining indicated that 65 percent of the attached biomass was either damaged or dead.

4.3.2 Plasmid copy number and multimer analysis.

In the chemostat, the plasmid copy number of *E. coli* ATCC pEGFP grown in LB broth only fell below detectable levels by 72 h **(Figure 4.1A)**. Plasmid loss occurred at a slower rate in LB broth containing ampicillin. In biofilms, there was an initial decrease in the band intensity of plasmid extracted from biofilms grown without ampicillin relative to the inoculum **(Figure 4.1B)**, but subsequently band intensity increased over the course of the experiment. At 24 h, band intensity for biofilms cultivated in media containing 16 ppm ampicillin was greater than in biofilms cultivated in LB broth only, and increased

over the duration of the 144 h experiment **(Figure 4.1B)**. Biofilms grown in media containing concentrations of up to 200 ppm ampicillin showed similar band patterns and intensities (data not shown). Proportions of monomers and multimers remained similar in both biofilms and chemostats, with monomers accounting for 52 to 65 percent of plasmid DNA.

In the chemostat, densitometry measurements indicated that 100 ppm ampicillin led to increased PCN **(Figure 4.2, closed circles)**, but that 16 ppm ampicillin did not. In contrast, in the biofilm, 16 ppm ampicillin fostered a significant increase in PCN which did not increase at higher ampicillin concentrations **(Figure 4.2, open circles)**. In the chemostat, the PCN declined steadily as a function of time **(Figure 4.3A)**. In LB broth only or media containing 16 ppm ampicillin, the PCN decreased by nearly 90 percent relative to inoculum levels by 57 h. In LB broth containing 100 ppm ampicillin, a decline in PCN was still evident, but the rate was slower than at 16 ppm. In the biofilm, following an initial decrease in PCN relative to the inoculum, the PCN increased for both growth conditions over the course of the experiment **(Figure 4.3B)**. The PCN was significantly higher in biofilms grown with ampicillin present compared to biofilms grown without ampicillin at 24 h ($p = 0.035$), 48 h ($p = 0.000036$), and 96 h ($p = 0.016$). The PCN at 144 h was the same for both growth conditions ($p = 0.60$).

4.3.3 Analysis of biofilm structure and growth.

All biofilms showed well-established structures at 24 h with a loose “sponge-like” arrangement, punctuated with densely populated clusters. At 48 h, there was a confluent

bottom layer several cells thick, larger clusters and well-defined channels. The accumulation of strain pEGFP biomass by 48 h was similar to *E. coli* ATCC 33456 over the same time period (Niu & Gilbert, 2004). Biomass continued to increase in height and cell density through 144 h. The effect of antibiotic selective pressure on the biofilm structure was modest **(Table 4.1)**. With respect to time, there was also a significant increase in percent substratum coverage and maximum diffusion distance after 24 h. In contrast, the surface area to volume ratio decreased significantly between 24 and 144 h. The average biofilm doubling time was estimated using data collected from COMSTAT analyses. Doubling times based on biomass and substratum coverage parameters were 8.7 h and 9.6 h, respectively. This was approximately nine times slower than the growth of strain pEGFP in the chemostat.

4.3.4 HPP dynamics.

Visual inspection under UV light of colonies cultured from resuspended biofilms identified three distinct populations: one which fluoresced strongly, a second which fluoresced moderately and a non-fluorescent population. Each of the populations could be distinguished from the others by flow cytometry **(Figure 4.4)**. Cells with an FL1-H value of 40 - 9910 were considered strongly fluorescent, those from 3 - 40 were designated as moderately fluorescent, and cells with FL1-H values of less than 3 were considered non-fluorescent. The average GFP production of the strongly fluorescent population was 0.16 mg GFP mL^{-1}, accounting for 17 percent of total cell protein, and the average GFP production by the moderately fluorescent population corresponded to 0.01 mg GFP mL^{-1},

approximately 1 percent of total cell protein. The dynamics of the three populations in chemostats and biofilms were monitored as a function of time.

The effect of ampicillin concentration on cell fluorescence was considered. In the chemostat, the majority of cells grown in media containing 0 or 16 ppm ampicillin were non-fluorescent by 48 h, **(Figure 4.5A)**, and for 100 ppm ampicillin, a small strongly fluorescent population was detectable. In biofilms grown in media containing 0 ppm ampicillin, the population split into distinct non-fluorescent and fluorescent populations. A shift to the right indicating increased average fluorescence was visible in biofilms grown in media containing 16 and 100 ppm ampicillin. In the chemostat, non-fluorescent events accounted for 50 – 55 percent of the total events collected, and fewer than 10 percent of events were strongly fluorescent by 48 h **(Figure 4.5B)**. In the biofilm, a decrease in the moderately fluorescent population occurred with increasing ampicillin concentration with a corresponding increase in the size of the strongly fluorescent population.

The dynamics of fluorescence during growth in biofilms and chemostats was compared. In the chemostat, the strongly fluorescent population accounted for less than 3 percent of the total counts by 48 h **(Figures 4.6A, 4.6B)**. Non-fluorescent and moderately fluorescent populations stabilized by 48 h and accounted for approximately half each of the total events. In biofilms grown in the absence of ampicillin, fluorescent cells comprised approximately 85 percent of the population for all time points **(Figure 4.6C)**. With ampicillin present, the strongly fluorescent population was less than 1 percent at 24 h, but steadily increased in size to 50 percent at 144 h. The non-fluorescent population

was largest at 24 h, but dropped to less than 3 percent for all other time points **(Figure 4.6D)**.

4.4 DISCUSSION

Recombinant protein production based on *E. coli* is advantageous for reasons that include its ability to grow using inexpensive substrates, rapid high-density growth, high level gene expression, and the potential to control protein folding (Baneyx, 1999; Baneyx & Mujacic, 2004). The presented research supports the concept that *E. coli* growing in biofilms could benefit HPP. First, a low concentration of antibiotics enhanced plasmid maintenance and HPP in biofilms, whereas no comparable benefit was detected in the chemostat. Second, high plasmid copy number was maintained in biofilms over extended periods in the absence of antibiotic selective pressure. A factor that may have contributed to this result was the slower average doubling time for *E. coli* ATCC 33456 in the biofilm environment. Third, the presence of plasmid multimers did not lead to plasmid loss over time. Although plasmid multimerization is sometimes a prelude to the heterogeneous distribution of plasmids within a population, direct measurements of plasmid copy number and multimer percentages supported the conclusion that plasmids were maintained. Moreover, the non-fluorescent population of cells within the biofilm either remained stable in size or declined over time, augmenting this point of view. Fourth, 90 percent or more of cells in the biofilms contained significant levels of heterologous protein by 6 days, even in the absence of selective pressure. This behavior could have been promoted by the larger gene dosage that resulted from enhanced plasmid retention.

The high percentage of cells containing GFP suggests that heterologous enzymes produced within *E. coli* biofilms could serve as an effective catalyst.

Continuous biofilm cultures for HPP have advantages with respect to chemostats for retention of plasmid-bearing cells. Significant loss of plasmid from cells cultured in the chemostat occurred, similar to the findings of other investigators (Lu-Chau *et al.*, 2004; Ryan & Parulekar, 1991; Yazdani & Mukherjee, 2002) In contrast, high-density fed-batch cultures have been effectively managed for HPP with minimal loss of plasmid (Hu *et al.*, 2003; Lau *et al.*, 2004). However, maintaining optimal operation of fed-batch reactors is challenging for reasons that include substrate solubility limitations, dissolved oxygen delivery limitations, and toxic metabolite accumulation (Lee, 1996; Riesenberg & Guthke, 1999). A continuous biofilm culture may represent a compromise between the comparative ease of operating a continuous flow system and the high yield and plasmid stability that can be achieved in fed-batch culture. It should be noted that Sharp *et al.*, 1998) saw comparable rates of plasmid loss in both biofilms and planktonic culture. We think that the difference between our results and theirs is attributable to the significantly larger size of the TOM_{31C} plasmid (108 kbp), a pGEM family vector, relative to plasmid pEGFP (3.5 kbp), which may have placed a greater metabolic burden on *Burkholderia cepacia* 17616 (Sharp *et al.*, 1998).

The stable maintenance of high copy number vectors for HPP by *E. coli* biofilms could benefit metabolic engineering processes. For example, *E. coli* biofilms comprised of multiple subpopulations and each carrying requisite genes on different vectors, could be used to assemble composite metabolic pathways. This approach could be

advantageous in cases where recruitment of the genes of a pathway into a single organism proved to be unfeasible due to gene instability, metabolic burden or kinetic limitations. A related approach could involve multiple bacterial species, each with different metabolic capabilities. These constructed multispecies biofilms could take advantage of microenvironments within biofilms to support diverse populations of bacteria. The rational design of multispecies biofilms has been proposed, based on the *E. coli* surface adhesin antigen 43 (Kjaergaard *et al.,* 2000), and could potentially incorporate cells harboring high copy number vectors. Recent work with high resolution spatial patterning of bacteria on surfaces could foster efforts in this area (Cowan *et al.,* 2001; Xu *et al.,* 2004). In general, the ability of biofilms to maintain high copy number vectors in the absence of selective pressure or a plasmid addiction system should continue to be evaluated for industrial applications.

TABLE 4.1. COMSTAT analysis of biofilm structure.

Parameter	Growth period, h							
	24		48		96		144	
	LB only	LB + amp[a]	LB only	LB + amp	LB only	LB + amp	LB only	LB + amp
Maximum thickness (μm)	12 ± 0	22 ± 2	19 ± 4	15 ± 4	16 ± 2	45 ± 4	23 ± 3	30 ± 5
Biomass ($\mu m^3/\mu m^2$)	0.04 ± 0.01	0.17 ± 0.05	1.7 ± 0.9	0.72 ± 0.32	0.14 ± 0.13	4.03 ± 2.91	0.92 ± 0.36	1.14 ± 0.48
Percent substratum coverage	1 ± 0	4 ± 1	23 ± 11	17 ± 8	1 ± 1	27 ± 19	7 ± 3	9 ± 2
Roughness coefficient[b,c]	2.0 ± 0.008	1.9 ± 0.04	1.5 ± 0.2	1.3 ± 0.3	1.9 ± 0.00	1.2 ± 0.1	1.8 ± 0.07	1.7 ± 0.1
Maximum diffusion distance (μm)	1.8 ± 0.2	1.9 ± 0.1	3.8 ± 1.2	3.7 ± 0.5	3.3 ± 0.5	6.3 ± 0.9	5.2 ± 0.9	7.5 ± 1.2
Surface area to volume ratio ($\mu m^2/\mu m^3$)	4.4 ± 0.3	4.4 ± 0.4	3.9 ± 0.6	5.1 ± 0.7	3.8 ± 0.4	2.6 ± 0.2	3.3 ± 0.3	2.5 ± 0.4

[a] LB broth + 16 ppm ampicillin

[b] Unitless measurement

[c] Area of microcolony at the substratum

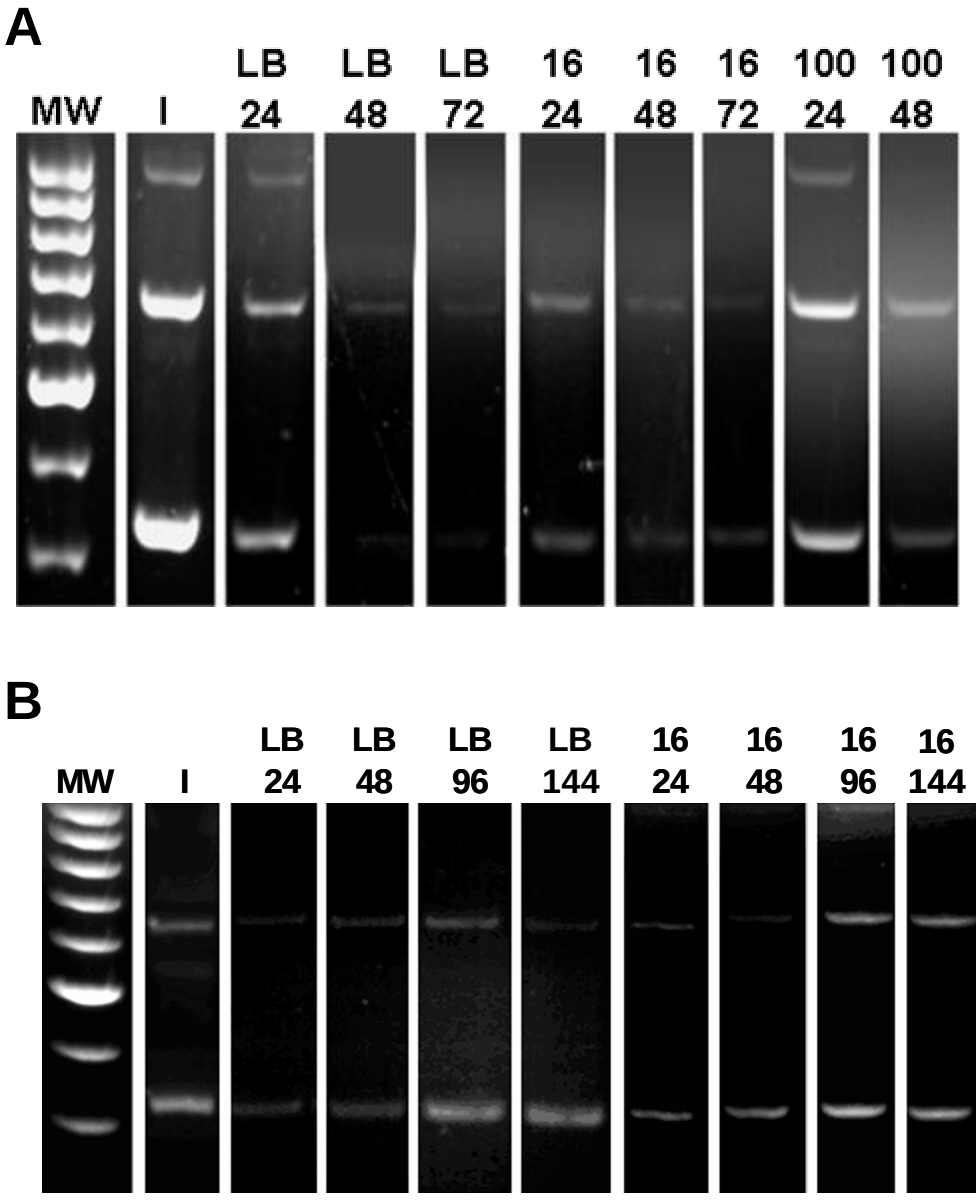

Figure 4.1. Gel electrophoresis of pEGFP DNA extracted from time-course experiments with (A) chemostats and (B) biofilms. MW: Supercoiled plasmid marker, 2 – 10 kbp. I: Inoculum. LB: Cultures grown in LB broth only. 16 and 100: Cultures grown in LB broth and either 16 ppm ampicillin or 100 ppm ampicillin. Plasmid DNA collected at 24 h intervals. Representative lanes shown.

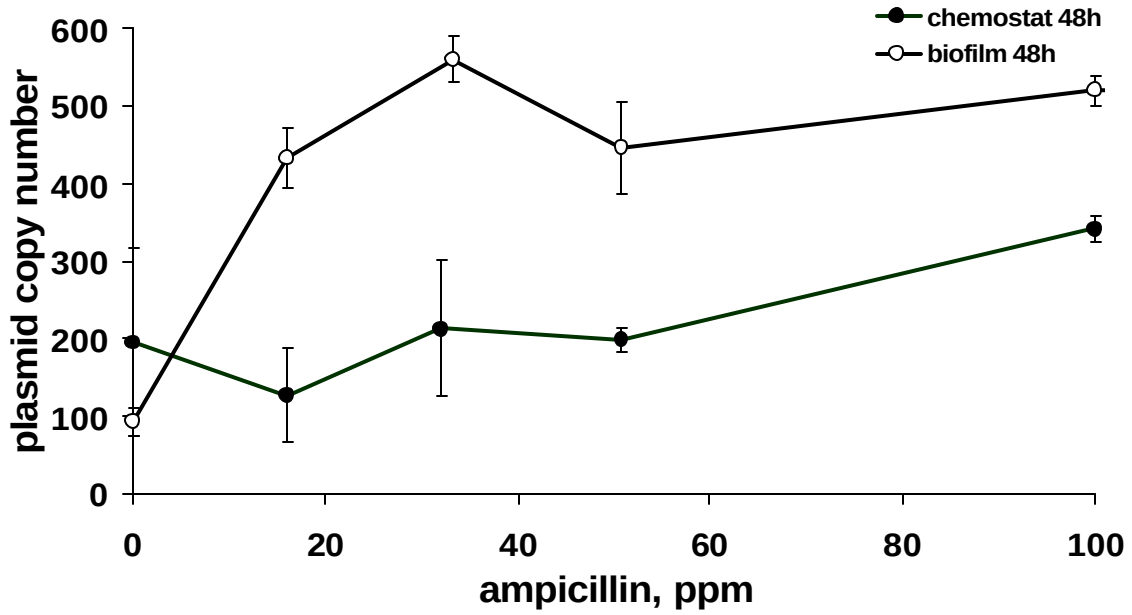

Figure 4.2. Plasmid copy number at 48 h for cells cultured in either chemostats or biofilms (n = 4 to 7) versus ampicillin concentration. Closed squares: chemostat, open squares: biofilm.

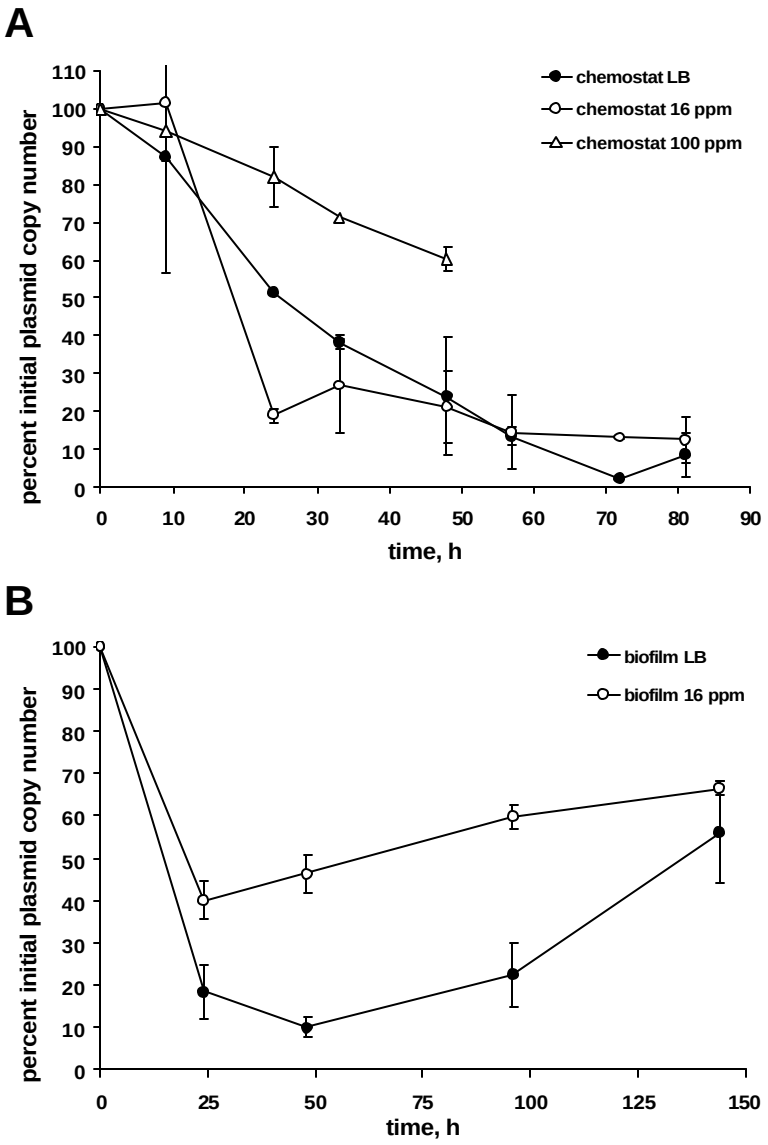

Figure 4.3. Change in PCN versus time in chemostats and biofilms. Plasmid DNA concentrations are reported as the percentage of the inoculum PCN. Closed circles: Cultures grown in LB broth only. Open circles: Cultures grown in LB containing 16 ppm ampicillin. Open triangles: Cultures grown in LB containing 100 ppm ampicillin. (A) Chemostats, (B) biofilms.

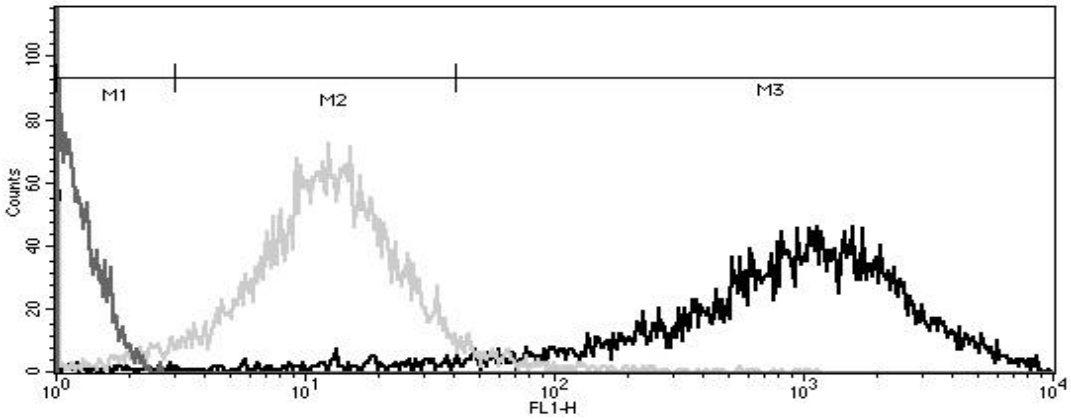

Figure 4.4. Three populations of cells with differing levels of GFP expression detected by flow cytometry. M1: non-fluorescent control cells. M2: moderately fluorescent *E. coli* ATCC 33456 pEGFP. M3: strongly fluorescent *E. coli* ATCC 33456 pEGFP.

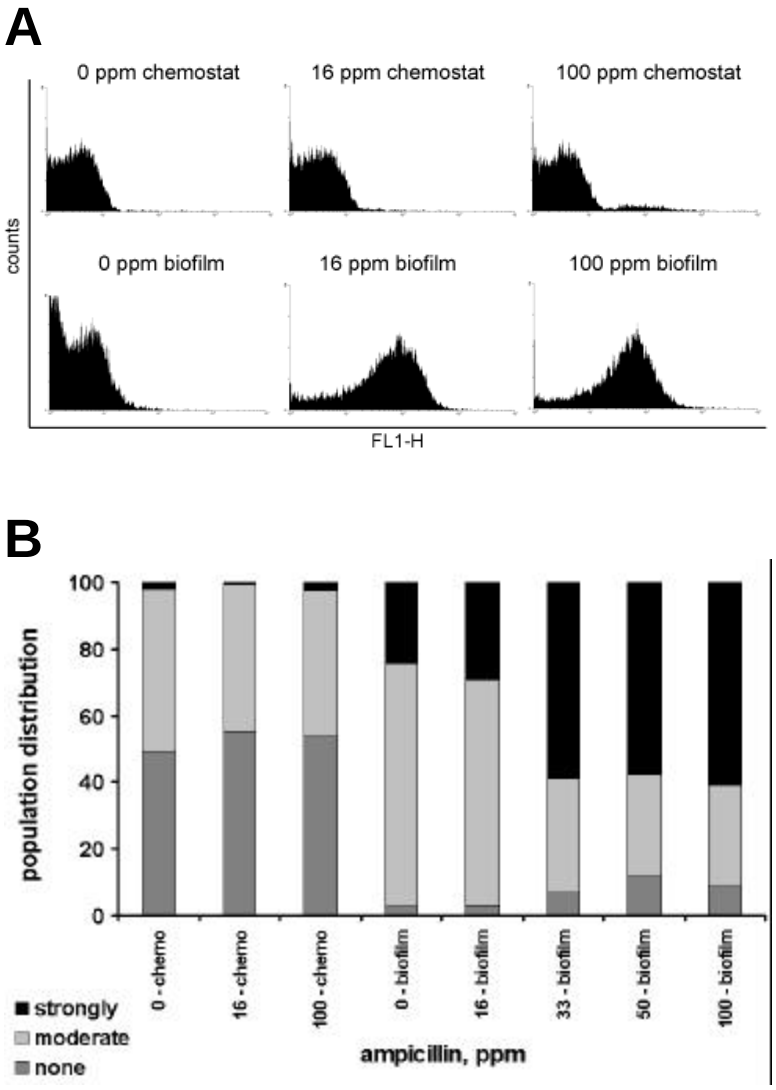

Figure 4.5. Distribution of fluorescent populations versus ampicillin concentration in chemostats and biofilms. Analysis by flow cytometry after 48 h growth. (A) Representative histograms of chemostats and biofilms grown in media containing either 0, 16, or 100 ppm ampicillin. FL1-H: GFP fluorescence. B: Percent distribution of non-fluorescent, moderately fluorescent, and strongly fluorescent cells. Ampicillin concentrations of culture media and cultivation mode are indicated on the x-axis.

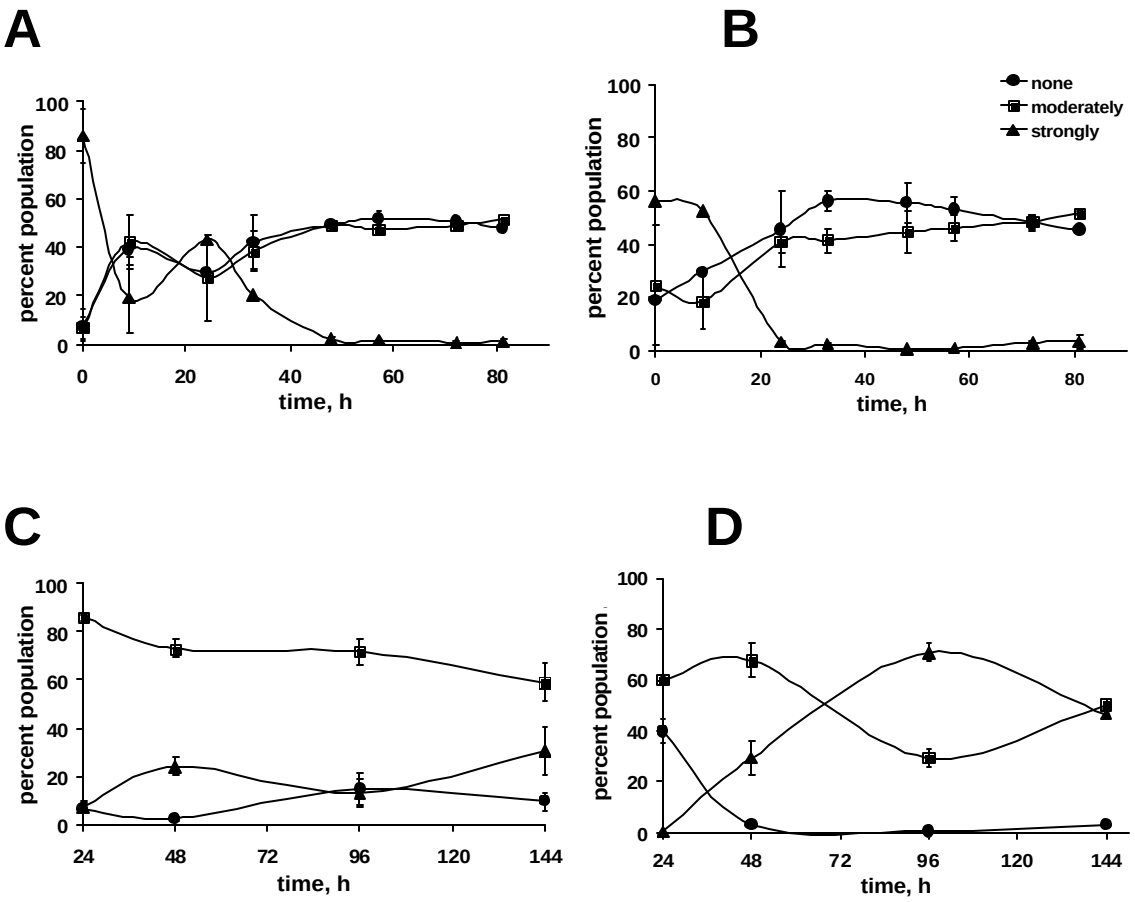

Figure 4.6. Changes in the distribution of fluorescent populations versus time in chemostats and biofilms. Analysis by flow cytometry. (A) Chemostats grown in LB broth only. (B) Chemostats grown in LB broth containing 16 ppm ampicillin. (C) Biofilms grown in LB broth only. (D) Biofilms grown in LB broth containing 16 ppm ampicillin.

CHAPTER 5 CONCLUSION

5.1 Introduction of two techniques.

A chemostat cultivation technique and an image analysis program were developed during this research. The chemostat system **(Figure. 5.1)** was developed using items such as sidearm flasks and Pyrex bottles that are available in most microbiology laboratories. This setup features simple construction, modular sterilization, and ease of operation relative to commercially available systems. Additionally, this system can be used with minimal training, making steady-state liquid culture experiments for comparison to biofilms more feasible.

A software program was developed in conjunction with the Georgia State University Department of Computer Sciences, the details of which are in Appendices A and B. Simultaneous counts of differently labeled cells, measurements of the centroid to centroid distance between cells, and counts of user-defined cell groups lend a better understanding of attachment events that shape later biofilm growth.

5.2 The novelty and significance of each chapter in this work.

Prior to this research, commensal protection of an antibiotic sensitive organism by a resistant organism, a phenomenon referred to as indirect pathogenesis, had only been observed in beta-lactamase producing bacteria (Brook, 1994; Brook, 2004; Budhani, 1998). This dissertation research demonstrated similar protection to a nonpathogenic target in a model system, laying the foundation for applications using clinically relevant

organisms. The commensal detoxification of spectinomycin by attached cells is novel because aminoglycoside inactivation in the biofilm setting is sufficient to support a sensitive organism, whereas no protection is observed in comparable liquid environments. Many previous studies have focused on antibiotic resistance in established biofilms, instead of examining attachment and early growth (Costerton, 1999; Donlan & Costerton, 2002; Fux *et al.,* 2005). Many infections involve multiple species growing attached to surfaces as biofilms, as opposed planktonic growth (Brook 2002; Gilbert *et al.,* 2002). This inactivation of antibiotics by non-target resistant organisms is significant, and should be factored into antibiotic treatment of infections.

Previous research has created a wealth of knowledge in the areas of combination therapies of pure culture biofilms (Rossolini & Mantengoli 2005; Rahal, 2006), and single-antibiotic treatment of polymicrobial biofilms (Lin *et al.,* 2006; Brook 2002). The research in Chapter 3 is novel because it demonstrates the ability of two organisms to produce biofilm in media containing inhibitory concentrations of two antibiotics. This community dependent resistance to multiple antibiotics requires a minimum number of individual cells of both strains to attach in proximity to each other.

This research demonstrated that biofilms stabilize high copy number plasmids in the absence of antibiotic selective pressure. Traditionally, biofilms have been viewed as a source of biofouling, a nuisance in high-density chemostat cultures. However, the attached nature of biofilms prevents the washout of the cells which have slower growth rates due to the metabolic demands imposed by the maintenance of high copy plasmids and their associated heterologous protein production (Reisner *et al.,* 2006; Bathe *et al.,*

2004). Using biofilms for heterologous protein production may be useful because it would increase yield per cell, and could reduce the costs associated with purchasing exogenous compounds (such as antibiotics) required to apply selective pressure.

Overall, this body of research underscores the contributions that biofilms make to plasmid maintenance and non-inherited mechanisms of antibiotic resistance. First, by providing a nidus of attachment for cells containing high copy number plasmids, biofilms can aid industrial processes. Second, understanding the interactions between the members of antibiotic resistant polymicrobial biofilms lays the foundation for developing therapies that will better eradicate infections, or prevent their formation.

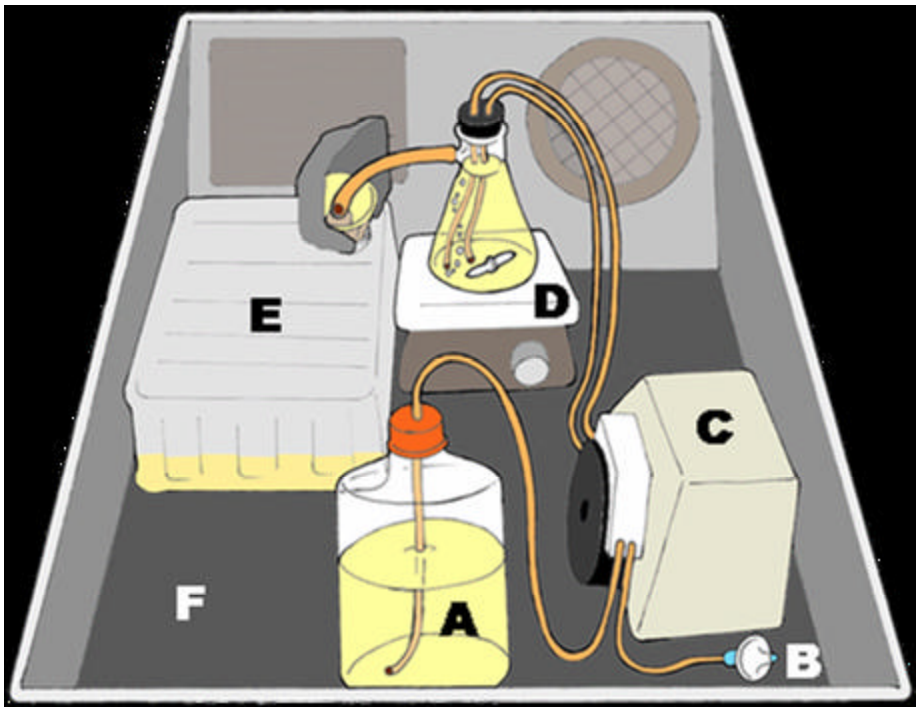

Figure 5.1. A diagram of the chemostat used for this project. A: Reservoir bottle containing sterile media. B: 0.2 micron pore size filter, sterile air intake. C: Adjustable flow pump. D. Stir plate with sidearm flask reactor. E: Hooded waste container. F: Chest incubator.

REFERENCES

Adair, C.G., Gorman, S.P., Feron, B.M,, Byers, L.M., Jones, D.S., Goldsmith, C.E., Moore, J.E., Kerr, J.R., Curran, M.D., Hogg, G. and others. (1999). Implications of endotracheal tube biofilm for ventilator-associated pneumonia. *Intensive Care Medicine* **25**, 1072 - 1076.

Ahmed, M., Yamany, S., Mohamed, N., Farag, A., Moriarty, T. (2002). A Modified Fuzzy C-Means Algorithm for Bias Field Estimation and Segmentation of MRI Data. *IEEE Transactions On Medical Imaging* **21**, 193-199.

An D., Danhorn, T., Fuqua, C., Parsek, M.R. (2006). Quorum sensing and motility mediate interactions between *Pseudomonas aeruginosa* and *Agrobacterium tumefaciens* in biofilm cocultures. *Proc Natl Acad Sci U S A* **103**, 3828-3833.

Asaka, O., Ano, T., Shoda, M. (1994). A rapid and simple method for plasmid copy number determination. *Biotechnol Tech* **8**, 865-868.

Baneyx, F. (1999). Recombinant protein expression in *Escherichia coli. Curr Opin Biotechnol* **10**, 411-421.

Baneyx, F., Mujacic, M. (2004). Recombinant protein folding and misfolding in *Escherichia coli*. *Nat Biotechnol* **22**, 1399-1408.

Basu, S., Banerjee, A., Mooney, R. (2004). Active Semi-Supervision for Pairwise Constrained Clustering. *Proceedings of the SIAM SDM*.

Bathe, S., Mohan, T.V., Wuertz, S., Hausner, M. (2004). Bioaugmentation of a sequencing batch biofilm reactor by horizontal gene transfer. *Water Sci Technol* **49**, 337-344.

Belanger, L., Figueira, M.M., Bourque, D., Morel, L., Beland, M., Laramee, L., Groleau, D., Miguez, C.B. (2004). Production of heterologous protein by *Methylobacterium extorquens* in high cell density fermentation. *FEMS Microbiol Lett* **231**, 197-204.

Belkasim, S., Ghazal, A., Basir, A. (2003). Phase-based optimal image thresholding. *Digital Signal Processing* **13**, 636-655.

Belkasim, S., Shridhar, M., Ahmdi, M. (1995). New method for contour detection and automatic thresholding. *Can J Elect and Comp Eng* **20,** 165-172.

Binnie, C., Cossar, J.D., Stewart, D.I. (1997). Heterologous biopharmaceutical protein expression in *Streptomyces*. *Trends Biotechnol* **15**, 315-320.

Bollmann, A., Bar-Gilissen, M.J., Laanbroek, H.J. (2002). Growth at low ammonium concentrations and starvation response as potential factors involved in niche differentiation among ammonia-oxidizing bacteria. *Appl Environ Microbiol* **68**, 4751-4757.

Brook, I. (1994). Indirect Pathogenicity. *Infectious Diseases in Clinical Practice* **3**, S21-S27.

Brook, I. (2002). Microbiology of polymicrobial abscesses and implications for therapy. J Antimicrob Chemother, **50**, 805-810.

Brook, I. (2004). Beta-lactamase-producing bacteria in mixed infections. Clin Microbiol Infect **10**, 777-784.

Bryers, J.D., Huang, C-T. (1995). Recombinant plasmid retention and expression in bacterial biofilm cultures. Water Science and Technology **31**, 105-115.

Budhani, R.K. Struthers, J.K. (1998). Interaction of *Streptococcus pneumoniae* and *Moraxella catarrhalis*: investigation of the indirect pathogenic role of beta-lactamase-producing moraxellae by use of a continuous-culture biofilm system. *Antimicrob Agents Chemother* **42**, 2521-2526.

Burlage, R.S., Hooper, S.W., Sayler, G.S. (1989). The TOL (pWW0) catabolic plasmid. Appl Environ Microbiol **55**, 1323-1328.

Ceri, H., Olson, M., Stremick, C., Read, R., Morck, D., Buret, A. (1999). The calgary biofilm device: New technology for rapid determination of antibiotic susceptibilities of bacterial biofilms. *Journal of Clinical Microbiology* **37**, 1771-1776.

Chen, B., Li, Y. (1999). Numerical modeling of biofilm growth at the pore scale. *Proceedings of the 1999 Conference on Hazardous Waste Research*.

Cheng, H., Jiang, Y., Wang, J. (2001). Color image segmentation: advances and prospects. Pattern Recognition **34**, 2259-2281.

Christensen, B.B. Haagensen, J., Heydorn, A., Molin, S. (2002). Metabolic commensalism and competition in a two-species microbial consortium. Appl Environ Microbiol. **68**, 4481-4485.

Costerton, J.W., Lewandowski, Z., Caldwell, D.E., Korber, D.R. (1995). Microbial biofilms. Annu Rev Microbiol **49**, 711-745.

Costerton, J.W., Stewart, P., Greenberg, E.P. (1999). Bacterial biofilms: a common cause of persistent infections. *Science* **284**, 1318-1322.

Cotton, J.C., Pometto, A.L., Gvozdenovic-Jeremic, J. (2001). Continuous lactic acid fermentation using a plastic composite support biofilm reactor. *Appl Microbiol Biotechnol* **57**, 626-630.

Cowan, S., Gilbert, E., Liepmann, D., Keasling, J. (2000). Commensal interactions in a dual-species biofilm exposed to mixed organic compounds. Appl Environ Microbiol **66**, 4481-5.

Cowan, S.E., Liepmann, D., Keasling, J.D. (2001). Development of engineered biofilms on poly-l-lysine patterned surfaces. *Biotechnol Lett* **23**, 1235-1241.

Donlan, R.M., Costerton, J.W. (2002). Biofilms: survival mechanisms of clinically relevant microorganisms. *Clin Microbiol Rev* **15**, 167-193.

Ehrlich, G.D., Hu, F.Z., Shen, K., Stoodley, P., Post, J.C. (2005). Bacterial plurality as a general mechanism driving persistence in chronic infections. *Clin Orthop Relat Res* **437**, 20-4.

Erb, R.W., Eichner, C.A., Wagner-Dobler, I., Timmis, K.N. (1997). Bioprotection of microbial communities from toxic phenol mixtures by a genetically designed pseudomonad. Nat Biotechnol **15**, 378-82.

Fux, C.A., Costerton, J.W., Stewart, P.S., Stoodley, P. (2005). Survival strategies of infectious biofilms. Trends Microbiol **13**, 34-40.

Gauch, J., Hsia, C. (1992). A comparison of three color image segmentation algorithm in four color spaces. *Visual Communications and Image Processing '92* **1818**, 1168-1181.

Gilbert, E., Keasling, J. (2004). Bench scale flow cell for nondestructive imaging of biofilms. *In:* Spencer, J., Ragout de Spencer, A., editors. *Environmental Microbiology Methods and Protocols.* Totowa, NJ: Humana Press.

Gilbert, E., Walker, A., Keasling, J. (2003). A constructed microbial consortium for biodegradation of the organophosphorus insecticide parathion. Applied Microbiology and Biotechnology **61**, 77-81.

Gilbert, P., Allison, D.G., McBain, A.J. (2002). Biofilms in vitro and in vivo: do singular mechanisms imply cross-resistance? *J Appl Microbiol* **92**, 98S-110S.

Gilbert, P., Collier, P., Brown, M. (1990). Influence of growth rate on susceptibility to antimicrobial agents: biofilms, cell cycle, dormancy, and stringent response. *Antimicrobial Agents and Chemotherapy* **34**, 1865-1868.

Gordan, M., Kotropoulos, C., Georgakis, A., IPitas, I. (2002). A new fuzzy c-means based segmentation strategy. applications to lip region identification. *IEEE-TTTC International Conference on Automation, Quality and Testing, Robotics*.

Hansen, M., Palmer, R.J., Udsen, C., White, D., Molin, S. (2001). Assessment of GFP fluorescence in cells of *Streptococcus gordonii* under conditions of low pH and low oxygen concentration. *Microbiology* **147**, 1383-1391.

Hedhammar, M., Stenvall, M., Lonneborg, R., Nord, O., Sjolin, O., Brismar, H., Uhlen, M., Ottosson, J., Hober, S. (2005). A novel flow cytometry-based method for analysis of expression levels in *Escherichia coli*, giving information about precipitated and soluble protein. *J Biotechnol* **119**, 133-146.

Heydorn, A., Nielsen, A., Hentzer, M., Sternberg, C., Givskov, M., Ersboll, B.K., Molin, S. (2000). Quantification of biofilm structures by the novel computer program COMSTAT. Microbiology **146**, 2395-2407.

Hu, Y-C., Tsai, C-T., Chang, Y-J., Huang, J-H. (2003). Enhancement and Prolongation of Baculovirus-Mediated Expression in Mammalian Cells: Focuses on Strategic Infection and Feeding. *Biotechnol Prog* **19**, 373-379.

Husmann, L.K., Yung, D.L., Hollingshead, S.K., Scott, J.R. (1997). Role of putative virulence factors of *Streptococcus pyogenes* in mouse models of long-term throat colonization and pneumonia. *Infect Immun* **65**, 1422-1430.

Jana, S., Deb, J.K. (2006). Molecular understanding of aminoglycoside action and resistance. *Appl Microbiol Biotechnol* **70**, 140-150.

Ji, S., Park, H. (1998). A new method of color image segmentation based on intensity and hue clustering. *International Conference on Image Processing* **1**, 80-83.

Jones, K.L., Kim, S.W., Keasling, J.D. (2000). Low-copy plasmids can perform as well as or better than high-copy plasmids for metabolic engineering of bacteria. *Metab Eng* **2**, 328-338.

Jorgensen, J.H., Turnidge, J.D. (2003). Susceptibility test methods: dilution and disk diffusion methods. *In:* Murray, P.R., Baron, E.J., Jorgensen, J.H., Pfaller, M.A.,

Yolken, R.H., editors. *Manual of Clinical Microbiology*. 8 ed. Washington, DC: ASM Press. p 1115-1116.

Kaieda, S., Yano, H., Okitsu, N., Hosaka, Y., Okamoto, R., Inoue, M., Takahashi, H. (2005). In vitro investigation of the indirect pathogenicity of beta-lactamase-producing microorganisms in the nasopharyngeal microflora. *Int J Pediatr Otorhinolaryngol* **69**, 479-485.

Kamel, M., Belkasim, S., Mendonca, A., Campelho, A. (2001). A Neural Network Approach for the Automatic Detection of Microaneurysms in Retinal Angiograms. *Proceedings of the 2001 INNS-IEEE International Joint Conference on Neural Networks*, 595-599.

Kanungo, T., Mount, D., Netanyahu, N., Piatko, C., Wu, A. (2002). An efficient k-means clustering algorithm: analysis and implementation. IEEE Transactions On Pattern Analysis And Machine Intelligence **24**, 881-892.

Kirkpatrick, C., Maurer, L.M., Oyelakin, N.E., Yoncheva, Y.N., Maurer, R., Slonczewski, J.L. (2001). Acetate and formate stress: opposite responses in the proteome of *Escherichia coli*. *J Bacteriol* 183, 6466-6477.

Kjaergaard, K., Schembri, M.A., Ramos, C., Molin, S., Klemm, P. (2000). Antigen 43 facilitates formation of multispecies biofilms. *Environ Microbiol* **2**, 695-702.

Kreft, J.U. (2004). Biofilms promote altruism. *Microbiology* **150**, 2751-2760.

Kreth, J., Merritt, J., Shi, W., Qi, F. (2005). Competition and coexistence between *Streptococcus mutans* and *Streptococcus sanguinis* in the dental biofilm. *J Bacteriol* **187**, 7193-7203.

Kunduru, M.R., Pometto, A.L. (1996). Continuous ethanol production by *Zymomonas mobilis* and *Saccharomyces cerevisiae* in biofilm reactors. *J Ind Microbiol* **16**, 249-456.

Lau, J., Tran, C., Licari, P., Galazzo, J. (2004). Development of a high cell-density fed-batch bioprocess for the heterologous production of 6-deoxyerythronolide B in *Escherichia coli. J Biotechnol* **110**, 95-103.

LeBlanc, D., Lee, L., Inamine, J. (1991). Cloning and nucleotide base sequence analysis of a spectinomycin adenyltransferase AAD(9) determinant from *Enterococcus faecalis*. *Antimicrob Agents and Chemother* **35**, 1804-1810.

Lee, SY. (1996). High cell-density culture of *Escherichia coli. Trends Biotechnol* **14**, 98-105.

Leriche, V., Briandet, R., Carpentier, B. (2003). Ecology of mixed biofilms subjected daily to a chlorinated alkaline solution: spatial distribution of bacterial species suggests a protective effect of one species to another. *Environ Microbiol* **5**, 64-71.

Lescure, P., Meas-Yedid, V., Dupoisot, H., Stamon, G. (1999). Color segmentation on biological microscope images. Proceeding of SPIE, *Application of Artificial Neural Networks in Image Processing* **4**, 182-93.

Lewis, K. (2005). Persister cells and the riddle of biofilm survival. *Biochemistry (Mosc)* **70**, 267-274.

Li, Y., Ku, C.Y., Xu, J., Saxena, D., Caufield, P.W. (2005). Survey of oral microbial diversity using PCR-based denaturing gradient gel electrophoresis. *J Dent Res* **84**, 559-564.

Lin WJ, Lo WT, Chu CC, Chu ML, Wang CC. (2006). Bacteriology and antibiotic susceptibility of community-acquired intra-abdominal infection in children. J Microbiol Immunol Infect **39**, 249-254.

Littmann, E., Ritter, H. (1997). Adaptive color segmentation - a comprehension of neural and statistical methods. *IEEE Trans Neural Network* **8**, 175-85.

Livermore, D., Moosdeen, F., Lindridge, M., Khog, P., Williams, J. (1986). Behaviour of TEM-1 beta -lactamase as a resistance mechanism to ampicillin, mezlocillin and azlocillin in *Escherichia coli*. J Antimicrobl Chemother **17**, 139-146.

Lu-Chau, T.A., Guillan, A., Nunez, M.J., Roca, E., Lema, J.M. (2004). Anaerobic and aerobic continuous cultures of *Saccharomyces cerevisiae*: comparison of plasmid stability and EXG1 gene expression. *Bioprocess Biosyst Eng* **26**, 159-163.

Mateus, C., Crow, S.A., Ahearn, D.G. (2004). Adherence of *Candida albicans* to silicone nduces immediate enhanced tolerance to fluconazole. *Antimicrob Agents Chemother* **48**, 3358-3366.

Molin, S., Tolker-Nielsen, T. (2003). Gene transfer occurs with enhanced efficiency in biofilms and induces enhanced stabilization of the biofilm structure. *Curr Opin in Biotechnol* **14**, 255-261.

Niu, C., Gilbert, E.S. (2004). Colorimetric method for identifying plant essential oil components that affect biofilm formation and structure. *Appl Environ Microbiol* **70**, 6951-6956.

O'Callaghan, C.H., Morris, A., Kirby, S.M., Shingler, A.H. (1972). Novel method for detection of beta-lactamases by using a chromogenic cephalosporin substrate. *Antimicrob Agents Chemother* **1**, 283-288.

O'Connell, H.A., Kottkamp, G.S., Eppelbaum, J.L., Stubblefield, B.A., Gilbert, S.E., Gilbert, E.S. (2006). Influences of biofilm structure and antibiotic resistance mechanisms on indirect pathogenicity in a model polymicrobial biofilm. Appl Environ Microbiol **72**, 5013-5019.

Ong, S., Yeo, N., Lee, K., Venkatesh, Y., Cao, D. (2002). Segmentation of color images using a two-stage self-organizing network. *Image and Vision Computing* **20**, 279-289.

O'Toole, G.A., Kolter, R. (1998). Flagellar and twitching motility are necessary for *Pseudomonas aeruginosa* biofilm development. *Mol Microbiol* **30**, 295-304.

Palmer, R.J., Kazmerzak, K., Hansen, M.C., Kolenbrander, P.E. (2001). Mutualism versus independence: strategies of mixed-species oral biofilms in vitro using saliva as the sole nutrient source. *Infect Immu.* **69**, 5794-5804.

Parsek, M.R., Singh, P.K. (2003). Bacterial biofilms: an emerging link to disease pathogenesis. *Annu Rev Microbiol* **57**, 677-701.

Paterson, D.L. (2006). The epidemiological profile of infections with multidrug-resistant *Pseudomonas aeruginosa* and *Acinetobacter* species. *Clin Infect Dis* **43**, S43-S48.

Patterson, G., Knobel, S., Sharif, W., Kain, S., Piston, D. (1997). Use of the green fluorescent protein and its mutants in quantitative fluorescence microscopy. *Biophys J* **73**, 2782-2790.

Peietikainen, M. (1996). Accurate color discrimination with classification based on feature distributions. *International Conference on Pattern Recognition*, 833-838.

Pickering, S., Bayston, R., Scammell, B. (2003). Electromagnetic augmentation of antibiotic efficacy in infection of orthopaedic implants. *J Bone Joint Surg Br.* **85**, 588-593.

Piddock, L.J. (2006). Multidrug-resistance efflux pumps - not just for resistance. *Nat Rev Microbiol* **4**, 629-636.

Puri, J., Mishra, B., Mal, A., Murthy, N.S., Thakur, A., Dogra, V., Singh, D. (2002). Catheter associated urinary tract infections in neurology and neurosurgical units. *J Infect* **44**, 171-175.

Rachid, S., Niki, N., Nishitani, H., Nakamura, S., Mori, S. (1997). Segmentation of sputum color image for lung cancer diagnosis. *Proceedings of the 1997 International Conference on Image Processing* **1**, 243-246.

Rahal, J.J. (2006). Novel antibiotic combinations against infections with almost completely resistant *Pseudomonas aeruginosa* and *Acinetobacter* species. *Clin Infect Dis* **43**, S95-S99.

Rao, D., Webb, J.S., Kjelleberg, S. (2005). Competitive interactions in mixed-species biofilms containing the marine bacterium *Pseudoalteromonas tunicata.* Appl Environ Microbiol **71**, 1729-1736.

Rasmussen, K., Lewandowski, Z. (1998). Microelectrode measurements of local mass transport rates in heterogeneous biofilms. *Biotechnol Bioeng* **59**, 302-309.

Reisner, A., Haagensen, J.A., Schembri, M.A., Zechner, E.L., Molin, S. (2003). Development and maturation of *Escherichia coli* K-12 biofilms. *Mol Microbiol* **48**, 933-946.

Reisner, A., Holler, B.M., Molin, S., Zechner, E.L. (2006). Synergistic effects in mixed *Escherichia coli* biofilms: conjugative plasmid transfer drives biofilm expansion. *J Bacteriol* **188**, 3582-3588.

Remans, T., Schenk, P., Manners, J., Grof, C., Elliott, A. (1999). A protocol for fluorometric quantification of mGFP5-ER and sGFP(S65T) in transgenic plants. *Plant Molectular Biology Reptr* **17**, 385-395.

Riesenberg, D., Guthke, R. (1999). High-cell density cultivation of microorganisms. *Applied Microbiol and Biotechnol* **51**, 422-430.

Riley, M.A., Gordon, D.M. (1999). The ecological role of bacteriocins in bacterial competition. *Trends Microbiol* **7**, 129-133.

Ronald, A. (2003). The etiology of urinary tract infection: traditional and emerging pathogens. *Dis Mon* **49**, 71-82.

Rossolini, G.M., Mantengoli, E. (2005). Treatment and control of severe infections caused by multiresistant *Pseudomonas aeruginosa*. *Clin Microbiol Infect* **11,** S17-S32.

Ryan, W., Parulekar, S. (1991). Recombinant protein synthesis and plasmid instability in continuous cultures of *Escherichia coli* JM103 harboring a high copy number plasmid. *Biotechnol Bioeng* **37**, 415-429.

Schembri, M.A., Kjaergaard, K, Klemm, P. (2003). Global gene expression in *Escherichia coli* biofilms. *Mol Microbiol* **48**, 253-27.

Sharp, R.R., Bryers, J.D., Jones, W.G. (1998). Activity and stability of a recombinant plasmid-borne TCE degradative pathway in biofilm cultures. *Biotechnol Bioeng* **59**, 318-327.

Shen, H., Wang, Y.T. (1993). Characterization of enzymatic reduction of hexavalent chromium by *Escherichia coli* ATCC 33456. *Appl Environ Microbiol* **59**, 3771-3777.

Shintani, H., Hayashi, F., Sakakibara, Y., Kurosu, S., Miki, A., Furukawa, T. (2006). Relationship between the contamination of the nurse's caps and their period of use in terms of microorganism numbers. *Biocontrol Sci* **11**, 11-16.

Stewart, P.S., Roe, F., Rayner, J., Elkins, J.G., Lewandowski, Z., Ochsner, U.A., Hassett, D.J. (2000). Effect of catalase on hydrogen peroxide penetration into *Pseudomonas aeruginosa* biofilms. Appl Environ Microbiol **66**, 836-838.

Stone, G., Wood, P., Dixon, L., Keyhan, M., Matin, A. (2002). Tetracycline rapidly reaches all the constituent cells of uropathogenic *Escherichia coli* biofilms. *Antimicrobial Agents and Chemother* **46**, 2458-2461.

Stoodley, P., Sauer, K., Davies, D.G., Costerton, J.W. (2002). Biofilms as complex differentiated communities. *Annu Rev Microbiol* **56**, 187-209.

Triandafillu, K., Balazs, D., Aronsson, B.O., Descouts, P., Tu Quoc, P., van Delden, C., Mathieu, H.J., Harms, H. (2003). Adhesion of *Pseudomonas aeruginosa* strains to untreated and oxygen-plasma treated poly(vinyl chloride) (PVC) from endotracheal intubation devices. *Biomaterials* **24**, 1507-1518.

Tsien, R. (1998). The green fluorescent protein. *Annu Rev Biochem* **67**, 509-544.

Umesh, A.P,. Chaudhuri, B. (1998). Analysis of volumetric images of filamentous bacteria in industrial sludge. *Proceedings of the Fourteenth International Conference on Pattern Recognition* **2**, 1735-1737.

Von Canstein, H., Kelly, S., Li, Y., Wagner-Dobler, I. (2002). Species diversity improves the efficiency of mercury-reducing biofilms under changing environmental conditions. *Appl Environ Microbiol* **68**, 2829-2837.

Watnick, P., Kolter, R. (2000). Biofilm, city of microbes. *J Bacteriol* **182**, 2675-2679.

Wei, Z.Q., Chen, Y.G., Yu, Y.S., Lu, W.X., Li, L.J. (2005). Nosocomial spread of multi-resistant *Klebsiella pneumoniae* containing a plasmid encoding multiple beta-lactamases. *J Med Microbiol* **54**, 885-888.

Wilke, M.S., Lovering, A.L., Strynadka, N.C. (2005). Beta-lactam antibiotic resistance: a current structural perspective. *Curr Opin Microbiol* **8**, 525-533.

Wright, G.D. (2005). Bacterial resistance to antibiotics: enzymatic degradation and modification. *Adv Drug Deliv Rev* **57**, 1451-1470.

Xu, T., Petridou, S., Lee, E., Roth, E., Vyavahare, N., Hickman, J., Boland, T. (2004). Construction of high-density bacterial colony arrays and patterns by the ink-jet method. *Biotechnol Bioeng* **85**, 29-33.

Yazdani, S., Mukherjee, K. (2002). Continuous-culture studies on the stability and expression of recombinant streptokinase in *Escherichia coli*. *Bioprocess Biosyst Eng* **24**, 341-346.

Zhang, C., Wang, P. (2000). A new method of color image segmentation based on intensity and hue clustering. *15th International Conference on Pattern Recognition* **3**, 613-616.

Zhong, X., Yan, H. (2000). Color image segmentation using color space analysis and fuzzy clustering. *Proceedings of IEEE Signal Processing Society Workshop on Neural Networks for Signal Processing X* **2**, 624-633.

APPENDIX A

The 2004 International Conference on Mathematics and Engineering Techniques in Medicine and Biological Sciences (METMBS '04), Las Vegas, NV, USA.

MULTI RESOLUTION IMAGE SEGMENTATION FOR QUANTIFYING SPATIAL HETEROGENEITY IN MIXED POPULATION BIOFILMS

Saeid Belkasim, Jian Gu, Gordana Derado, Eric Gilbert and Heather O'Connell

A.1. ABSTRACT

Mutualistic interactions among microorganisms in multispecies biofilms contribute to economically relevant processes, ranging from tooth decay to wastewater treatment. Understanding interactions in multispecies biofilms may contribute to treatment of polymicrobial biofilm infections as well as rational design of engineered biofilms. Multi resolution image segmentation offers many powerful tools for the analysis of such interactions. The Biofilm Image Segmentation (BIS) algorithm has been developed to assist in quantifying the spatial heterogeneity of microbial populations within biofilms. The algorithm deploys multi resolution clustering and segmentation tools to measure the distance between clusters of homogeneous microbial populations within two-dimensional sections of biofilms visualized by confocal laser scanning microscopy. The concept underlying multi resolution image segmentation is that the number of clusters will be larger for higher resolution image and smaller for lower resolution image. This hierarchical structure analysis can be used to simplify the problem in well-mixed

populations. The algorithm combines Fuzzy C-Means, SOM and LVQ Neural networks to segment and identify clusters. The outcome of the segmentation is quantified by the number of clusters of each kind of microorganism within sections of the biofilm, and the centroid distances between the identified clusters. Initial experimental evaluations of the algorithm showed its effectiveness in analyzing the distribution of microbial populations in the substratum layer of a model two-member biofilm comprised of an ampicillin resistant and an ampicillin sensitive strain of *Escherichia coli*, each with a distinct red or green fluorescent label.

A.2. INTRODUCTION

Biofilms are communities of microorganisms attached to surfaces and develop a complex heterogeneous three-dimensional structure. Multispecies biofilms occur in diverse environments, and may foster commensal and mutualistic (beneficial) interactions, often by processes of nutrient exchange or detoxification (Chen & Li 1999; Costerton *et al.*, 1995; Gilbert *et al.*, 2003). Understanding interactions in multispecies biofilms may contribute to treatment of polymicrobial biofilm infections as well as rational design of engineered biofilms (Rachid *et al.*, 1997; Umesh & Chaudhuri, 1998). Analysis of microbial biofilms by confocal laser scanning microscopy (CLSM) yields a stack of digital images that can be combined to give a three-dimensional view of the biofilm, and that are also amenable to quantitative analysis. Information on the relationships among bacteria in multispecies biofilms can be obtained from CLSM image stacks by combining pattern recognition and image processing techniques such as clustering and segmentation. Multi-dimensional clustering methods are simple and

powerful tools for classifying and segmenting pixels. Although most of the clustering methods require the number of clusters be known, that requirement does not represent any burden for this work since the maximum number of clusters in all biofilm bacteria images is always three (Gauch & Hsia, 1992; Gordan *et al.,* 2002). The k-means clustering algorithm and fuzzy c-means clustering algorithm are the most popular techniques applied in image processing (Zhong & Yan, 2000). Other techniques such as artificial neural networks are extensively used for pattern recognition. Their extended parallel structure is particularly useful for classification and clustering (Ahmed *et al.,* 2002; Ji & Park, 1998; Kanungo *et al.,* 2002; Littmann & Ritter 1997; Peietikainen, 1996; Zhang & Wang, 2000). Neural networks can be used to represent a very complex nonlinear system. Some self-organizing neural networks such as Self Organizing Maps (SOM) and Learning Vector Quantization Neural Networks (LVQNN) have been applied for image segmentation and their results are satisfying (Kamel *et al.,*2001; Lescure *et al.,* 1999). The Self-Organizing Map neural network is a powerful classifier for data clustering. The most interesting feature of SOM is its ability of unsupervised learning, which means the training of the network is entirely data driven and the target outputs are not needed which is a very useful feature when the amount of training data is limited or not available. Multi resolution image segmentation offers many powerful tools for simplifying the biofilm data clustering and segmentation. Biofilm Image Segmentation can be used to assist in quantifying the spatial heterogeneity of microbial populations within biofilms. Multi resolution clustering combined with image segmentation can be used to measure the distance between clusters of homogeneous microbial populations

within two-dimensional sections of biofilms visualized by confocal laser scanning microscopy. The concept underlying multi resolution image segmentation is that the number of clusters will be larger for higher resolution image and smaller for lower resolution image. This hierarchical structure analysis can be used to simplify the problem in well-mixed populations of biofilm bacteria images. Capitalizing on the features of each of the previous techniques we developed an algorithm named BISS (Biofilm Image Segmentation Software) that combines FCM, LVQ and SOM methods to perform image clustering and segmentation. The algorithm initiates an analysis by segmenting images using a Fuzzy C-Means approach followed by two stage SOM or LVQ Neural network to identify clusters. The outcome of the segmentation is quantified by the number of clusters of each kind of microorganism within sections of the biofilm, and the centroid distances between the identified clusters. Initial experimental evaluations of the algorithm showed its effectiveness in analyzing the distribution of microbial populations in the substratum layer of a model two-member biofilm comprised of an ampicillin resistant and an ampicillin sensitive strain of *Escherichia coli,* each with a distinct red or green fluorescent label. Section 2 of this paper describes the multi resolution border extraction. Performance evaluation is given in section 3, followed by experimental results and conclusions in sections 4 and 5.

A.3. IMAGE ANALYSIS BASED ON MULTI RESOLUTION BORDER EXTRACTION

The analysis of all objects in the image can be very tedious and time consuming particularly if all the details small or large are considered. In this section we outline a

scheme that selects the amount of details to be considered based on their size. Larger objects are normally more visible and dominate the image while smaller or finer details are less visible and may be overshadowed by larger objects.

This multiresolution image analysis scheme is based on extracting all objects in the image using their borders or contours. The size of contour can be used to define the level of resolution and hence the analysis. Fine details are represented by small size contours while coarser details are represented by larger contours or borders. The simplest way to extract the borders in an image is to binarize the image using optimum thresholding and perform contour tracking or border following procedure (Belkasim ***et al.,*** 1995). The optimum thresholding procedure is needed to efficiently segment the image into objects and background (Belkasim ***et al.,*** 2003).

The methodology for the segmentation procedure can be outlined in the following:

1- Optimally threshold the image to transform it to binary level image.

2- Perform edge detection and border following routines to produce the borders of each object.

3- Label the objects; starting with top left pixel, traversing from left to right and top to bottom.

4- Build a tree structure for the traced object borders as shown in Fig.1 and Fig. 2 (**Figures A.1 and A.2)**.

5- The root of the tree represents the large bordered objects.

6- The leaves represent the smallest contours or borders of objects.

7- Borders can be used to extract objects using their labels.

The object extraction procedure is based on matching the inner space of the closed contour to the corresponding space in the original image and copying it to a new object array. This can be easily achieved by filling the border inner space with pixel values of unity and the outer pixels with zero values. The multiplication of the two image arrays pixel by pixel will result of an object extraction of non-zero values.

A.4. PERFORMANCE EVALUATION

An image segmentation problem is basically one of psychophysical perception (Cheng *et al.,* 2001). The psycho-visual response in judging the accuracy of segmentation results may be quite different from person to person, even for those experts who have a priori knowledge about the original image. Many researchers used reference images to evaluate different segmentation results. However, an ideally segmented reference image may not be available in many cases. An evaluation criterion based on the sum of the pair-wise inter-cluster distance is very appropriate for judging the success of the segmentation of bacteria images (Basu *et al.*,2004; Ong *et al.*,2002).

The degree of "mixedness" of populations is one of many important parameters that need to be analyzed to study the behavior of biofilms. The different states of "mixedness" or patchiness among populations are categorized by labeling regions or segments of bacteria in mixed population biofilms.

The basic analysis is based on the assumption that the degree of "mixedness" of two populations can be described by the average distance between neighboring clusters of different color. Less mixed populations will have larger clusters, and thus longer inter-

cluster distances. Measuring the centroids of each cluster is needed to determine the inter cluster distances.

A.5. EXPERIMENTAL RESULTS

The image segmentation algorithms described in the previous sections have been implemented using Matlab for the segmentation and analysis of several bacteria images. The results from the segmentation stage are used for identifying the various levels of mixedness among each patch of biofilm data. The developed image segmentation software package (BISS) measures the distance between clusters of homogeneous microbial populations within two-dimensional sections of biofilms visualized by confocal laser scanning microscopy. A screen shot of the main window of BISS is displayed in Figure.6. The concept underlying BISS is that the intercluster distance will be larger for "patchy" biofilms and smaller for well-mixed populations. BISS initiates an analysis by segmenting images using a Fuzzy C-Means approach, followed by training a neural network to identify clusters. BISS calculates the centroid distances between the identified clusters which can then be used to analyze the image. The cluster identification process is preceded with the multi resolution analysis scheme outlined in section 3. The benefit of the multi resolution border extraction step can be seen from Table 1 where the number of clusters is decreasing as the resolution level is decreased. Figure 3 **(Figure A.3)** shows the three resolution levels that relates to the data in Table 1 **(Table A.1)**. The smaller number of cluster results in shorter training period for the neural network.

Several color biofilm bacteria images were extracted from slices of 512×512 color scans obtained by confocal scanning laser microscope (CSLMs). Each image, as shown in Fig.3, contains three parts; the red part (*E. coli* ATCC 33446 pUCSpec), the green part (*E. coli* ATCC 33446 pEGFP) and the dark background. The first major step is to separate these parts with the minimum overlap or error. The process starts by selecting a suitable color space, then applying the multi resolution segmentation technique.

In an initial study, BISS was used to evaluate the distribution of microbial populations in the substratum layer of a model two-member biofilm comprised of an ampicillin resistant and an ampicillin sensitive strain of *Escherichia coli*, each with a distinct red or green fluorescent label. The analysis indicated the presence of smaller clusters (centroid distance, 5 ± 1 microns) for biofilms cultivated in Luria-Bertani (LB) broth containing 51 ppm ampicillin, and larger clusters (centroid distance, 21 ± 12 microns) for biofilms grown in LB broth only. Sample images are shown in Fig. 4 and 5 **(Figures A.4, A.5)**. The average intercluster distances were calculated and are shown below superimposed on the images used for the analysis.An algorithm has been designed and implemented to perform the biofilm analysis A 2D confocal microscope image of a biofilm is imported into the Biofilm Image Segmentation Software (BISS). The image segmentation program which is based on combining several clustering techniques, defines each pixel in terms of red, green or black color. This process differentiates biomass and empty space. BISS identifies clusters of each population based on patterns developed during the neural network training stage. BISS segment the image into separate black, red and green populations. The multi resolution border selection stage

simplifies the clustering problem by reducing the number of clusters present for each population. Upon identifying the required clusters, the cluster centroids and intercluster distances can be computed.

The number of clustered pixels and the coordinates of the centroids for red, green and black pixels are listed in Table 2 **(Table A.2)**. This table also lists the summation of the Euclidean distances between the cluster centroids obtained by different segmentation methods. These results are based on the assumption that better separation between cluster centroids leads to better segmentation, which means a high value will indicate the superiority of a method. Table 3 **(Table A.3)** represents the misclassified pixels error rate in comparison to the optimal case which represents supervised assignments of pixels. The table shows the LVQ neural network achieved the lowest misclassification rate.

A.6. CONCLUSIONS

A multi resolution image analysis utilizing image contours as boundaries for extracting objects at multi resolution levels has been successfully implemented. The scheme reduced the complexity of the segmentation problem considerably and simplified the clustering process.

Several clustering algorithms have been tested in RGB and HSV color spaces for segmenting the bacteria biofilm images. Extensive and rigorous testing of the various algorithms in several combinations of color components was used to evaluate their effectiveness. A two-stage SOM/LVQ clustering algorithm was introduced and evaluated. The test results indicate that the two stage neural network is very effective in clustering the biofilm images. The neural network LVQ/SOM has very close results for

both the HV or RG color planes. The RG plane is more effective than the HV plane for the FCM method.

A possible future improvement of this research is to combine the present segmentation model with image retrieval and other database query systems to efficiently build a biofilm bacteria database to be used in testing and analyzing larger amount of biofilm data. Another useful extension is to implement an algorithm to extract and analyze spatial features. These features can be used to categorize and retrieve the different clusters of biofilms. This step involves the selection of best features for cluster recognition, the automation of cluster enumeration, reduction of background noise, the exclusion of individual cells not associated with clusters. Development of three dimensional analysis utilizing multiple image stacks or frames is also among the future aims of this research.

Table A.1. The effect of changing the resolution level on the number of detected clusters.

Resolution level	Image size in pixels	Number of clusters
1	512x512	654
2	256x256	349
3	128x128	155

Table A.2. Number of pixels, centroids and sum of distances with an optimally clustered image.

Method	Color Space	Red Channel		Green Channel		Background		Total distance
		pixels	centroid	pixels	centroid	pixels	centroid	
FCM	RG	28360	(0.181,0.334)	13874	(0.130,0.723)	219910	(0.167,0.029)	1.39
	HV	89518	(0.086,0.037)	26709	(0.154,0.587)	145917	(0.218,0.047)	1.23
LVQ	RG	17918	(0.092,0.510)	13582	(0.241,0.542)	230644	(0.168,0.041)	1.13
	HV	15779	(0.085,0.547)	14919	(0.241,0.521)	231446	(0.167,0.041)	1.16
SOM	RG	16640	(0.072,0.504)	21897	(0.225,0.476)	223607	(0.168,0.032)	1.08
	HV	11268	(0.070,0.615)	12899	(0.222,0.609)	237977	(0.168,0.047)	1.29

Table A.3. Misclassification percentages compared.

LVQ (RGB)	FCM(HSV)	SOM (RGB)
6.94 %	8.59 %	14.14 %

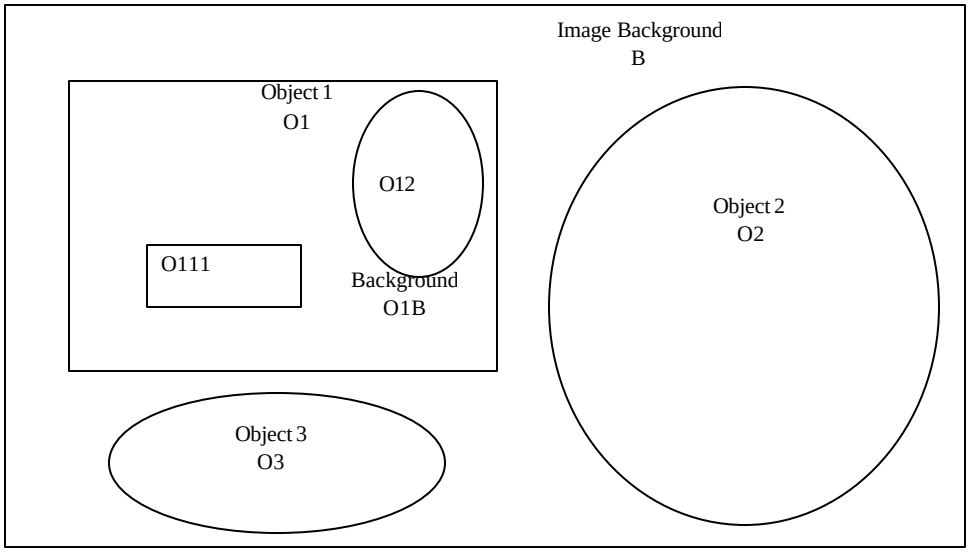

Figure A.1. The multi resolution border segmentation process

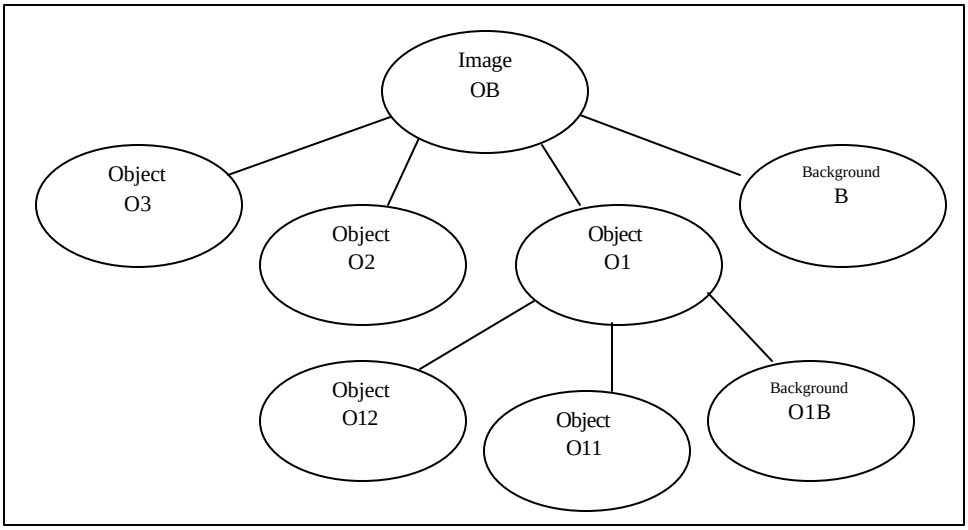

Figure A.2. The tree structure of the segmented image.

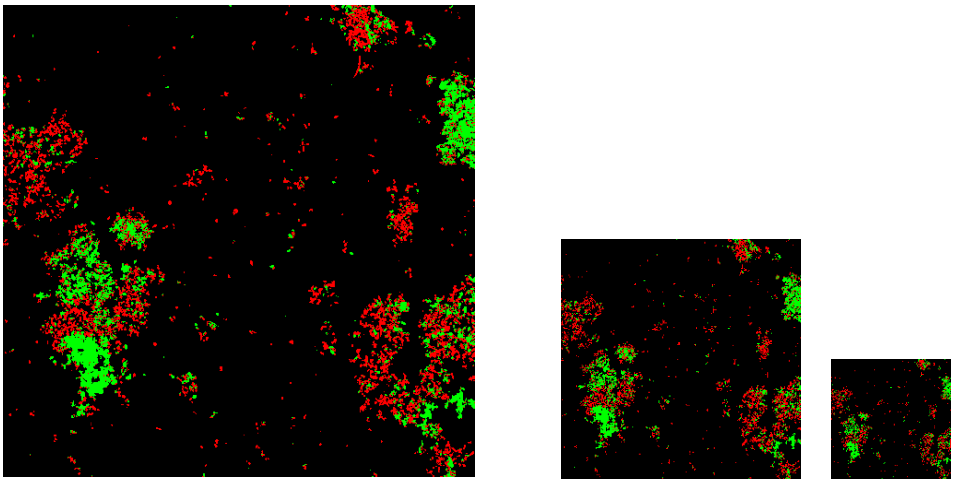

Figure A.3. Image sizes corresponding to 512x512, 256x256 and 128x128 for three resolution levels 1,2 and 3 respectively. Level 1 represents an original slice of a biofilm bacteria image taken by CSLM.

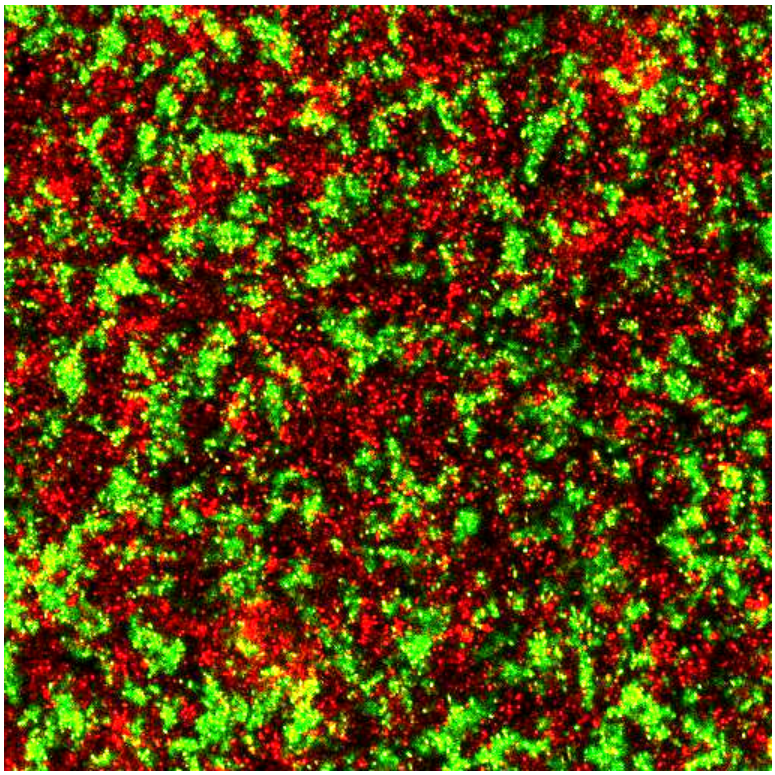

Fig A.4. The result of initial segmentation of biofilm bacteria image containing 0 ppm ampicillin; cluster centroids of 21 ± 12 micron.

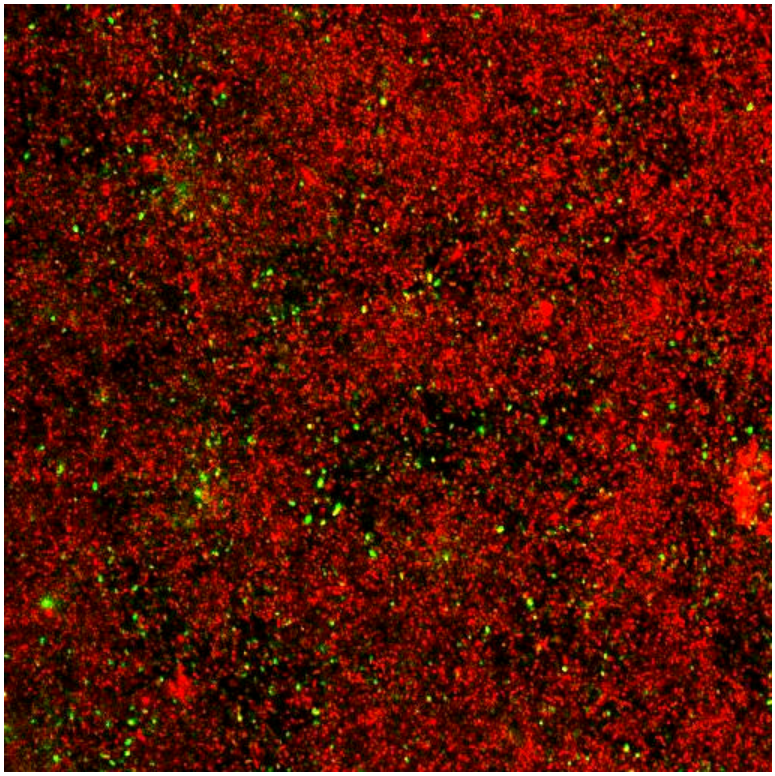

Figure A.5. The result of initial segmentation of biofilm bacteria image containing 50.8 ppm ampicillin; cluster centroids of 5 ± 1 micron.

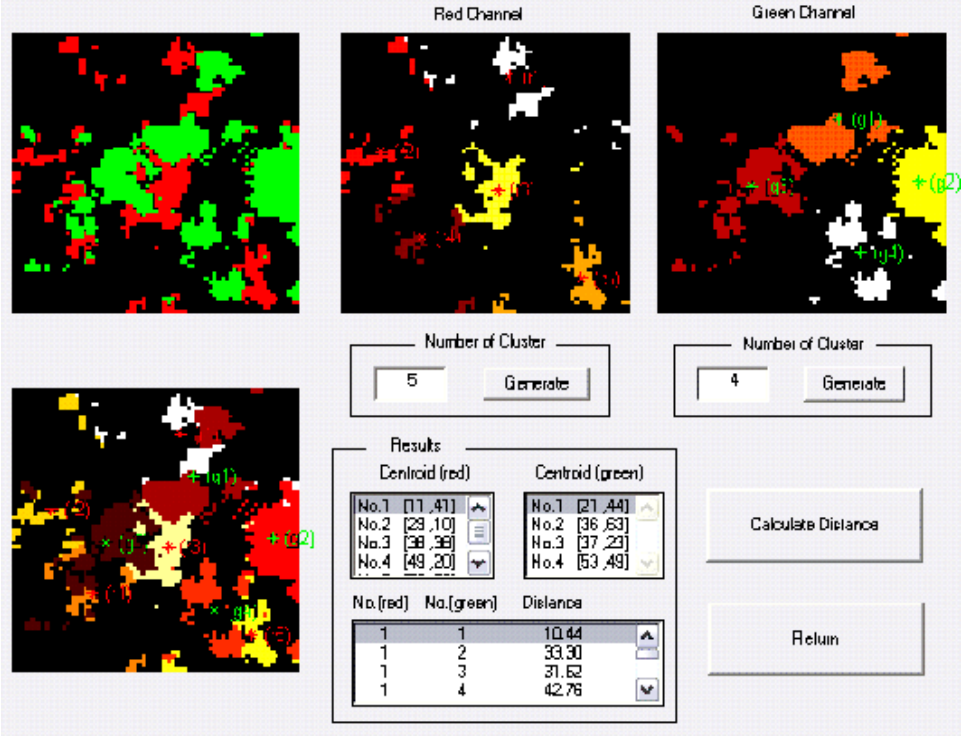

Figure A.6. Screen shot of BISS window interface.

APPENDIX B

Proceedings of the 47th IEEE International Midwest Symposium on Circuits and Systems, July 25-28, 2004, Hiroshima, Japan.

THE EFFECTIVENESS OF MULTI RESOLUTION IMAGE SEGMENTATION FOR MEASURING SPATIAL HETEROGENEITY IN MIXED POPULATION BIOFILMS

S. Belkasim, G. Derado, E. Gilbert and H. O'Connell

B.1 ABSTRACT

Multi resolution image segmentation offers many powerful tools for the analysis of interactions in mixed populations of biofilms. Multi resolution clustering and segmentation tools has been developed to measure the distance between clusters of homogeneous microbial populations within two-dimensional sections of biofilms visualized by confocal laser scanning microscopy. The concept underlying multi resolution image segmentation is that the number of clusters will be larger for higher resolution image and smaller for lower resolution image. This hierarchical structure analysis can be used to simplify the problem in well-mixed populations. The algorithm combines Fuzzy C-Means, SOM and LVQ Neural networks to segment and identify clusters. The outcome of the segmentation is quantified by the number of clusters of each kind of microorganism within sections of the biofilm, and the centroid distances between

the identified clusters. Experimental evaluations of the algorithm showed its effectiveness in analyzing mixed populations of biofilms

B.2 INTRODUCTION

Biofilms are biological communities of microorganisms attached to surfaces and develop a complex heterogeneous three-dimensional structure. Understanding interactions in multispecies biofilms may contribute to treatment of polymicrobial biofilm infections as well as rational design of engineered biofilms (Chen & Li, 1999; Costerton *et al.*,1995; Gauch & Hsia, 1992; Gilbert *et al.*,2003; Rachid *et al.*,1997; Umesh & Chaudhuri, 1998). Analysis of microbial biofilms by confocal laser scanning microscopy (CLSM) yields a stack of digital images that can be combined to give a three-dimensional view of the biofilm. Information on the relationships among bacteria in multispecies biofilms can be obtained from CLSM image stacks by combining pattern recognition and image processing techniques such as clustering and segmentation. Multi-dimensional clustering methods are simple and powerful tools for classifying and segmenting pixels. Although most of the clustering methods require the number of clusters be known, that requirement does not represent any burden for this work since the maximum number of clusters in all biofilm bacteria images is always three (Gordan *et al.*,2002). The k-means clustering algorithm and fuzzy c-means clustering algorithm are the most popular techniques applied in image processing (Zhong & Yan, 2000). Other techniques such as artificial neural networks are extensively used for pattern recognition. Their extended parallel structure is particularly useful for classification and clustering (Littmann & Ritter 1997; Peietikainen, 1996). Neural networks can be used to represent a very complex

nonlinear system. Some self-organizing neural networks such as Self Organizing Maps (SOM) and Learning Vector Quantization Neural Networks (LVQNN) have been applied for image segmentation and their results are satisfying (Kamel *et al.*, 2001; Lescure *et al.*, 1999). The Self-Organizing Map neural network is a powerful classifier for data clustering. The most interesting feature of SOM is its ability of unsupervised learning, which means the training of the network is entirely data driven and the target outputs are not needed which is a very useful feature when the amount of training data is limited or not available. Multi resolution image segmentation offers many powerful tools for simplifying the biofilm data clustering and segmentation. Biofilm Image Segmentation can be used to assist in quantifying the spatial heterogeneity of microbial populations within biofilms. Multi resolution clustering combined with image segmentation can be used to measure the distance between clusters of homogeneous microbial populations within two-dimensional sections of biofilms visualized by confocal laser scanning microscopy. The concept underlying multi resolution image segmentation is that the number of clusters will be larger for higher resolution image and smaller for lower resolution image. This hierarchical structure analysis can be used to simplify the problem in well-mixed populations of biofilm bacteria images. Capitalizing on the features of each of the previous techniques we developed an algorithm named BISS (Biofilm Image Segmentation Software) that combines FCM, LVQ and SOM methods to perform image clustering and segmentation. The algorithm initiates an analysis by segmenting images using a Fuzzy C-Means approach followed by two stage SOM or LVQ Neural network to identify clusters. The outcome of the segmentation is quantified by the number of clusters

of each kind of microorganism within sections of the biofilm, and the centroid distances between the identified clusters. Initial experimental evaluations of the algorithm showed its effectiveness in analyzing the distribution of microbial populations in a model two-member biofilm comprised of an ampicillin resistant and an ampicillin sensitive strain of *Escherichia coli,* each with a distinct red or green fluorescent label. Section 2 of this paper describes the multi resolution border extraction. Performance evaluation is given in section 3, followed by experimental results and conclusions in sections 4 and 5.

B.3. MULTI RESOLUTION BORDER EXTRACTION

The analysis of all objects in the image can be very tedious and time consuming particularly if all the details small or large are considered. In this section we outline a scheme that selects the amount of details to be considered based on their size. Larger objects are normally more visible and dominate the image while smaller or finer details are less visible and may be overshadowed by larger objects.

This multiresolution image analysis scheme is based on extracting all objects in the image using their borders or contours. The size of contour can be used to define the level of resolution and hence the analysis. Fine details are represented by small size contours while coarser details are represented by larger contours or borders. The simplest way to extract the borders in an image is to binarize the image using optimum thresholding and perform contour tracking or border following procedure (Belkasim ***et al.,*** 1995). The optimum thresholding procedure is needed to efficiently segment the image into objects and background (Belkasim ***et al.,*** 2003).

The methodology for the segmentation procedure can be outlined in the following:

1. Optimally threshold the image to transform it to binary level image.
2. Perform edge detection and border following routines to produce the borders of each object.
3. Label the objects; starting with top left pixel, traversing from left to right and top to bottom.
4. Build a tree structure for the traced object borders as shown in Fig.1 **(Figure B.1)** and Fig. 2 **(Figure B.2)**.
5. The root of the tree represents the large bordered objects.
6. The leaves represent the smallest contours or borders of objects.
7. Borders can be used to extract objects using their labels **(Figure B.3)**.

The object extraction procedure is based on matching the inner space of the closed contour to the corresponding space in the original image and copying it to a new object array. This can be easily achieved by filling the border inner space with pixel values of unity and the outer pixels with zero values. The multiplication of the two image arrays pixel by pixel will result of an object extraction of non-zero values.

B.4 BIOFILM IMAGE SEGMENTATION AND CLUSTERING

In this section we explain our edge based technique for the biofilm images segmentation and clustering. We use the pixel neighbourhood elements for determining the pixel connectivity and performing image segmentation.

The basic algorithm consists of the following steps:

1. The original image is converted into RGB color space and processed to include only red, green (bacteria) and black (background) color **(Figure B.4.)**.
2. Smoothing of the image is preformed first, followed by a statistical analysis of the 3x3 window of each image pixel. Each pixel is assigned the value of the dominant color (red, green, or black) in its 3x3 neighborhood
3. Borders (contours) of the "potential clusters" are detected for the red or green image component by extracting all contours using the contour tracking (border following) procedure outlined in (Belkasim et al. 1995).
4. After the borders are detected and border pixels for each detected "cluster" registered, a step in which interiors of the clusters are registered is preformed. In this step some of the "potential" clusters, which normally represent holes or voids inside bigger clusters are also detected and removed.
5. Once all clusters are detected, they are categorized into "small", "large", and "medium" size clusters based on their size (not the border size, but the total size). The category is determined in comparison with the largest cluster detected **(Figure B.6, Figure B.7, Figure B.8)**.
6. The centroids and the distances of the centroids among the clusters in each of the categories are calculated.

Step two is performed to reduce the number of "too mixed" areas. Some areas consist of two many individual bacteria and are not of much interest in studying the "global" behavior and level of "mixedness" of the two species of bacteria. This step also reduces the small gaps which allow merging of dissimilar regions (i.e. clusters of different color). Another important reason for this step is to reduce the complexity of the computations to be performed later.

Step three is the most computationally expensive step. Parallelization of this step would contribute the most to speeding of the algorithm. However, it is not easy to parallelize it.

The procedure is repeated for each bacteria (color) on the same (original) image, and is used to calculate the average distances between the clusters of "opposite" colors. This distance is used in the analysis of the level of "mixedness" and the behaviour of the two mixed bacteria under different treatment conditions.

The evaluation stage is quite complex and difficult in particular the part that deals with evaluating the clustering and segmentation success. This is due to the fact that an image segmentation problem is basically one of psychophysical perception (Cheng *et al.*, 2001). The psycho-visual response in judging the accuracy of segmentation results may be quite different from person to person, even for those experts who have a priori knowledge about the original image. Many researchers used reference images to evaluate different segmentation results. However, an ideally segmented reference image may not be available in many cases. An evaluation criterion based on the sum of the pair-wise

inter-cluster distance is very appropriate for judging the success of the segmentation of bacteria images (Basu *et al.*, 2004; Ong *et al.*, 2002).

The degree of "mixedness" of populations is one of many important parameters that need to be analyzed to study the behavior of biofilms. The different states of "mixedness" or patchiness among populations are categorized by labeling regions or segments of bacteria in mixed population biofilms.

The basic analysis is based on the assumption that the degree of "mixedness" of two populations can be described by the average distance between neighboring clusters of different color. Less mixed populations will have larger clusters, and thus longer inter-cluster distances. Measuring the centroids of each cluster is needed to determine the inter cluster distances.

B.5 EXPERIMENTAL RESULTS

The image segmentation algorithms described in the previous sections have been implemented using Matlab for the segmentation and analysis of several bacteria images. The results from the segmentation stage are used for identifying the various levels of mixedness among each patch of biofilm data. The cluster identification process is preceded with the multi resolution analysis scheme outlined in section 3. The benefit of the multi resolution border extraction step can be seen from Table.1 where the number of clusters is decreasing as the resolution level is decreased. Figure 3 shows the three resolution levels that relates to the data in Table 1 **(Table B.1)**. The smaller number of cluster results in shorter training period for the neural network.

Several color biofilm bacteria images were extracted from slices of 512×512 color scans obtained by confocal scanning laser microscope (CSLMs). Each image, as shown in Fig.3 **(Figure B.3)**, contains three parts; the red part (*E. coli* ATCC 33456 pUCSpec), the green part (*E. coli* ATCC 33456 pEGFP) and the dark background. The first major step is to separate these parts with the minimum overlap or error. The process starts by selecting a suitable color space, then applying the multi resolution segmentation technique.

The distribution of microbial populations in the substratum layer of a model two-member biofilm comprised of an ampicillin resistant and an ampicillin sensitive strain of *Escherichia coli*, each with a distinct red or green fluorescent label has been analyzed. The image segmentation process which is based on combining several clustering techniques, defines each pixel in terms of red, green or black color. This process differentiates biomass and empty space. The multi resolution border selection stage simplifies the clustering problem by reducing the number of clusters present for each population. Upon identifying the required clusters, the cluster centroids and intercluster distances can be computed.

The number of clustered pixels and the coordinates of the centroids for red, green and black pixels are listed in Table 2 **(Table B.2)**. This table also lists the summation of the Euclidean distances between the cluster centroids obtained by different segmentation methods. These results are based on the assumption that better separation between cluster centroids leads to better segmentation, which means a high value will indicate the superiority of a method. The results of this table indicate that FCM is the one that gives

a higher separation and leads to better segmentation over the other two methods. The drawback is the in the complexity of the method and the processing time needed for this method. Using this method in a multistage clustering process may be a good choice that will use the benefits of both methods.

B.6 CONCLUSIONS

A multi resolution image analysis utilizing image contours as boundaries for extracting objects at multi resolution levels has been successfully implemented. The scheme reduced the complexity of the segmentation problem considerably and simplified the clustering process.

This research is at a preliminary stage. The next stage is to combine the present segmentation model with image retrieval and other database query systems to efficiently build a biofilm bacteria database to be used in testing and analyzing larger amount of biofilm data. Another useful extension is to implement an algorithm to extract and analyze spatial features. These features can be used to categorize and retrieve the different clusters of biofilms. This step involves the selection of best features for cluster recognition, the automation of cluster enumeration, reduction of background noise, the exclusion of individual cells not associated with clusters. Development of three dimensional analysis utilizing multiple image stacks or frames is also among the future aims of this research.

Table B.1. The effect of changing the resolution level on the number of detected clusters.

Resolution level	Image size in pixels	Number of clusters
1	512x512	654
2	256x256	349
3	128x128	155

Table B.2. Number of pixels, centroids and cluster separation distance

Method	Color Space	Red Clusters		Green Clusters		Euclidean distance
		pixels	centroid	pixels	centroid	
FCM	RG	28360	(0.181,0.334)	13874	(0.130,0.723)	0.392
	HV	89518	(0.086,0.037)	26709	(0.154,0.587)	0.436
LVQ	RG	17918	(0.092,0.510)	13582	(0.241,0.542)	0.149
	HV	15779	(0.085,0.547)	14919	(0.241,0.521)	0.158
SOM	RG	16640	(0.072,0.504)	21897	(0.225,0.476)	0.156
	HV	11268	(0.070,0.615)	12899	(0.222,0.609)	0.152

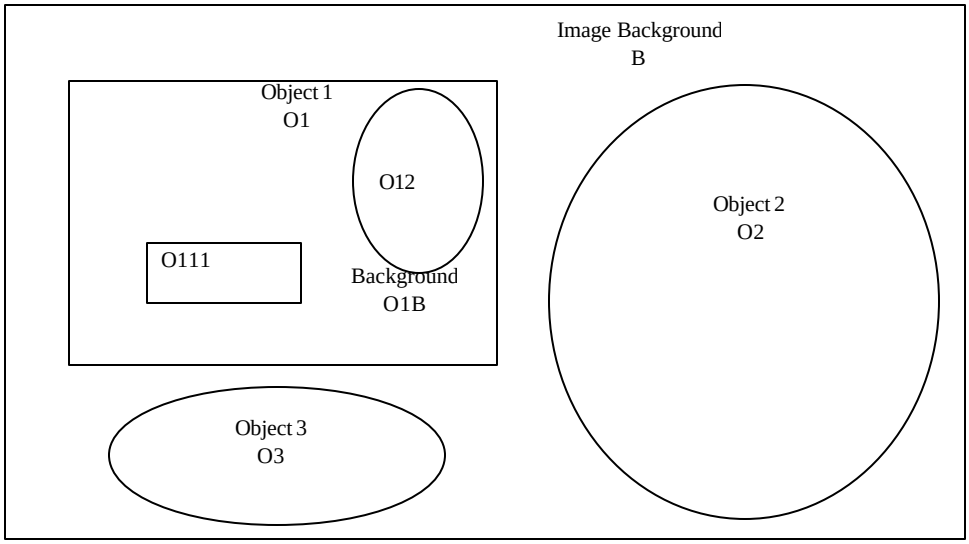

Figure B.1. The multi resolution border segmentation process.

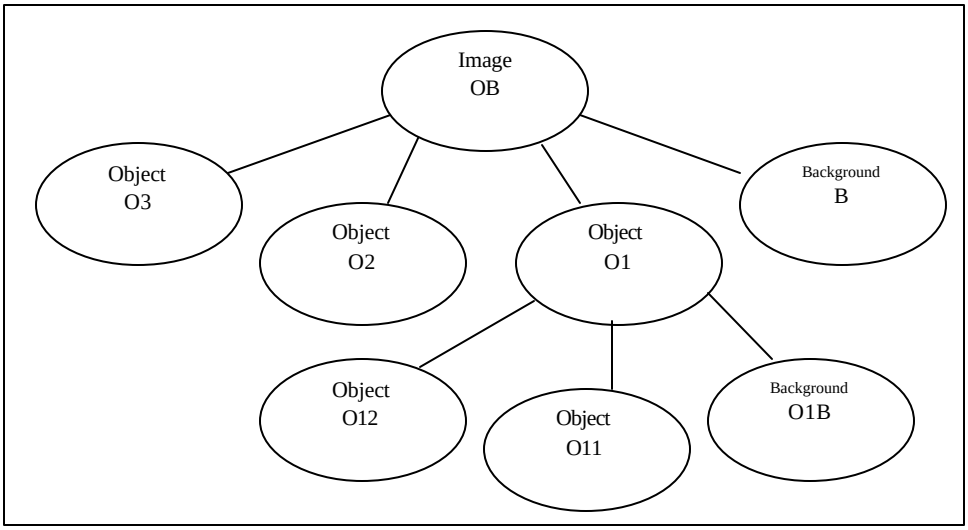

Figure B.2. The tree structure of the segmented image.

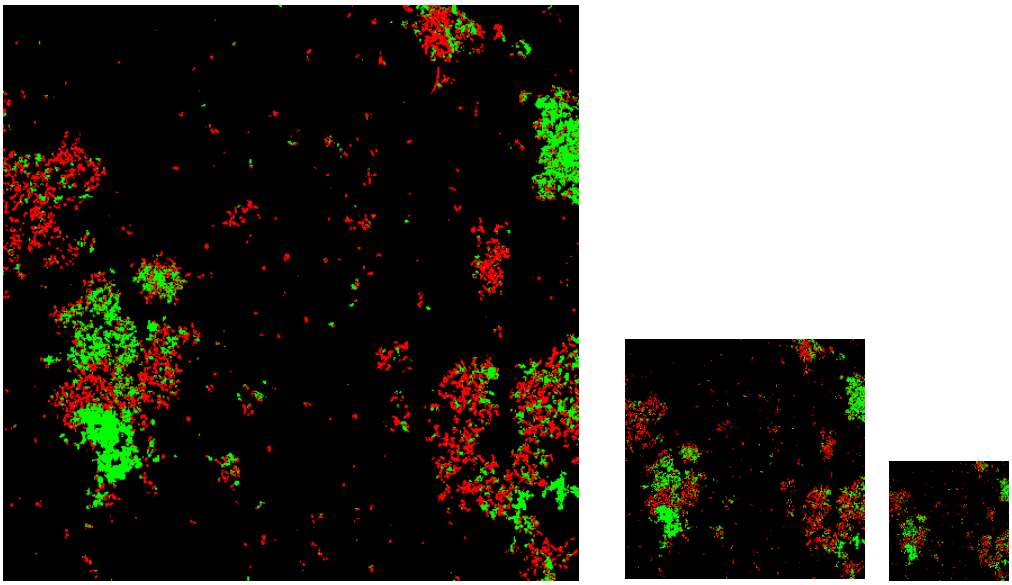

Figure B.3. Image sizes corresponding to 512x512, 256x256 and 128x128 for three resolution levels 1,2 and 3 respectively. Level 1 represents an original slice of a biofilm bacteria image taken by CSLM

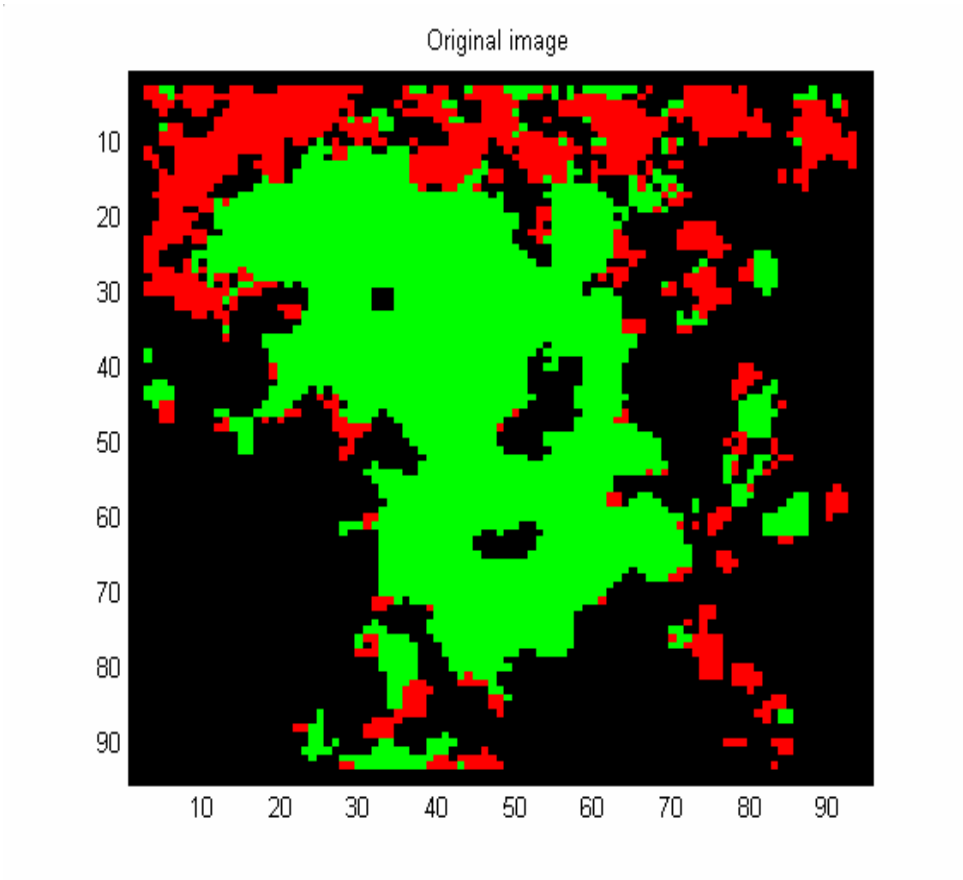

Figure B.4. An original biofilm bacteria image

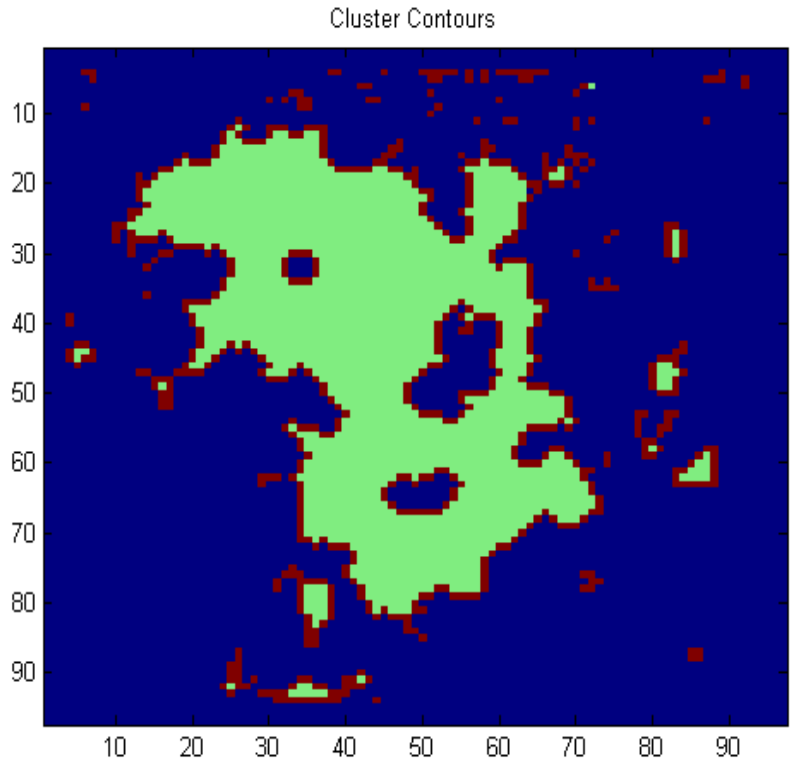

Figure B.5. The result of initial segmentation with the object contours highlighted with black color.

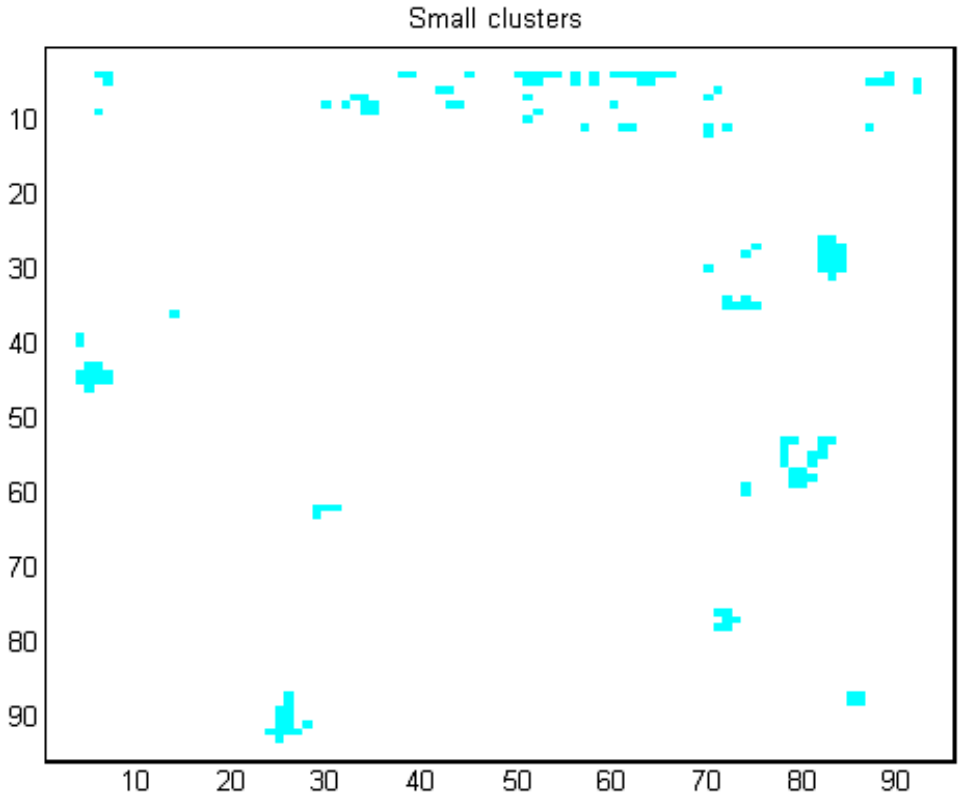

Figure B.6. Green bacteria small contours.

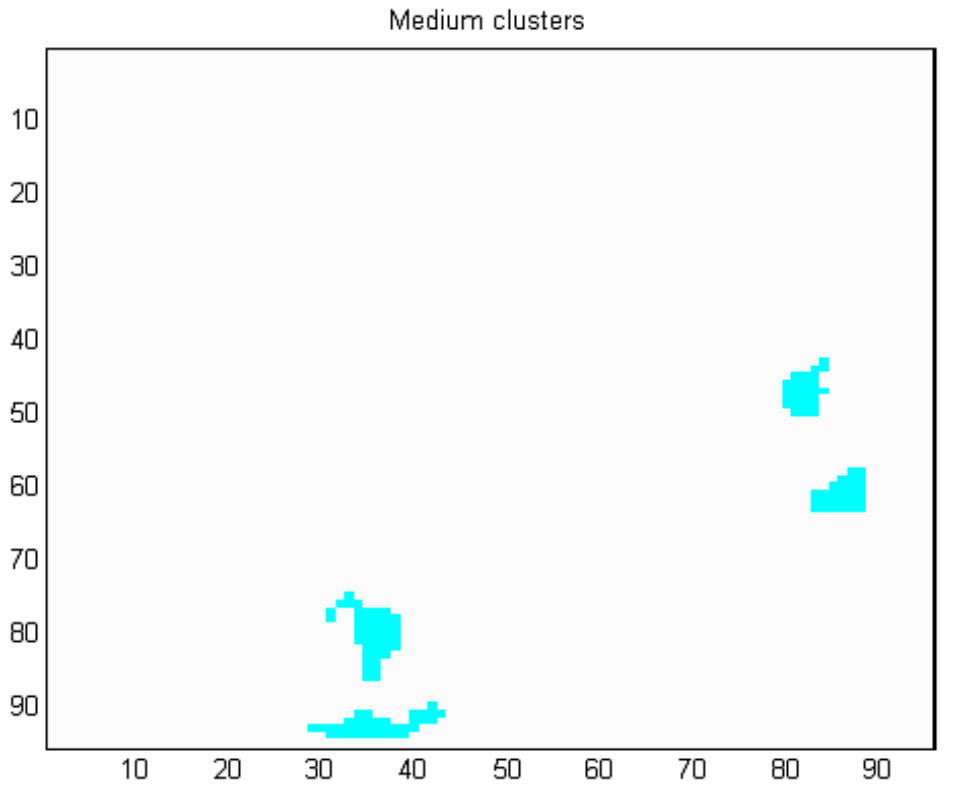

Figure B.7. Green bacteria medium contours.

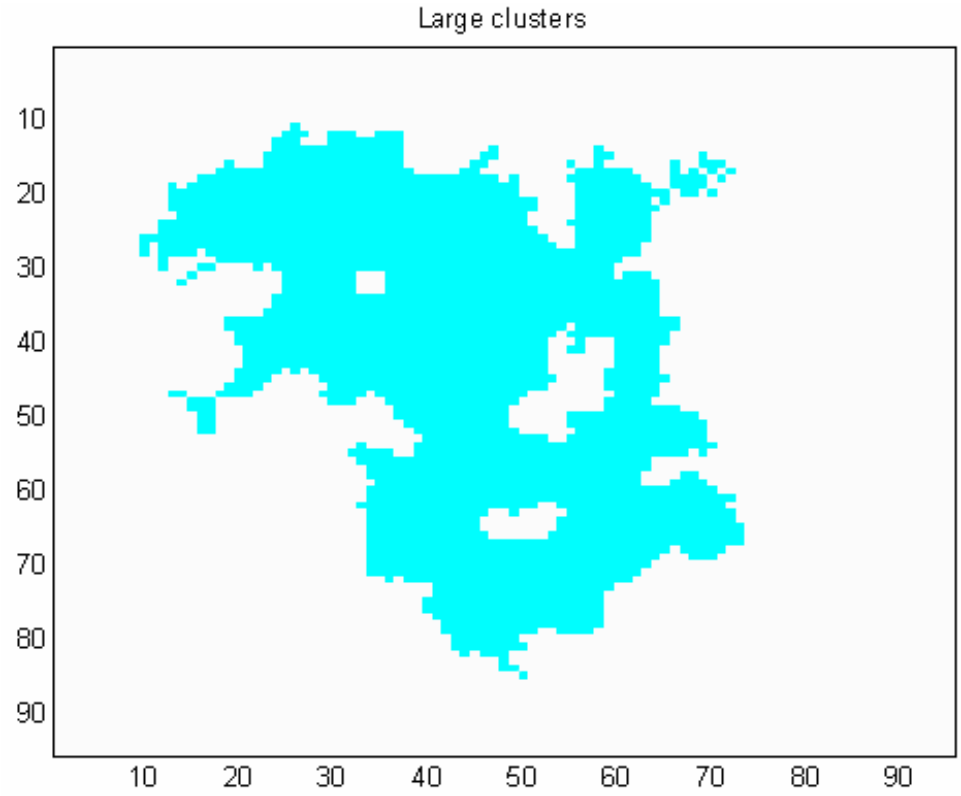

Figure B.8. Green bacteria large contours.